Title

Identification of novel protein targets of metronidazole in drug sensitive and resistant strains of Trichomonas vaginalis and examination of the role of Mycoplasma hominis in secretion of cytokines released from primary human monocytes

Author

Diala, Fitz Gerald Iheanyichukwu

Publication Date

2020

Peer reviewed|Thesis/dissertation

UNIVERSITY OF CALIFORNIA

Los Angeles

Identification of novel protein targets of metronidazole in drug sensitive and resistant strains of *Trichomonas vaginalis* and examination of the role of *Mycoplasma hominis* in secretion of cytokines released from primary human monocytes

A dissertation submitted in partial satisfaction of

the requirement for the degree Doctor of Philosophy

in Molecular Biology

by

Fitz Gerald Iheanyichukwu Diala

2020

ABSTRACT OF THE DISSERTATION

Identification of novel protein targets of metronidazole in drug sensitive and resistant strains of *Trichomonas vaginalis* and examination of the role of *Mycoplasma hominis* in secretion of cytokines released from primary human monocytes

by

Fitz Gerald Iheanyichukwu Diala

Doctor of Philosophy in Molecular Biology

University of California, Los Angeles, 2020

Professor Patricia J. Johnson, Chair

Trichomonas vaginalis, an extracellular, flagellated protozoan parasite, is the etiologic agent for trichomoniasis, the most common non-viral sexually transmitted infection, trichomoniasis. While asymptomatic presentation is commonplace, symptomatic infections typically present as vaginitis and cervicitis in women, and urethritis in men. Only 5-nitroimidazole class of drugs, metronidazole (Mz) and tinidazole, is FDA-approved for treatment of infections. To overcome the knowledge gap in Mz targets in *T. vaginalis,* we used metronidazole-alkyne analog and we employed copper(I)-catalyzed azide-alkyne cycloaddition (CuAAC) "click" reaction to enrich these protein targets. Using tandem mass tag quantitative proteomics, we identified novel protein targets in Mz-sensitive and -resistant parasites. We also determined through activity-based protein profiling that metronidazole binds to cysteine residues

and subsequently identified cysteine residues that are bound by metronidazole. As the nature of immune response to *T. vaginalis* infection appears to vary, we also explored whether *T. vaginalis* parasites harboring *M. hominis*, an endosymbiont, induce the production of different cytokines from primary human monocytes compared to parasites that do not harbor the endosymbiont. Indeed, we observe that more cytokines are elaborated in response to *M. hominis* infected parasites. Together, these studies illuminate our knowledge of this important human pathogen, pharmacologically and immunologically.

The dissertation of Fitz Gerald Iheanyichukwu Diala is approved.

Linda G. Baum

Peter J. Bradley

David A. Campbell

Marcus A. Horwitz

Patricia J. Johnson, Committee Chair

University of California, Los Angeles

2020

DEDICATION

To my loving and supportive parents; to my sisters who have always cheered loudly; to my grandparents, especially Da Rose, who always believed in my education even though she didn't have the opportunity; to late Justice Joseph Ogu Ugoagwu who saw this achievement long before it was reality; to Promise Chidubem.

TABLE OF CONTENTS

ACKNOWLEDGEMENTS

Nothing is possible without life and health. I thank God for life and I feel very blessed to be in this position. I would like to thank my advisor Prof. Patricia J. Johnson who has been supportive and instrumental in my development as a scientist. As difficult as experimental science is, I am glad to have had a mentor who is insightful, wise, and kind. I am also thankful for my thesis committee members who also shepherded me on this journey, ensuring that I didn't lose focus.

I am thankful to the various research members of the Johnson lab, past and present, with whom I forged different nurturing relationships: Drs. Angelica Riestra, Brian Janssen, Augusto Barbosa, Sharon Alterzon, Audrey Dubourg, Francie Mercer, Anand Rai, Azeez Aranmolate, Fernanda Santiago, Katie Muratore, Yi-Pei Chen, and Edward Wang. Also, Brenda Molgora, Taylor Brown, Charlie Ho, Anna Shvartsur, Ramiro Patino, and Grace Boatman. I am equally indebted to the undergrads lab helpers, past and present, who made reagents, helped to keep the lab functioning so that I could spend more time on experiments: Emily Xu, Benny Teng, Lilian Fung, Kaycee Flores, Susan Lei, Leonardo Hernandez, Mahlet Mekonnen, Elizabeth Elton, Brianna Empson and Kaitlyn Richardson. I am especially thankful to Mirrat Adil who also helped me with some experiments as I was recovering from surgery.

The work presented in Chapter 2 could not have been possible without the help of many individuals across several laboratories. I am indebted to Profs. Valery Fokin (USC) and Lars Eckmann (UCSD) for synthesizing and kindly sharing metronidazole-alkyne, which underpins the study. I am grateful to Dr. Brian Janssen for guiding me throughout the early stages as the project evolved. I am grateful to Shannon Stone and Brett Babin from the Tirrell lab at Caltech for their expertise and generous support. Working in collaboration with the Proteome

Exploration Laboratory, Division of Biology and Biological Engineering, Beckman Institute at the California Institute of Technology, I thank Drs. Mike Sweredoski, Annie Moradian and Sonja Hess for advice, help with sample preparation, and data analysis. Dr. Sweredoski has been especially invaluable, making himself available for any and all conversations about how to look at the data and make sense of it. As with all evolving projects, I am also thankful to my other collaborators Drs. Katie Muratore, Jian Cao, and Keriann Backus who were instrumental in our pivot towards identifying cysteine residues bound by metronidazole. Dr. Cao prepared those samples, ran the mass spec, and performed that analysis.

The work presented in Chapter 3 is the main work of Dr. Frances Mercer with Prof. Johnson as the PI. As a rotation student in the laboratory, I worked with Dr. Mercer, contributing what would be Figure 5 in the paper. I enjoyed engaging on this project with Dr. Mercer and our discussions were remarkably synergistic with my infectious diseases block in medical school.

The parasitology community at UCLA has been a great forum to engage with other laboratories, providing and receiving feedback on different projects over the years. I am grateful to all members of that community, past and present.

I am equally grateful for the administration and support staff of the UCLA-Caltech Medical Scientist Training Program. The MBI staff throughout the years has also been supportive, decreasing administrative burden that can sometimes add unnecessary stress. Thank you so much.

The road to UCLA MSTP could not have been possible without programmatic support from the NIH-funded MARC Program under the direction of late Prof. Jolinda A. Traugh, as well as HHMI-funded Medical Scholars Program under Ms. Teresa Cofield. These two programs provided funding support and created an environment that allowed me to become open to

scientific research in addition to my interests in patient care. I am forever grateful to some of undergraduate faculty who supported, encouraged, and believed in my aspirations. They include Dr. Clyde Webster, Prof. Raphael Zidovetzki, Prof. David A. Biggs, and Prof. Leah T. Haimo. Prof Haimo's encouragement opened my eyes to research and her sustained support and advising throughout my undergraduate study was superb. Prof. Katherine A. Borkovich allowed me great latitude in her lab. My curiosity for scientific investigation was born and nourished there.

As a young black man navigating higher education, science, and medicine, finding a relatable mentor can be life-changing. Dr. Ernest Levister, Jr. has been a steadfast mentor throughout the time I have known him beginning during my early days at UCR. I cannot thank him enough for advocating on my behalf. He inspires me to be a strong mentor and advocate for other students. Dr. Margarita Loeza has been an invaluable mentor throughout my years at UCLA. Under her mentorship, I have grown to appreciate medicine in many settings.

Beyond the laboratory, my family and friends have been invaluable. They have listened and comforted me. I am especially grateful for the following friends who have stood firmly with me through some portion of this journey: Adewunmi Adelaja, Yuxi Tian, Aschlyee Braswell, Anand Rai, Samuel Olanrewaju, Kabita Parajuli, David Lyons, Chidubem Amaraegbu, Brenda Molgora, and Azeez Aranmolate.

VITA

Education

Year	Degree	Major/Minor	School	Location
2013 – Present	Doctor of Medicine (in progress)	Medicine	David Geffen School of Medicine at UCLA	Los Angeles, California
2008 – 2012	Bachelor of Science	Biochemistry	University of California, Riverside	Riverside, California

Experience

2013-present **University of California, Los Angeles**
Graduate research with Patricia J. Johnson, PhD in the Department of Microbiology, Immunology & Molecular Genetics on *Trichomonas vaginalis* protein targets of metronidazole and response of primary human monocytes to *T. vaginalis*.

2009-2012 **University of California, Riverside**
Undergraduate research with Katherine A. Borkovich, PhD in the Department of Microbiology & Plant Pathology on Two-component signaling in *Neurospora crassa*.
NIH/Minority Access to Research Careers (MARC) Trainee

2012 **University of California, San Francisco**
Summer undergraduate research with Alexander Johnson, PhD in the Department of Microbiology and Immunology on farnesol-induced cell death of *Candida albicans* opaque-state cells.
Amgen Scholars Program Student

2011 **Baylor College of Medicine**
Summer undergraduate research with Qizhi Cathy Yao, MD, PhD in the Department of Molecular Virology & Microbiology on gene regulatory network of mesothelin (MSLN) in pancreatic cancer.
NIH/Minority Access to Research Careers (MARC) Trainee

Publications

Mercer F, **Diala FG**, Chen Y-P, Molgora B, Ng SH, Johnson PJ. Leukocyte lysis and cytokine induction by the human sexually-transmitted parasite *Trichomonas vaginalis.* PLoS Negl Trop Dis. 2016 Aug 16;10(8):e0004913.

Park G, Servin JA, Turner GE, Altamirano L, Colot HV, Collopy P, Litvinkova L, Li L, Jones CA, **Diala FG**, Dunlap JC, Borkovich KA. Global Analysis of Serine-Threonine Protein Kinase Genes in *Neurospora crassa*. *Eukaryot Cell*. 10:1553-64, 2011. (*Recommended as very good by Faculty of 1000).*

Fellowships and Award

Fellowships & scholarships

2013 - Present	UCLA-Caltech Medical Scientist Training Program
2018 - 2019	UCLA, Microbial Pathogenesis Training Grant
2015 - 2017	UCLA, Microbial Pathogenesis Training Grant
2010 - 2012	NIH/Minority Access to Research Careers (MARC) Trainee
2010	UCR, Medical Scholars Program HHMI Research Fellowship

Awards

2012	Phi Beta Kappa Honors Society
2012	Rosemary S.J. Schraer Outstanding Science Student Award
	UCR, Science Circle Award
	UCSF, Summer Research Training Program, Amgen Scholar
2011	UCR Dean of Student Affairs, Outstanding Leadership Award for African Student Programs
	NAACP Riverside Chapter W.E.B. DuBois Scholar
2010	UCR, Neil Campbell Outstanding Undergrad Research Award
	UCR, Research Grant Spring 2010
2009	Housing Corporation of America Scholarship

Chapter 1 : General Introduction

Trichomonas vaginalis is a microaerophilic protozoan parasite that is the causative agent of trichomoniasis, a sexually transmitted infection afflicting men and women[1]. The estimated prevalence of trichomoniasis is over 250 million worldwide[1], with about 3.7 million cases in the United States[2], making trichomoniasis the most prevalent non-viral STI in the world and the US[1]. As an extracellular parasite, *T. vaginalis* has to adhere and lyse host cells[3] to obtain nutrient[4] and establish infection.

Importantly, the bulk of infections are asymptomatic; however, symptomatic presentation result from pain and inflammation of affected urogenital organs[1]. In women, symptoms include vaginitis, cervicitis, and vaginal discharge[1], with complications including pelvic inflammatory disease[5] and Fitz-Hugh-Curtis syndrome[6], as well as premature rupture of membranes, premature delivery, and low birth weight babies in pregnant women[7]. In men, urethritis[1] and prostatitis[2] are notable symptoms. Trichomoniasis is also associated with increased risk of HIV infection and transmission[1], presumably because of increased traffic of immune cells into the urogenital tract of infected patients[8,9].

Trichomoniasis treatment and mechanism

The absence of symptoms in infected individuals might lead them to not seek treatment[10], thus leading to increased spread of infection. Given the potential for harm to infected patients, it is important to have robust treatment regimens for trichomoniasis. Trichomoniasis is responsive to treatment with 5-nitroimidazole drugs, with metronidazole and tinidazole the only FDA-approve ones[11]. Both metronidazole and tinidazole are prodrugs that differ only in their side chains. Unfortunately, resistance to metronidazole has been reported ranging from 4.3% of isolates in the US[11] to 17.4% in the Goroka region of Papua New Guinea[12].

Metronidazole diffuses passively into the parasite[13], and is activated by redox enzymatic processes in the hydrogenosome[14,15], a mitochondria-related organelle[16], and in the cytoplasm[17]. Activated drug then binds to macromolecules[18]. *In vitro* evidence exists that the drug is able to bind to proteins in susceptible anaerobic and microaerophilic parasites *T. vaginalis*[17], *Entamoeba histolytica*[19], and *Giardia duodenalis*[20], and to DNA[18].

While the activated metronidazole is a promiscuous nitroradical anion[21], previous work had only demonstrated the identification of very few proteins[17,19,20] and suggested specific limited number of targets[17]. It is likely that metronidazole activation in the hydrogenosome and cytoplasm results in adduction to more proteins than previously reported.

Immune cells' response to *Trichomonas vaginalis*

Effective immune response to trichomoniasis is very important, especially given the possible documented complications with this infection. Given that partner reinfection is common[1], thus necessitating the empiric treatment of the patient's sexual partners, it highlights the fact that adaptive immune response formed following infection might not be fully protective. Lysis of the epithelial layer allows for possible interaction between *T. vaginalis* and cells of the immune system, which traffic to the site of injury[22]. *T. vaginalis* is a phagocytic organism that is able to phagocytose different cells, including bacteria and human cells, including leukocytes[4,23]. Vaginal discharge is one symptom of *T. vaginalis* infection, and has been demonstrated to contain neutrophils[8]. *T. vaginalis* isolates can exhibit a range of differences, including adherence and cytotoxicity[3], which are necessary for infection. The impact of varied virulence of *T. vaginalis* strains on the quality of immune response mounted in response to infection deserves exploration. In addition to virulence differences secondary to expression of different proteins in

different strains[24], differences have also been attributed to the presence of an endosymbiont, *Mycoplasma hominis*[25].

The overall goals of this dissertation are to better understand drug treatment of *T. vaginalis* infection with metronidazole as well as factors that underpin the immune response to infection. In Chapter 2, identification of the protein targets as well as the adducted amino acid residues are explored using a more sensitive approach. The adaptation of a terminal alkyne analog of metronidazole allows the identification of more proteins than previously published and also demonstrate adducted cysteine residues for the first time. In Chapter 3, differences in cytokine elaborated from primary human monocytes exposed to a *T. vaginalis* strain with or without the endosymbiont *M. hominis* is explored. Together, these studies illuminate our knowledge of this important human pathogen, laying the foundation for potential exploration of future drug targets as well as providing insight into the observed range and severity of symptoms in infected patients.

References:

1. Schwebke, J. R. & Burgess, D. Trichomoniasis. *Clinical Microbiology Reviews* vol. 17 794–803 (2004).

2. Meites, E. *et al.* A Review of Evidence-Based Care of Symptomatic Trichomoniasis and Asymptomatic Trichomonas vaginalis Infections. *Clin. Infect. Dis.* (2015) doi:10.1093/cid/civ738.

3. Lustig, G., Ryan, C. M., Secor, W. E. & Johnson, P. J. Trichomonas vaginalis contact-dependent cytolysis of epithelial cells. *Infect. Immun.* **81**, 1411–1419 (2013).

4. Midlej, V. & Benchimol, M. Trichomonas vaginalis kills and eats - Evidence for phagocytic activity as a cytopathic effect. *Parasitology* **137**, 65–76 (2010).

5. Moodley, P., Wilkinson, D., Connolly, C., Moodley, J. & Sturm, A. W. Trichomonas vaginalis Is Associated with Pelvic Inflammatory Disease in Women Infected with Human Immunodeficiency Virus. *Clin. Infect. Dis.* **34**, 519–522 (2002).

6. Woo, S. Y. *et al.* Clinical outcome of Fitz-Hugh-Curtis syndrome mimicking acute biliary disease. *World J. Gastroenterol.* **14**, 6975–6980 (2008).

7. Cotch, M. F. *et al.* Trichomonas vaginalis associated with low birth weight and preterm delivery. *Sex. Transm. Dis.* **24**, 353–360 (1997).

8. Lazenby, G. B., Soper, D. E. & Nolte, F. S. Correlation of leukorrhea and Trichomonas vaginalis infection. *J. Clin. Microbiol.* **51**, 2323–2327 (2013).

9. Menezes, C. B., Frasson, A. P. & Tasca, T. Trichomoniasis – are we giving the deserved attention to the most common non-viral sexually transmitted disease worldwide? *Microbial Cell* vol. 3 404–419 (2016).

10. Jackson, D. J., Rakwar, J. P., Bwayo, J. J., Kreiss, J. K. & Moses, S. Urethral Trichomonas vaginalis infection and HIV-1 transmission [5]. *Lancet* **350**, 1076 (1997).

11. Kirkcaldy, R. D. *et al.* Trichomonas vaginalis antimicrobial drug resistance in 6 US cities, STD surveillance network, 2009-2010. *Emerg. Infect. Dis.* **18**, 939–943 (2012).

12. Upcroft, J. A. *et al.* Metronidazole resistance in Trichomonas vaginalis from highland women in Papua New Guinea. *Sex. Health* **6**, 334–338 (2009).

13. Muller, M. & Lindmark, D. G. Uptake of metronidazole and its effect on viability in trichomonads and Entamoeba invadens under anaerobic and aerobic conditions. *Antimicrob. Agents Chemother.* **9**, 696–700 (1976).

14. Yarlett, N., Gorrell, T. E., Marczak, R. & Müller, M. Reduction of nitroimidazole

derivatives by hydrogenosomal extracts of Trichomonas vaginalis. *Mol. Biochem. Parasitol.* **14**, 29–40 (1985).

15. Hrdý, I., Cammack, R., Stopka, P., Kulda, J. & Tachezy, J. Alternative pathway of metronidazole activation in Trichomonas vaginalis hydrogenosomes. *Antimicrob. Agents Chemother.* **49**, 5033–5036 (2005).

16. Shiflett, A. M. & Johnson, P. J. Mitochondrion-Related Organelles in Eukaryotic Protists. *Annu. Rev. Microbiol.* **64**, 409–429 (2010).

17. Leitsch, D. *et al.* Trichomonas vaginalis: Metronidazole and other nitroimidazole drugs are reduced by the flavin enzyme thioredoxin reductase and disrupt the cellular redox system. Implications for nitroimidazole toxicity and resistance. *Mol. Microbiol.* **72**, 518–536 (2009).

18. Ings, R. M. J., McFadzean, J. A. & Ormerod, W. E. The mode of action of metronidazole in Trichomonas vaginalis and other micro-organisms. *Biochem. Pharmacol.* **23**, 1421–1429 (1974).

19. Leitsch, D., Kolarich, D., Wilson, I. B. H., Altmann, F. & Duchêne, M. Nitroimidazole action in Entamoeba histolytica: A central role for thioredoxin reductase. *PLoS Biol.* **5**, 1820–1834 (2007).

20. Leitsch, D., Schlosser, S., Burgess, A. & Duchêne, M. Nitroimidazole drugs vary in their mode of action in the human parasite Giardia lamblia. *Int. J. Parasitol. Drugs Drug Resist.* **2**, 166–170 (2012).

21. Moreno, S. N. & Docampo, R. Mechanism of toxicity of nitro compounds used in the chemotherapy of trichomoniasis. *Environ. Health Perspect.* **64**, 199–208 (1985).

22. Wira, C. R., Fahey, J. V., Sentman, C. L., Pioli, P. A. & Shen, L. Innate and adaptive immunity in female genital tract: cellular responses and interactions. *Immunol. Rev.* **206**, 306–335 (2005).

23. Rendón-Maldonado, J. G., Espinosa-Cantellano, M., González-Robles, A. & Martínez-Palomo, A. Trichomonas vaginalis: In vitro phagocytosis of lactobacilli, vaginal epithelial cells, leukocytes, and erythrocytes. *Exp. Parasitol.* **89**, 241–250 (1998).

24. De Miguel, N. *et al.* Proteome analysis of the surface of trichomonas vaginalis reveals novel proteins and strain-dependent differential expression. *Mol. Cell. Proteomics* **9**, 1554–1566 (2010).

25. Vancini, R. G., Pereira-Neves, A., Borojevic, R. & Benchimol, M. Trichomonas vaginalis harboring Mycoplasma hominis increases cytopathogenicity in vitro. *Eur. J. Clin. Microbiol. Infect. Dis.* **27**, 259–267 (2008).

Chapter 2 : Identification of novel protein targets of metronidazole in drug sensitive and resistant strains of *Trichomonas vaginalis*.

Abstract:

Trichomonas vaginalis is an obligate, extracellular, flagellated protozoan parasite that causes the most common non-viral sexually transmitted infection, trichomoniasis. The infection is treated with 5-nitroimidazole drugs of which metronidazole (Mz) is the most widely used. Parasite death results from adduction of activated drug to proteins and consequent loss of function. While in use since 1960, known protein targets of the drug in *T. vaginalis* are limited. To identify the targets of Mz, we adapted a terminal alkyne analog of Mz (Mz-alkyne) that retains the capacity to be activated and to kill *T. vaginalis*. We determined that Mz-alkyne is able to bind to proteins in sensitive and resistant strains; that metronidazole binds to cysteine residues. We used a chemical labeling approach to identify more metronidazole protein targets in both a sensitive and resistant strain of the parasite, and found that more hydrogenosomal proteins are adducted in the Mz-sensitive strain. Furthermore, for the first time, we identify cysteine residues on some target proteins to which metronidazole adducts.

Introduction:

Trichomonas vaginalis is a microaerophilic protozoan parasite that causes trichomoniasis, the most common non-viral sexually transmitted infection worldwide[1]. Most of the estimated quarter billion annual infections[2] are asymptomatic. However, symptomatic cases present as vaginitis and cervicitis in women and urethritis and prostatitis in men[1].

5-nitroimidazole drugs metronidazole and tinidazole are the sole FDA-approved drugs for treating trichomoniasis[3,4]. Both are prodrugs and differ only in their side chains. Metronidazole (Mz), diffuses passively into cells[5]. Susceptible cells, including some anaerobic bacteria and

microaerophilic protozoans—like *Trichomonas, Entamoeba,* and *Giardia*—have the requisite redox potential to reduce Mz, and lack oxygen, which would otherwise regenerate the nontoxic-parent compound, Mz[6,7]. Different redox pathways that reduce Mz to active metabolites are implicated in bacteria[8] and protozoa[6,9–11].

T. vaginalis contains an unusual organelle, called the hydrogenosome[12], which is the site of carbohydrate catabolism, amino acid synthesis and Fe-S cluster assembly. While there is evidence that different hydrogenosomal processes reduce Mz in *T. vaginalis*[7,9], evidence of cytosolic activation equally exists[6,13]. Previous work in *T. vaginalis*, *E. histolytica*, and *G. lamblia* identified seven, five, and eight Mz-adducted proteins, respectively, leading the authors to conclude that limited number of proteins are adducted to the drug[6,10,11]. Since activated Mz is an anion free radical[14], and thus likely promiscuous, we hypothesize that there are more protein targets than previously reported[6,10,11].

In this work, we have adapted the use of an alkyne analog of metronidazole, Mz-alkyne—which was synthesized and generously provided by Valery Fokin (University of Southern California) and Lars Eckmann (UCSD)—to functionally tag, potentially, the full complement of Mz targeted proteins in *T. vaginalis*. As terminal alkynes react specifically with azides under copper(I)-catalyzed azide-alkyne cycloaddition (CuAAC) "click" reaction[15], target proteins can be bound by clicking to agarose-azide resin followed by enrichment. The resulting Mz targeted proteins were identified and quantified with tandem mass tag (TMT)-based proteomics. We have assessed target proteins in both metronidazole sensitive[16,17] and resistant *T. vaginalis*. We report here the identification of 61 putative metronidazole targets between these metronidazole–sensitive and –resistant strains. In addition, we have been able to resolve the adducted cysteine residues on eight additional putative target proteins, bringing our total to 69

proteins, the highest reported in any such study. While cysteine, free and protein-bound, has been implicated in binding to activated metronidazole[10,18], direct evidence for Mz binding to cysteine has not been reported until this study.

Results:

CuAAC enables detection of many *T. vaginalis* proteins adducted by Mz-alkyne

Copper(I)-catalyzed azide-alkyne cycloaddition (CuAAC) is known to be specific between a terminal alkyne and an azide[15], and given that a terminal alkyne analog of metronidazole (Mz-alkyne) is equally as trichomonocidal as the parent drug (Lars Eckmann, unpublished data), we first wanted to evaluate the specificity of Mz-alkyne adduction in *Trichomonas vaginalis*. To examine Mz-alkyne adduction in both metronidazole-sensitive and -resistant strains, we used highly resistant strain B7268[17,19] as well as the drug sensitive, standard laboratory strain G3[16]. We treated metronidazole-sensitive strain G3[16] and -resistant strain B7268[17,19] parasites with 50 μM Mz, 50 μM Mz-alkyne, or DMSO. 300 μg of lysates were reacted with biotin-azide in 300 μl total CuAAC reaction, using sodium ascorbate as the reducing agent, for 1 hr. After incubation, 8 μg of reaction lysates were resolved by SDS-PAGE, and labeling was visualized by streptavidin blot. An antibody against *T. vaginalis* GAPDH served as a loading control (Fig. 2-1A). With DMSO-treated lysate reacted with biotin-azide as the background, we observed detection of multiple bands in Mz-alkyne-treated lysates from both G3 and B7268 parasites, equivalent to 3.6 fold and 2.8 fold increases over background, respectively (Fig. 2-1B). These data suggested that Mz-alkyne adduction might not be restricted to few proteins, as had been previously published[6]. We did not observe appreciable labeling over

background in CuAAC reactions with Mz-treated lysate or when Mz-alkyne-treated lysate CuAAC reaction lacked biotin-azide. As Mz has an alcohol handle instead of a terminal alkyne, the observation is in line with our expectation. Furthermore, observed adduction of Mz-alkyne to B7268 parasites (Fig. 2-1A), demonstrates that aerobic resistance, which is present in the parasite[6,17] does not completely abrogate binding of activated Mz to target proteins.

Mz-alkyne-treated parasites and CuAAC reaction allows identification of putative metronidazole targets in Mz-sensitive and -resistant parasites

Having observed that proteins of different sizes are adducted by Mz-alkyne and can be detected by functionalizing the terminal alkyne handle to an azide-containing molecule, we next sought to determine the molecular identity of the proteins targeted by using Click-&-Go Protein Enrichment Kit for alkyne-modified proteins from Click Chemistry Tools (#1039) and following the enrichment scheme shown in (Fig. 2-2A). We used metronidazole-highly resistant strain B7268-Res[17] and this strain expressing flavin reductase 1 (B7268-Sens) which results in >64X sensitivity to metronidazole[17]. *T. vaginalis* parasites were treated with Mz-alkyne or Mz-OH as a negative control. Following treatment, the parasites were lysed and the protein extracts subjected to click reaction with the agarose-azide resin. To eliminate non-specific binding of *T. vaginalis* proteins to the agarose resin, we reacted lysates from Mz-OH treatment. The beads were stringently washed to eliminate non-bound proteins and subjected to on-bead trypsin digestion, prior to TMT 10-plex labeling. For each strain, we performed TMT 10-plex labeling, according to manufacturer's protocol, of equal peptides derived from biological triplicates of clicked Mz-alkyne and Mz-OH "mock" reactions. All samples were then analyzed by tandem LC-MS/MS, and the spectra were searched against UniProt *T. vaginalis* sequences[20] and a contaminant

database including proteins like trypsin and human keratins. A decoy database of reversed sequences was also included to estimate the false discovery rate.

Excluding proteins that were either decoys, contaminants, "only identified by site", or matched by only a single peptide from quantitative analysis, 885 protein groups were identified in B7268-Res while 904 protein groups were identified in B7268-Sens. Abundance ratios of "click" vs "mock" were calculated for all protein groups and moderated t-test performed. As seen in the volcano plot of Log_2 enrichment ratio versus $-Log_{10}$ p-value, distribution of protein groups identified in B7268-Res and B7268-Sens in large part mirror each other (Fig. 2-2B). To determine protein groups that are putative targets of metronidazole, we selected those that are enriched (click/mock) at least two-fold and whose Benjamini and Hochberg adjusted p-value were less than 0.05 (boxed). This yielded 31 protein groups in B7268-Res and 39 protein groups in B7268-Sens, with 9 protein groups overlapping between the two strains.

More hydrogenosomal targets of metronidazole identified in Mz-sensitive B7268-Sens than in Mz-resistant B7268-Res

Previous investigation of metronidazole targets in *T. vaginalis* using two-dimensional gel (2DE) identified seven cytosolic proteins, including thioredoxin reductase[6]. None of the seven were identified in this study; however, a thioredoxin reductase ortholog (TVAG_125360) with cytosolic and hydrogenosomal pattern of expression[21], was identified in this study (Table 2-1). Thioredoxin reductase has been shown to be a key cytosolic activator of metronidazole[6,13], and subsequent adduction of activated metronidazole decreases its activity[6].

Of the 31 proteins found in drug-resistant B7268-Res strain, only five of them—a small GTPase (TVAG_079570), Signal recognition particle subunit SRP72 (TVAG_039020), Clathrin heavy chain-related protein (TVAG_562550), a thioredoxin reductase (TVAG_125360), and a ribosomal protein (TVAG_128790)—(16.1%) have been published as hydrogenosomal proteins, with four coming from a proteome of the hydrogenosome[22], and the other coming from a study of *T. vaginalis* thioredoxin reductases, which found TVAG_125360 to localize to the cytoplasm and hydrogenosome[21]. In contrast, 11 out of 39 protein groups (28.2%) identified in drug-sensitive B7268-Sens strain were previously published in the hydrogenosome proteome (Table 1).

Broad single functional categorization of all 61 proteins showed that several pathways are affected by metronidazole (Fig. 2-3A & Fig. S1), with gene ontology annotations tabled in Supplementary Table 2-1. 9 proteins are shared between the proteomes from both strains (Fig. 2-3B), and of them, only the ribosomal protein (TVAG_128790) is hydrogenosomal[22] (Table 2-1). Functions were assigned in line with TrichDB annotation[23], the published hydrogenosome proteome[22], other studies[21,24], UniProt[20] and QuickGO[25] gene ontology annotations, or Phyre2 predictions[26]. 34.42% of all proteins are represented in the "other" and "unknown" functional grouping. Other functional groups include amino acid metabolism, energy metabolism, sugar metabolism, peptidases, translation, redox proteins, cytoskeletal proteins and hydrolases. Hydrolase classification include proteins annotated as hydrolases as well as phosphatases, which also perform similar reactions.

While the hydrogenosome was originally recognized as the canonical site of metronidazole activation[27], more recent evidence has demonstrated that cytosolic enzymes play an important role in drug activation too[6,13]. Only 15 of the 61 putative targets identified have been identified as hydrogenosomal proteins[21,22], (Fig. 2-3C). A machine learning algorithm was

developed to predict proteins that localize to the hydrogenosome based on the entire predicted protein-coding genes of *T. vaginalis*[28]. To evaluate the predictive value of using the model output scores[28] to predict hydrogenosome localization of our identified putative targets, we determined the scores for published hydrogenosomal proteins[22] (Table S2-2). The machine learning algorithm was developed with the entire proteome of *T. vaginalis* taking into consideration proteins that had previously been shown to localize to the hydrogenosome[28]. In addition, because some hydrogenosome proteins have a targeting sequence while others do not[21,22], two predictive scores based on presence of recognizable hydrogenosomal targeting signal sequence (HTS) (MOT+) and lack thereof (MOT-) were developed[28]. Scores and ranks from the algorithm were matched to the previously published hydrogenosomal proteome[22] containing the 569 proteins with their accession numbers, annotation, functional group classification, presence of signal sequence and use in algorithm (Table S2-2). 94 of the 569 proteins had a MOT+ score ≥ 0.5 while 75 of 569 had MOT- score ≥ 0.5. Interestingly, only 7 of the 15 hydrogenosomal proteins[21,22] identified in our proteome had either score ≥ 0.5.

Six new total proteins could be labeled as hydrogenosomal using either MOT+ ≥ 0.5 or MOT- score ≥ 0.5. Using MOT+ score ≥ 0.5, five other proteins could be predicted as hydrogenosomal including an alanyl-tRNA synthetase family protein (TVAG_299450), a cysteine synthase protein (TVAG_071080), two 2-deoxyglucose-6-phosphate phosphatases (TVAG_117360 & TVAG_417190), and an uncharacterized protein (TVAG_487100), which is also one of only two proteins with MOT- score ≥ 0.5. The other is another 2-deoxyglucose-6-phosphate phosphatase (TVAG_463690). And of these six proteins, all three 2-deoxyglucose-6-phosphate phosphatases were enriched in both B7268-Res and B7268-Sens. The uncharacterized protein TVAG_487100 was also enriched in both strains, while alanyl-tRNA synthetase family

protein (TVAG_299450) and cysteine synthase protein (TVAG_071080) were enriched only in B7268-Sens. Cytosolic alanyl-tRNA synthetases have been demonstrated to have mitochondrial localization in *Saccharomyces cerevisiae* and apicoplast localization in *Plasmodium falciparum*[29], suggesting that *T. vaginalis* alanyl-tRNA synthetase could also have hydrogenosomal localization as predicted. Another annotated cysteine synthase protein was identified in the hydrogenosome proteome demonstrated cysteine metabolism in the hydrogenosome[22].

Even with six more proteins predicted to localize to the hydrogenosome across both strains, the higher proportion in B7268-Sens (16/39) compared to B7268-Res (9/31) suggests that there is likely more hydrogenosomal drug activation in the Mz-sensitive strain, B7268-Sens, than in the Mz-resistant strain, B7268-Res.

Mz decreases iodoacetamide alkyne (IAA) labeling of free cysteines and binds to cysteine residues

Cysteine residues are reactive, and are targeted by many drugs in use including anti-neoplastics, afatinib and ibrutinib, and antimicrobials showdomycin and leptomycin B[30]. *Trichomonas vaginalis* uses non-protein cysteine to scavenge for oxygen and maintain a microaerophilic environment[17]. In addition, when typical cysteine supplementation of culture medium is removed, parasites are more susceptible to lower concentration of metronidazole[31]. Moreover, canonical protein activators of metronidazole, ferredoxin and pyruvate ferredoxin oxidoreductase, as well as the cytosolic activator, thioredoxin reductase[6], have reactive cysteine active sites. To test the hypothesis that metronidazole binds to cysteine residues, we employed an

activity-based protein profiling (ABPP) approach[30]. We treated parasites with 50 μM, 500 μM metronidazole and DMSO, as solvent control, for 1 hr. Thereafter, lysates were prepared and labeled with iodoacetamide alkyne (IAA). IAA, like iodoacetamide, readily labels reduced cysteine residues in proteins, and can be clicked to rhodamine-azide using CuAAC, and visualized by in-gel fluorescence (Fig. 2-4A). We observed decreased IAA labeling of lysates from Mz-treated parasites compared to lysates from DMSO control-treated parasites, with two-fold reduction in IAA labeling in lysates from 50 μM Mz-treated parasites and four-fold reduction in IAA labeling in lysates from 500 μM Mz-treated parasites, suggesting that Mz adducts to cysteine residues on proteins. The observed labeling reduction was not due to amount of protein, as corresponding Coomassie staining of samples showed even loading (Fig. 2-4B). Interestingly, the highest prominent band on the gel corresponds to 55 kDa. While reports show that most *T. vaginalis* proteins are less than 70 kDa[32], it is unclear why larger proteins detected by Coomassie staining were not labeled appreciable by IAA, especially in lysates from DMSO-treated parasites.

Mz-alkyne efficient labeling of proteins enables resolution of adducted cysteine residues

Having identified protein targets and demonstrated that metronidazole adducts to cysteine residues, we wanted to identify the particular cysteine residues. In employing CuAAC click to agarose bead and on-bead digest, we were unable to resolve the amino acid residues to which Mz-alkyne adducted. Having demonstrated that Mz-alkyne binds to proteins in Mz-sensitive and -resistant parasites ~3-3.5 fold above background (Figs. 2-1A & 2-1B), we then quantified the binding to ensure that Mz-alkyne labeling was efficient enough to allow detection by mass spectrometry. To determine the efficiency of adduction by Mz-alkyne, we treated parasites with

50 μM Mz-alkyne, and subjected the lysate to CuAAC click to biotin-azide. DMSO control-treated parasite lysate labeled with various concentrations of IAA and clicked to biotin-azide under the same conditions were also examined. We observed that Mz-alkyne adducts to proteins with a greater efficiency than labeling with 100 μM IAA, about 1.6x as intense (Figs. 2-5A & 2-5B). This level of efficiency of labeling indicated that mass spec could be used to detect modified cysteine residues[33,34].

Thereafter, lysates from Mz-sensitive parasites treated with 50 μM Mz-alkyne were subjected to CuAAC click to biotin-azide[35]. Samples were prepared using standard protocols for CuAAC enrichment[36]. Samples were purified after DTT reduction and iodoacetamide alkylation with single-pot, solid-phase-enhanced sample-preparation (SP3) beads[37], and subjected to trypsin digest. Subsequent enrichment with neutrAvidin-agarose followed to obtain Mz-alkyne–modified peptides. To identify modified cysteine residues, lysates from Mz-OH–treated parasites were standardly prepared without CuAAC click. Peptides were desalted and analyzed by LC-MS/MS. Spectral searches were performed with IP2 ProLuCID. Using a differential modification search with fixed carbamidomethyl modification on cysteine, we expected a modification of 400.19978 Da based on cysteine elimination of activated nitro group on Mz-alkyne[38] and subsequent CuAAC with biotin-azide. We identified eight peptides corresponding to eight previously unidentified metronidazole target proteins (Table 2-2). Gene ontology annotation of these proteins are listed in Supplementary Table 2-3. None of these eight proteins was identified in the hydrogenosome proteome[22]; however, only dihydroorotate dehydrogenase family protein TVAG_186690 might be predicted to be hydrogenosomal with MOT+ score of 0.9998 and MOT- score of 0.8886[28]. Interestingly, while localization of dihydroorotate dehydrogenase

family proteins can be cytosolic or mitochondrial[39], previous investigation of pyrimidine metabolism in *T. vaginalis* concluded *de novo* pyrimidine synthesis to be absent in the parasite[40].

Discussion

In this study, we have extended the use of copper(I)-catalyzed azide-alkyne cycloaddition (CuAAC) towards addressing three important issues: identifying metronidazole target proteins in *Trichomonas vaginalis*, determining whether metronidazole binds to cysteine, and demonstrating the cysteine residues adducted by the drug. Previously indirect evidence implicated cysteine involvement in drug binding[10,18], however, this had not been definitively demonstrated, nor had particular residues been identified, as we have done here.

While the number of Mz-targeted proteins identified in total, 69, is over 9 times greater than the seven previously identified, it is likely that our adaptation failed to fully capture the number of proteins to which metronidazole binds. The Click Chemistry Tools kit (#1039) buffer with high urea and NaCl likely reduced the efficacy of CuAAC[41]. Most importantly, our results argue that metronidazole adducts widely and efficiently to proteins in the hydrogenosome and cytoplasm, a stark contrast to studies suggesting only a limited number of proteins[6,10,11].

In a previous study, resistance to metronidazole could be induced with the use of a flavin inhibitor, which ultimately leads to loss of activity of thioredoxin reductase, a flavin enzyme[13]. In B7268-Res where flavin reductase activity is absent, one possibility might be that thioredoxin reductase after having activated some drug, loses its activity, as some of the activated drug also binds to the enzyme[6]. Thus, if there is loss of drug activation, then the parasites are able to resist even higher amount of drug, as seen in the B7268-Res strain. This would essentially mimic the

observed decreased uptake of metronidazole into non-susceptible cells[42]. Identified Mz protein targets in both sensitive and resistant parasites revealed commonalities and differences likely owing to net drug activation capabilities of the parasites. It is possible that where greater net drug activation is present, a sensitive strain, more proteins are able to be bound, thus increasing the likelihood of their disruption.

We identified cysteine residues adducted by Mz-alkyne in Mz-sensitive G3 parasites. These eight proteins were not identified in either of B7268-Res or B7268-Sens. This might have been due to proteome differences between the G3 strain and any of the B7268 strains used. For example, in a surface proteome analysis including G3 and B7268, there were notable differences in the proteins present as well as the relative abundance between strains[43].

Moreover, further optimization and application of CuAAC to more Mz-resistant and -sensitive strains might allow greater understanding of different pathways that are likely to be disrupted in treated parasites. In a parasite where few essential genes are known, this might be a valuable means to begin to gain a foothold in that regard. Furthermore, understanding of said essential pathways could hold the key for discovering pathways that might not yet be explored as druggable targets.

Materials and Methods:

Growing cells

The *T. vaginalis* strains used in this study were G3 (ATCC PRA-98), BRIS/92/STDL/B7268. B7268-Res and B7268-Sens were generated and characterized in a previous study[17]. Parasites were cultured in Diamond's TYM medium supplemented with 10% horse serum (Sigma), 180 μM ferrous ammonium sulfate (Fisher), 28 μM sulfosalicylic acid (Fisher), 100 U/ml penicillin and 100 g/ml streptomycin (Thermo Fisher Scientific) (complete Diamond's media)[44]. MasterNeo-(HA [hemagglutinin]) plasmid bearing TVAG_517010 (flavin reductase (FR)1)-Sens or empty vector control (EV)-Res was overexpressed[17] and maintained with 100 g/ml of G418 (Gibco) for selection. Parasites were cultured at 37°C and passaged daily for 2 weeks or less.

Metronidazole treatments

Parasites were grown overnight in Complete Diamond medium without ascorbic acid, and washed with this media (3200 rpm 10 mins). 1 x 10^6 cells/ml parasites were seeded in tightly sealed plastic conical vials with complete Diamond (-ascorbic acid) with DMSO, as vehicle control, or Mz (or Mz-alkyne) as indicated. Parasites were incubated at 37 °C for 1-2 hrs, as indicated. Thereafter, parasites were washed with PBS (+5% sucrose) and lysed, sonicated (where indicated), and clarified by centrifugation at 14,000 rpm for 10 mins.

Detection of proteins bound by Mz-alkyne

300 μg of lysates in (2% SDS, 50 mM Tris, pH 7.5, 1x Halt Protease Inhibitor Cocktail (Thermo Fisher Scientific)) were CuAAC clicked to 31 μM biotin-azide (Cayman Chemical) in the presence of 2.5 mM THPTA (Sigma-Aldrich), 0.2 mM $CuSO_4$ (Sigma-Aldrich) and 5 mM

Na-ascorbate (Sigma-Aldrich) in 300 μL total volume for 1 hr at room temp. Samples were prepared and heat-denatured at 95 °C for 5 mins, and 8 μg separated by SDS-PAGE. Gels were blotted onto PVDF membrane at 100 V for 1 hr. For Streptavidin detection of biotin-azide click to Mz-alkyne, membrane was blocked with 1% BSA in PBS for 30 mins, followed by incubation with 1:10,000 Streptavidin-HRP (Thermo Fisher Scientific) for 1 hr, washed three times with PBS, and detection. TvGAPDH was probed as loading control. Membrane was blocked with 5% milk in 1x TBST for 30 mins, followed by probing with 1:10,000 anti-TvGAPDH primary antibody (Cocalico Biologicals) for 1 hr, three 10-min washes with 1x TBST, 1:25,000 horseradish peroxidase (HRP)-conjugated anti-rabbit secondary antibody (Jackson Laboratory) for 1 hr, and three 10-min washes with 1x TBST. Bio-Rad Gel Doc XR was used to capture images and ImageLab software (v. 5.1, Bio-Rad) used for analysis.

Detection of Mz competition for cysteine residues, leading to decreased iodoacetamide alkyne (IAA) labeling

200 μg of proteins from DMSO, 50 μM, or 500 μM Mz-treated parasites lysed in (1x PBS + 0.5% Triton X-100 + 2x Halt Protease Inhibitor Cocktail (Thermo Fisher Scientific)) were labeled with 0, 10, or 100 μM IAA in 200 μL volume for 1 hr at room temp. Thereafter, 100 μg labeled samples were CuAAC clicked to 22.3 μM rhodamine-azide in the presence of 91 μM TBTA, 0.89 mM $CuSO_4$ and 0.93 mM TCEP in 112 μL total volume for 1 hr at RT. Samples were prepared and heat-denatured at 95 °C for 5 mins, and 21 μg separated by SDS-PAGE. In-gel fluorescence was visualized on a Bio-Rad Gel Doc XR using the 605/50 fluorescence filter.

Detection of Mz-alkyne labeling efficiency

200 μg of proteins from DMSO-treated parasites lysed in (4% CHAPS, 1 M NaCl, 8 M Urea, 200 mM Tris pH 8, 2x Halt Protease Inhibitor Cocktail (Thermo Fisher Scientific)) were labeled with 0, 1, 10, or 100 μM IAA in 200 μL volume for 1 hr at room temp. After labeling, these IAA-labeled lysates as well as 200 μg lysate from Mz-alkyne-treated were CuAAC clicked to 0.38 mM biotin-azide in the presence of 4.25 mM THPTA, 0.425 mM $CuSO_4$ and 4.25 mM Na-ascorbate in 235 μL total volume for 1 hr at RT. Samples were prepared and heat-denatured at 95 °C for 5 mins, and 20 μg separated by SDS-PAGE. Gels were blotted onto PVDF membrane at 100 V for 1 hr. For Streptavidin detection of biotin-azide click to Mz-alkyne, membrane was blocked with 1% BSA in PBS for 30 mins, followed by incubation with 1:10,000 Streptavidin-HRP for 1 hr, washes with PBS, and detection. Bio-Rad Gel Doc XR was used to capture images and ImageLab software (v. 5.1, Bio-Rad) used for analysis.

Mass spectrometry identification of Mz adducted proteins by quantitative proteomics.

We adapted the Click-&-Go Protein Enrichment Kit for capture alkyne-modified proteins from Click Chemistry Tools (# 1039). Briefly, 500 μg of Mz-alkyne lysates lysed in (200 mM Tris pH 8, 4% CHAPS, 1 M NaCl, 8 M Urea, 1x Halt Protease Inhibitor Cocktail (Thermo Fisher Scientific)) were CuAAC clicked to agarose-azide beads overnight, rotating in a 30 °C chamber. Mock reaction with Mz-treated samples was also performed and samples were equally processed as below. The beads were washed with 1.8 mL water and then 1mL SDS wash buffer (100 mM Tris, 1% SDS, 250 mM NaCl, 5 mM EDTA, pH 8.0) before reduction with 10 mM DTT at 70 °C for 15 mins. After cooling, reduced proteins were subsequently alkylated with 80 mM iodoacetamide (incubated at room temp in the dark, rotating end-over-end for 30 mins). The reduced, alkylated resin-protein samples were transferred into 10 mL Bio-Rad Poly-Prep 30 micron chromatography columns for washes. Each sample was washed with 55 mL SDS wash

buffer, then 55 mL 8 M urea/100 mM Tris pH 8, and finally 55 mL 20% acetonitrile. Resin-protein samples were resuspended in digestion buffer (50 mM ammonium bicarbonate, 2 mM $CaCl_2$, 10% acetonitrile), transferred to microcentrifuge tube, spun, and excess buffer removed. 5 μL of 20 ng/μL trypsin was added and the samples incubated overnight in the dark at 37 °C. The resulting soluble fraction containing tryptic peptides was diluted to 1 mL before quenching the reaction with 2 μL trifluoroacetic acid. The acidified samples were dried in speed vac, resuspended in 0.2% formic acid and desalted by HPLC to desalt. The eluted samples from HPLC were dried in speed vac and resuspended in appropriate volume of 100 mM TEAB to achieve 0.25 ug/uL. Thermo TMT Label Reagents (# 90110) were equilibrated at room temp with anhydrous acetonitrile and 4.1 μL added to 2.5 ug peptides (10 μL). The reactions were incubated at room temp for 1 hr and subsequently quenched with 0.8 μL 5% hydroxylamine. Labeled samples were pooled together and desalted by HPLC. The elution was dried, resuspended and a fraction run on OrbiTrap Fusion (Thermo, Waltham MA) mass spectrometer.

Digested peptides were loaded onto a 26-cm analytical HPLC column (75 μm inner diameter) packed in-house with ReproSil-Pur C_{18AQ} 1.9-μm resin (120-Å pore size; Dr. Maisch, Ammerbuch, Germany). After loading, the peptides were separated with a 120-min gradient at a flow rate of 350 nl/min at 50°C (column heater) using the following gradient: 2–6% solvent B (7.5 min), 6–25% B (82.5 min), 25–40% B (30 min), 40–100% B (1 min), and 100% B (9 min), where solvent A was 97.8% H_2O, 2% ACN, and 0.2% formic acid, and solvent B was 19.8% H_2O, 80% ACN, and 0.2% formic acid. The Orbitrap Fusion was operated in data-dependent acquisition mode with SPS-MS3 to automatically switch between an MS1 scan (m/z = 400–1500) in the Orbitrap (120,000 resolution), an MS2 scan using CID fragmentation and detection in the ion trap (with turbo scan rate), and an SPS-MS3 scan using HCD fragmentation (65 NCE

on the top 10 most intense MS2 ions) and detection in the Orbitrap (60,000 resolution). The automatic gain control (AGC) targets of the MS1, MS2, and MS3 scans were 4E5, 1E4, and 1E5, respectively. Monoisotopic precursor selection was enabled, as well as charge state filtering (only charge states 2-7, ignoring undetermined charge states), minimum intensity threshold of 5000, and dynamic exclusion of 60 seconds.

Data analysis for identification of Mz target proteins

Thermo raw files were processed in MaxQuant with integrated search engine Andromeda (v. 1.6.10.43)[45,46]. Spectra were searched against UniProt *T. vaginalis* sequences (downloaded on 1/30/2020, 50752 entries) and a contaminant database including proteins like trypsin and human keratins (246 entries). A decoy database of reversed sequences was also included to estimate the false discovery rate. Trypsin was the specified digestion enzyme and up to two missed cleavages were allowed. Methionine oxidation and protein N-terminal acetylation were specified as variable modifications. Carbamidomethylation of cysteine, and TMT10plex modification of peptide N-teminus and lysine were specified as fixed modification. Precursor mass tolerance was 4.5ppm after mass recalibration, MS2 ion mass tolerance was 0.5 Da, and MS3 ion mass tolerance was 0.003 Da. Score thresholds were set to achieve a 1% false discovery rate at the protein, peptide, and peptide-spectrum match levels. Calculation of iBAQ values was enabled. Proteins that were either decoys, contaminants, "only identified by site", or matched only a single peptide were not included in quantitative analysis. The remaining proteins were further analyzed using limma[47], where a moderated t-test was performed between protein abundances in "clicked" samples and "mock" and "non-clicked" samples. Proteins whose 95% confidence interval of the abundance ratio indicated greater abundance in "clicked-enriched" than "mock enriched" and whose Benjamini and Hochberg adjusted p-value was less than 0.05 were

considered putative enriched targets of metronidazole. ***Selection criteria for targets:*** Log_2 ("clicked"/"mock") ratio greater than or equal to 1 with adj. p-value less than 0.05.

Sample preparation for site of labeling enrichment

200 μL of MZ-alkyne treated lysates (1 mg/mL) was subjected to CuAAC click chemistry with 400 μM of biotin-azide in the presence of 100 μM of TBTA, 1 mM of $CuSO_4$ and 1 mM TCEP for 1 hr at RT. Heat denaturation at 95 °C for 5 mins followed after reaction. Each sample was treated with 0.5 μL benzonase and incubated at 37 °C for 30 mins. 10 mM DTT in water (10 μL of a 200 mM stock in water) was added into each sample and the sample was incubated at 65 °C for 15 mins. To this 20 mM iodoacetamide (10 μL of 400 mM iodoacetamide in water) was added and the solution/mixture was allowed to react at 37 °C for 30 mins with shaking.

Sera-Mag SpeedBeads Carboxyl Magnetic Beads (SP3) were purchased from GE Healthcare Life Sciences. SP3 was performed at a bead/protein ratio of 10:1 (wt/wt). For each 200 μL lysates (1 mg/mL) sample, 20 μL of Sera-Mag SpeedBeads Carboxyl Magnetic Beads, hydrophobic (GE Healthcare, 65152105050250, 50 μg/μL, total 2mg) and 20 μL of Sera-Mag SpeedBeads Carboxyl Magnetic Beads, hydrophilic (GE Healthcare, 45152105050250, 50 μg/μL, total 2 mg) were aliquoted into a single Eppendorf tube and gently mixed. The tube was placed on a magnetic rack until the beads settled to the tube wall, and the supernatant was removed. The beads were reconstituted in 400 µL of molecular biology grade (MB) water off the magnetic rack, mixed and supernatant was removed on the magnetic rack. The process was repeated for another two times before reconstituting the beads in 50 – 100 μL MB water. The

reconstituted bead solution was transferred to the CuAAC click sample containing 0.5% SDS, allowing to shake at 1200 rpm for 5 mins at room temp. To this, 400 μL of 100% EtOH was added and it was allowed to incubate for 5 mins at room temp with shaking at 1200 rpm. The sample was then placed on a magnetic rack until the beads settled on the tube wall. The supernatant was removed and discarded. SP3 beads were further washed three times with 400 μL of 80% EtOH, vortexed, magnetized and the supernatant was discarded. Beads were then resuspended in 100 μL PBS containing 2 M urea followed by the addition of 10 μL of trypsin solution (1 mg/mL). The digestion was allowed to proceed overnight at 37 ºC with shaking. 3 μL formic acid was added into the digested sample and incubated for 5 mins at room temp with shaking at 1200 rpm. To this was added ~ 2 mL acetonitrile (> 95% of the final volume) and the mixture was incubated at room temp for 10 mins with shaking. Magnetic rack was applied to separate beads from liquid, and the beads were washed with 500 μL acetonitrile for 3 times. Peptides were then eluted off from SP3 beads with 100 μL of 2% DMSO in MB water at 37 °C for 30 mins with shaking at 1200 rpm.

NeutrAvidin enrichment of labeled peptides

For each sample, 50 μL of neutrAvidin-agarose beads slurry (Pierce, 29200) was washed twice in 10 mL IAP buffer (522 mg MOPS, 146.1 mg Na_2HPO_4 and 70.98 mg NaCl in 50 mL MB water) and then resuspended in 500 μL IAP solution. The eluted peptide solution was transferred to the suspension of neutrAvidin-agarose beads and the mixture was nutated for 2 hrs at ambient temp. After incubation, the beads were pelleted down by centrifugation (1,4800 rpm, 1 min) and washed (6 × 700 μL water). Bound peptides were eluted twice with 60 μL of 80% acetonitrile in MB water containing 0.1% formic acid (first at RT for 10 mins, second at 72 °C for 10 mins). After the first 10 mins incubation at RT, the sample was centrifuged (14,800 rpm, 1

min) and the top liquid layer was transferred into a Micro Bio-Spin columns with a receiving microcentrifuge tube and the bottom beads were then re-dissolved in 60 μL of 80% acetonitrile in water containing 0.1% formic acid. After the 10 min incubation at 72 °C, the mixture was transferred into the same bio-spin column. Elution was collected by centrifugation (14,800 rpm, 1 min). The combined elution was dried by speed-vacuum and resuspended in 40 μL water containing 5% acetonitrile and 1% formic acid. Digested and neutrAvidin enriched peptides were separated on C18 reversed phase for proteomics identification.

Mass spectrometry analysis for site of labeling peptides

Samples were run on a QExactive Hybrid Orbitrap Mass Spectrometer (Thermo, Waltham MA) and spectra processed with IP2 ProLuCID. Carbamidomethylation of cysteine was specified as fixed modification. For Mz-alkyne-adducted cysteine residues, we hypothesized that adduct formation resulted from substitution of activated nitro group on the drug by nucleophilic sulfur anion, as previously published (Girard 1993). Based on differential modification, we searched for 400.19978 Da modification net difference on peptides with cysteine residues corresponding to the mass change attributable to Mz-alkyne CuAAC clicked to biotin-azide.

Figures and tables

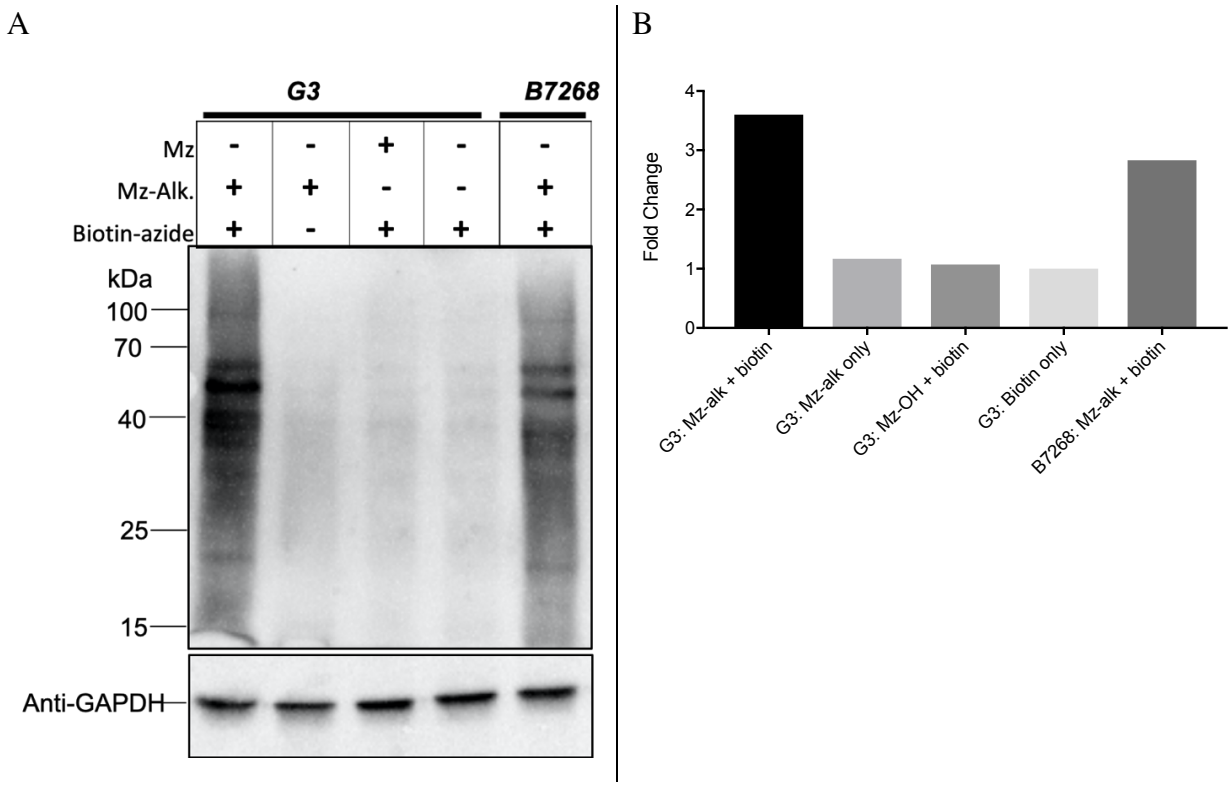

Figure 2-1. Biotin-azide labeling of protein lysate is Mz-alkyne-dependent. (A)Lysates were prepared from Mz-alkyne-, Mz-, and solvent-treated parasites. Lysates were clicked to biotin-azide under Cu(I) catalysis. Streptavidin-HRP WB shows proteins of different sizes in lysates from Mz-alkyne-treated cells, but not in those from Mz-treated cells or Mz-alkyne-treated cells not subjected to bioin-azide click catalysis. These data suggest Mz-alkyne adducts to different T. vaginalis proteins, and that click reaction is specific. (B) Lane intensities were quantified with ImageJ. G3 = T. vaginalis strain G3 lysates. B7268 = T. vaginalis strain B7268 lysates.

A

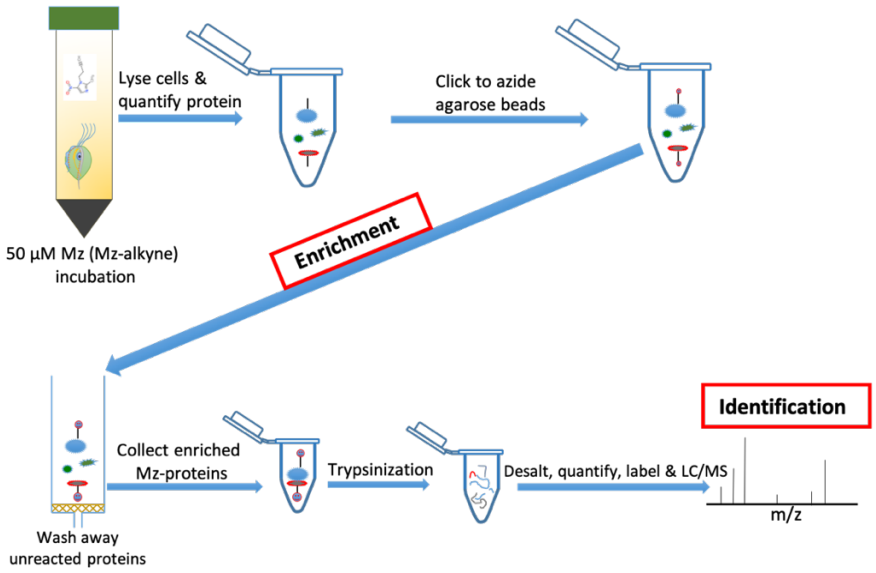

B

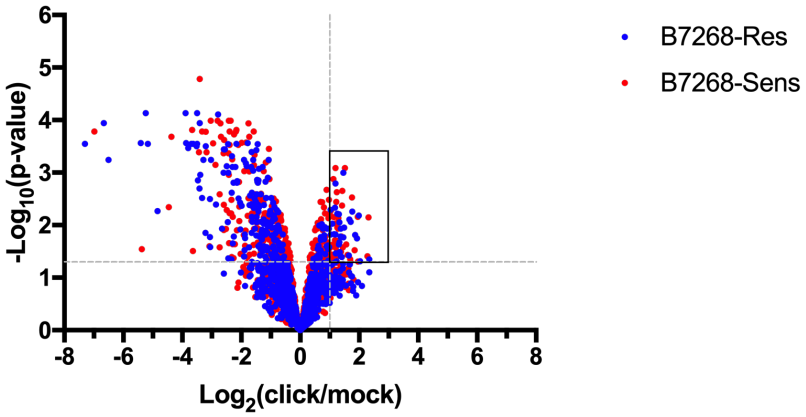

Figure 2-2. Reaction scheme to enrich and identify Mz targets. (A) T. vaginalis parasites were incubated with Mz or Mz-alkyne for two hours. Lysate was prepared from treated cells and CuAAC "clicked" to azide agarose beads. Reacted lysate and beads were then stringently washed to remove unreacted proteins. Bead-bound proteins were digested on-bead with trypsin, and peptides were labeled and identified by LC/MS. (B) Using Thermo tandem mass tag (TMT) 10-plex labeling for each strain, triplicates of peptides from Mz-alk "click" enrichment and Mz-OH mock enrichment were analyzed by LC-MS/MS. Protein groups demonstrating two-fold enrichment in click/mock with p-value < 0.05 are boxed in upper quadrant of graph. B7268-Res = drug resistant B7268 transfected with empty vector and B7268-Sens = drug sensitive B7268 transfected with flavin reductase 1[17].

Strain	Entry	Gene names	Protein names	Functional group	Unifying Functional Group Label	Previous evidence for hyd localization[22]	MOT + score[a]	MOT-score[a]	New hyd pred[b]
Res	A2EF89	TVAG_079570	Small GTP-binding protein, putative	Small GTPases and Associated Proteins	Hydrolase	Yes	0.0837	0.0002	
Res	A2E5L3	TVAG_039020	Signal recognition particle subunit SRP72	ER (protein targeting)	Other	Yes	0.0000	0.0000	
Res	A2GLT5	TVAG_562550	Clathrin heavy chain-related protein	Vesicle association	Other	Yes	0.0000	0.0001	
Res	A2F9L1	TVAG_125360	Thioredoxin reductase (EC 1.8.1.9)	Redox	Redox	Yes*	0.9999	0.9998	
Res	A2DLA9	TVAG_267590	WASH_WAHD domain-containing protein[U]	Cytoskeletal Proteins	Cytoskeleton		0	0	
Res	A2FLD2	TVAG_057830	WD_REPEATS_REGION domain-containing protein[U]	Cytoskeletal Proteins	Cytoskeleton		0	0	
Res	A2DAX3	TVAG_377820	4Fe-4S binding domain containing protein[U]	Energy Metabolism	Energy Metabolism		0	0	
Res	A2E222	TVAG_463690	2-deoxyglucose-6-phosphate phosphatase, putative	Hydrolase	Hydrolase		0.245	0.9803	Yes
Res	A2DLV5	TVAG_462440	Uncharacterized protein	Hypothetical proteins	Unknown		0	0.0002	
Res	A2EDW4	TVAG_363950	Ankyrin repeat protein, putative	Hypothetical proteins	Unknown		0.0003	0	
Res	A2FRN2	TVAG_327610	Ethanolamine-phosphate cytidylyltransferase, putative	Membrane lipid synthesis	Other		0.0012	0.0132	
Res	A2G214	TVAG_181540	Clan CA, family C19, ubiquitin hydrolase-like cysteine peptidase	Peptidases	Peptidases		0.0235	0	
Res	A2E3T7	TVAG_117470	Thioredoxin family protein	Redox	Redox		0	0	
Res	A2G881	TVAG_339630	Thioredoxin family protein	Redox	Redox		0.0004	0	
Res	A2E134	TVAG_388070	Zinc finger, C2H2 type family protein[U,O]	Ribosomal and Associated Proteins	Ribosomal and Associated Proteins		0	0	
Res	A2ER03	TVAG_016650	RNA polymerase Rpb3/Rpb11 dimerisation domain containing protein	Transcription	Other		0	0	

Res	A2DCT5	TVAG_237350	KOG2701 domain-containing protein	Golgi to plasma membrane transport	Cytoskeleton		0.0000	0.0000	
Res	A2DY82	TVAG_461080	Nucleolar GTP-binding protein 1	Small GTPases and Associated Proteins/biogenesis of the 60S ribosomal subunit	Translation		0.0001	0.0000	
Res	A2E6B9	TVAG_459140	SnoRNA binding domain containing protein	snoRNA binding	Other		0.0000	0.0000	
Res	A2EGV2	TVAG_497090	Eukaryotic translation initiation factor, putative	Translation initiation	Translation		9.30E-10	1.71E-07	
Res	A2EZW3	TVAG_273370	Haloacid dehalogenase-like hydrolase family protein	Hydrolase	Hydrolase		0.0281	0.0701	
Res	A2EZW4	TVAG_273380	6-phosphogluconate dehydrogenase, decarboxylating	Sugar Metabolism	Sugar Metabolism		0.0915	0.5354	
Res & Sens	A2E4D0	TVAG_128790; TVAG_189110	Ribosomal protein, putative	Ribosomal and Associated Proteins	Ribosomal and Associated Proteins	Yes	0	0	
Res & Sens	A2E3S6	TVAG_117360	2-deoxyglucose-6-phosphate phosphatase, putative	Hydrolase	Hydrolase		0.9759	0.0072	Yes
Res & Sens	A2F266	TVAG_154750; TVAG_432360	D-3-phosphoglycerate dehydrogenase[O]	Amino Acid Metabolism	Amino Acid Metabolism		0.0085	0.2978	
Res & Sens	A2ESH7	TVAG_417190	2-deoxyglucose-6-phosphate phosphatase, putative	Hydrolase	Hydrolase		0.7388	0.009	Yes
Res & Sens	A2DZD8	TVAG_487100	Uncharacterized protein	Hypothetical proteins	Unknown		0.9998	0.9986	Yes
Res & Sens	A2EC21	TVAG_137880	Peptidyl-prolyl cis-trans isomerase (PPIase) (EC 5.2.1.8)	Protein peptidyl-prolyl isomerization	Other		0.0037	0.0122	
Res & Sens	A2DGQ3	TVAG_110520; TVAG_064320	40S ribosomal protein S27	Ribosomal and Associated Proteins	Ribosomal and Associated Proteins		0	0	
Res & Sens	A2DU34	TVAG_277930	Uncharacterized protein	Ubiquitin E3 ligase[U]	Unknown		0.0081	0.0496	
Res & Sens	A2GEF2	TVAG_414560	dTDP-glucose 4,6-dehydratase, putative	Nucleoside sugar metabolism	Other		0.0001	0	
Sens	A2EIU6	TVAG_419720	Aspartate aminotransferase, putative	Amino Acid Metabolism	Amino Acid Metabolism	Yes	0.041	0.0217	

Sens	A2F0F6	TVAG_272760; TVAG_379130	Dihydrolipoyl dehydrogenase (EC 1.8.1.4)[U,O]	Amino Acid Metabolism	Amino Acid Metabolism	Yes	0.435	0.9999	
Sens	A2D9B6	TVAG_183790	AP65-3 adhesin	Energy Metabolism	Energy Metabolism	Yes	1	1	
Sens	A2D900	TVAG_182620	TvhydB protein, putative	Energy Metabolism	Energy Metabolism	Yes	1	0.9999	
Sens	A2FCW4	TVAG_037570; TVAG_361590	64kDa iron hydrogenase, putative	Energy Metabolism	Energy Metabolism	Yes	0.998	0.0155	
Sens	A2EVX8	TVAG_049830; TVAG_121610	Pyridine nucleotide-disulphide oxidoreductase family protein	Flavin Proteins	Redox	Yes	0.7181	0.0745	
Sens	A2EXK6	TVAG_260830	Uncharacterized protein	Hypothetical proteins	Other	Yes	0.002	0.0002	
Sens	A2G591	TVAG_001130	Uncharacterized protein	Hypothetical proteins	Other	Yes	0	0.0003	
Sens	A2FKA7	TVAG_293770	Phosphofructokinase, putative	Sugar Metabolism	Sugar Metabolism	Yes	0.4768	0.9551	
Sens	A2DKI5	TVAG_190580	Methionine aminopeptidase	Peptidases	Peptidases	Yes	0.0000	0.0000	
Sens	A2ECT4	TVAG_276530; TVAG_071080	Cysteine synthase, putative	Amino Acid Metabolism	Amino Acid Metabolism		0.9988	0.0403	Yes
Sens	A2EVS2	TVAG_299450	Alanyl-tRNA synthetase family protein	Amino Acid Metabolism	Amino Acid Metabolism		0.9774	0.0519	Yes
Sens	A2G4A3	TVAG_374870	Doublecortin domain-containing protein[U]	Cytoskeletal Proteins	Cytoskeleton		0.038	0.0007	
Sens	A2DI20	TVAG_402650	Uncharacterized protein	Cytoskeletal Proteins[U]	Cytoskeleton		0	0.0012	
Sens	A2DFE0	TVAG_436920	Quinoprotein alcohol dehydrogenase-like	Energy Metabolism	Energy Metabolism		0	0	
Sens	A2D7I8	TVAG_120430; TVAG_120280	4-alpha-glucanotransferase family protein	Host Cell Adherence	Other		0.1771	0.0003	
Sens	A2DJ99	TVAG_136170	Paramyosin, putative	Hypothetical proteins	Unknown		0	0	
Sens	A2FNN7	TVAG_427040	Cytosolic repetitive antigen, putative[U]	Hypothetical proteins	Unknown		0.0005	0	
Sens	A2G7Q7	TVAG_100270	Uncharacterized protein	Hypothetical proteins	Unknown		0	0	
Sens	A2E8E3	TVAG_044950	Uncharacterized protein	Hypothetical proteins	Hydrolase		0.0022	0	
Sens	A2E414	TVAG_074970	Clan SC, family S33, methylesterase-	Peptidases	Peptidases		0.0016	0	

			like serine peptidase						
Sens	A2F507	TVAG_029150	Clan CA, family C19, ubiquitin hydrolase-like cysteine peptidase	Peptidases	Peptidases		0.0002	0	
Sens	A2DKZ3	TVAG_146890	Serine/threonine-protein phosphatase (EC 3.1.3.16)	Phosphatase	Hydrolase		0	0	
Sens	A2E6A2	TVAG_458970	Translation initiation factor SUI1 family protein[U]	Ribosomal and Associated Proteins	Ribosomal and Associated Proteins		0.0325	0.0001	
Sens	A2EC78	TVAG_414060	Glucose-6-phosphate 1-dehydrogenase (EC 1.1.1.49)[U]	Sugar Metabolism	Sugar Metabolism		0.0295	0.0291	
Sens	A2E7M9	TVAG_344080	AP-1 complex subunit gamma	Vesicle mediated transport	Other		0.0012	0.0000	
Sens	A2E2S0	TVAG_212800	Clan MG, familly M24, aminopeptidase P-like metallopeptidase	Peptidases	Peptidases		0.0020	0.0001	
Sens	A2E347	TVAG_405290	Dentin sialophosphoprotein, putative	Hypothetical proteins	Unknown		0.0000	0.0000	
Sens	A2ERT0	TVAG_227780	Uncharacterized protein	Hypothetical proteins	Unknown		0.0000	0.0000	
Sens	A2FDI8	TVAG_315190	CAMK family protein kinase	Kinase	Other		0.0008	0.0000	

Table 2-1. Analysis of putative protein targets identified by Mz-alkyne. Displayed in the table are the 61 unique protein groups identified as putative targets by our selection criteria of two-fold increase in click over mock at p-value < 0.5. In light blue background are the 22 proteins found to be enriched only in B7268-Res strain, while the 9 proteins on green background are the proteins identified in both Res and Sens strains. And the 30 proteins on yellow background are proteins enriched significantly in only the Sens strain. Annotation of protein names are primarily from TrichDB[23], with some annotation coming from UniProt[20] and OrthoMCL[48] databases, as indicated. Functional group was assigned based on gene ontology classifications from UniProt[20] and QuickGO[25]. Unifying functional group label was assigned to help functionally categorize Mz-alkyne adducted proteins (Fig. 2-3A). As the hydrogenosome is canonically important in metronidazole activation, evaluating how many target proteins are hydrogenosomal is important in gleaning potential differences in drug activation in different strains. Of the 61 identified proteins, 14 were found in a previously published proteome[22] of the organelle while an additional protein, thioredoxin reductase, marked with an asterisk (*) was identified to dually localize to the cytoplasm and hydrogenosome[21]. To determine if more of the adducted proteins were likely hydrogenosomal proteins that were not identified previously, we

obtained the predicted hydrogenosomal scores from a previous machine learning study of hydrogenosomal proteins[28]. Selecting a predictive score of ≥ 0.7000, six additional proteins predicted to be hydrogenosomal, bringing the potential tally to 21 of 61 proteins, 34%, up from 24.5%.

[a] MOT+ & MOT- scores from: Burstein D, Gould SB, Zimorski V, et al. A machine learning approach to identify hydrogenosomal proteins in trichomonas vaginalis. *Eukaryot Cell*. 2012;11(2):217-228. doi:10.1128/EC.05225-11

[b] Prediction of hydrogenosomal localization from MOT+ & MOT- ≥ 0.7000

[U] Putative identities from UniProt database: D506-D515. UniProt: a worldwide hub of protein knowledge The UniProt Consortium. *Nucleic Acids Res*. 2019;47. doi:10.1093/nar/gky1049

[O] Putative identities from OrthoMCL database: Fischer S, Brunk BP, Chen F, et al. Using OrthoMCL to Assign Proteins to OrthoMCL-DB Groups or to Cluster Proteomes Into New Ortholog Groups. In: *Current Protocols in Bioinformatics*. Vol 35. Hoboken, NJ, USA: John Wiley & Sons, Inc.; 2011:6.12.1-6.12.19. doi:10.1002/0471250953.bi0612s35

* Mentel M, Zimorski V, Haferkamp P, Martin W, Henze K. Protein import into hydrogenosomes of Trichomonas vaginalis involves both N-terminal and internal targeting signals: A case study of thioredoxin reductases. *Eukaryot Cell*. 2008;7(10):1750-1757. doi:10.1128/EC.00206-08

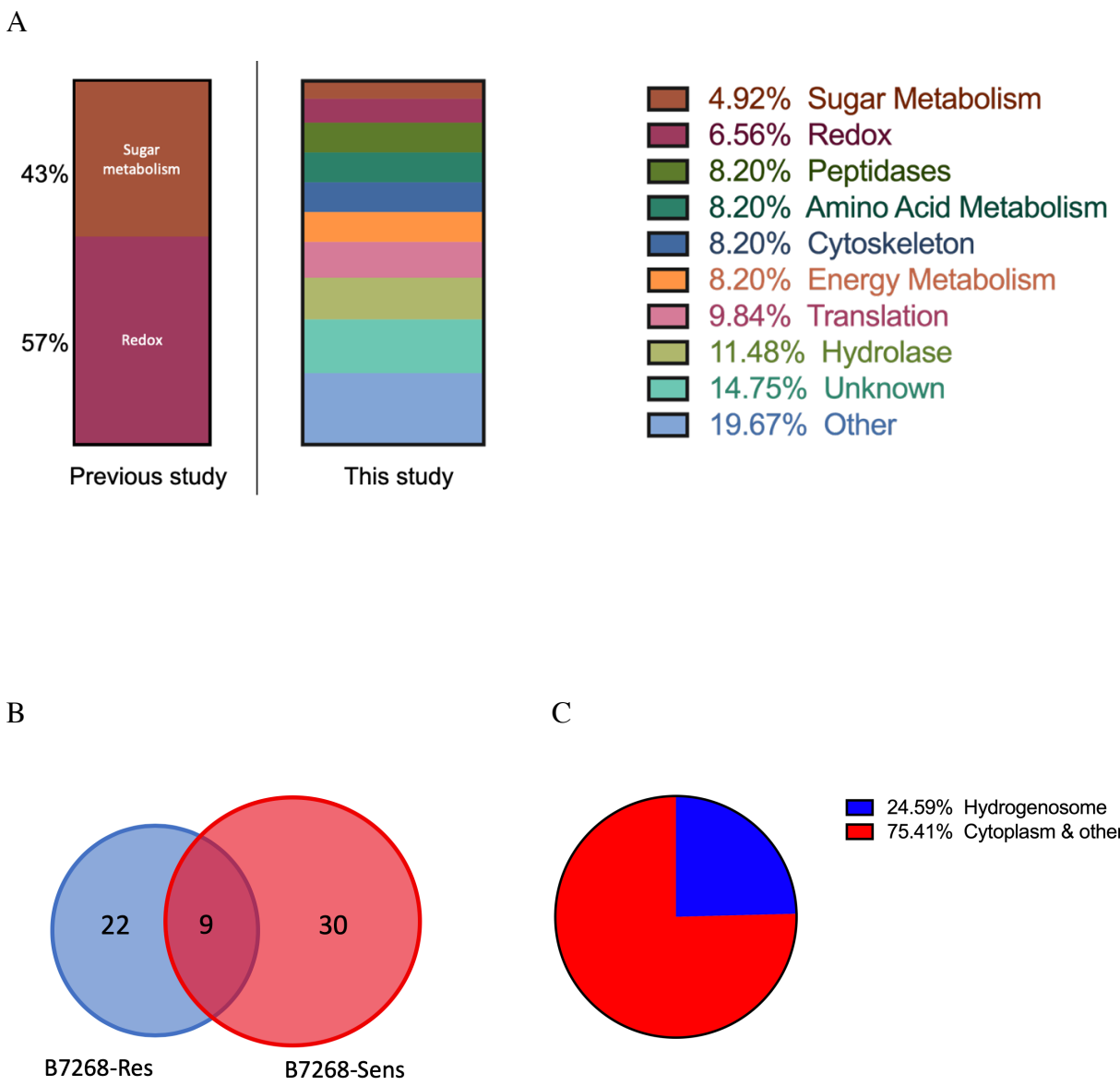

Figure 2-3. Mz targets in Mz-sensitive & -resistant parasites. (A) Broad functional categories of all 61 proteins are represented. Only seven proteins were identified in a previous study[6], with sugar metabolism and redox being the only represented functional category. In contrast, proteins identified in this study belong to more functional categories. 34% of all proteins are represented in the "other" and "unknown" functional grouping. (B) More proteins were identified in B7268-Sens than in B7268-Res. 9 identified proteins are shared between both strains. (C) Most proteins identified are predicted to be cytoplasmic. A quarter of all targets are hydrogenosomal proteins. Of the 12 classified as hydrogenosomal proteins, 11 were previously identified in a published hydrogenosomal proteome, and one, a thioredoxin reductase ortholog, was published in a separate report.

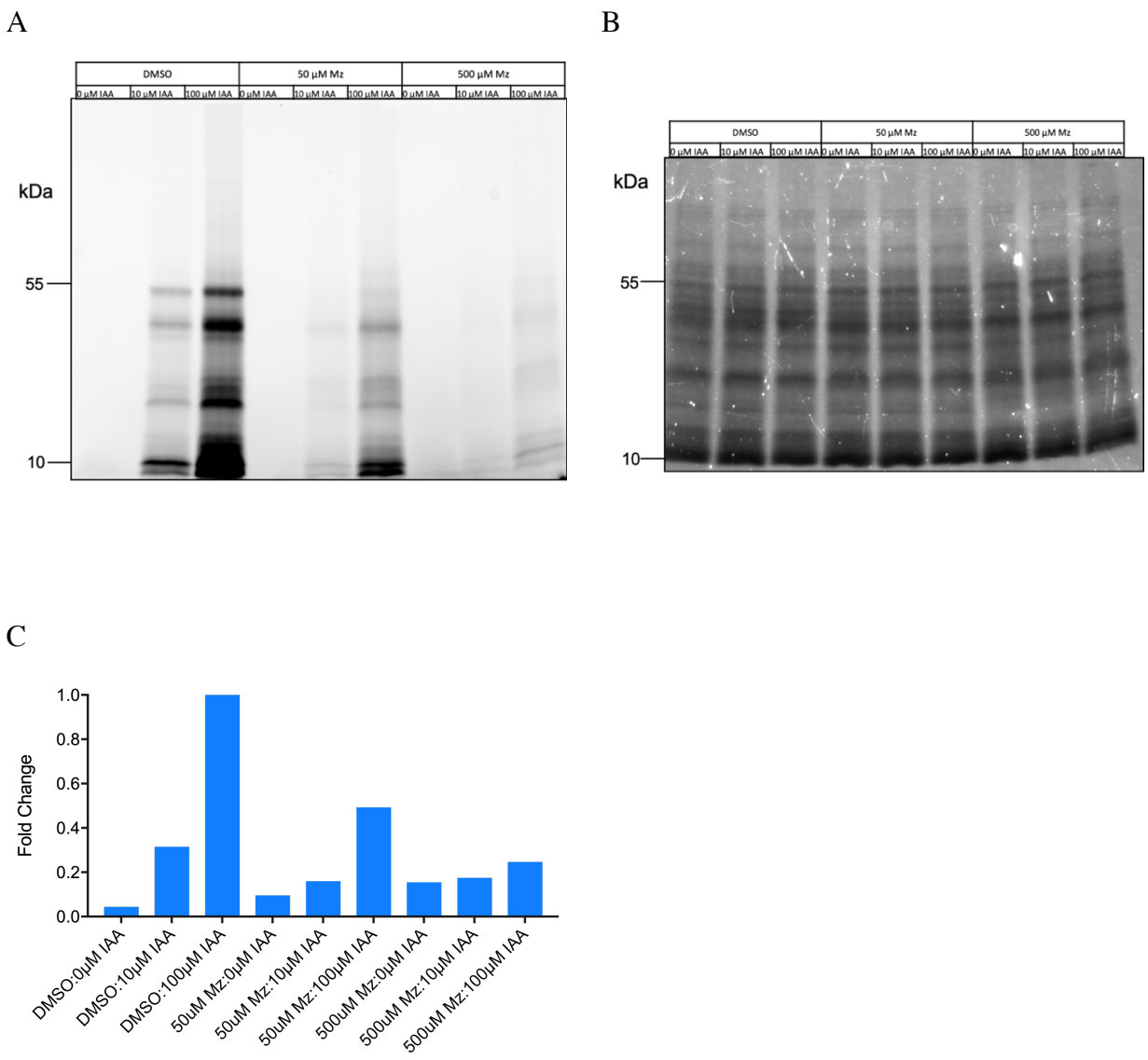

Figure 2-4. Increasing Mz concentration increasingly decreases IAA binding to cysteine residues. (A) Using activity-based protein profiling (ABPP) to evaluate if Mz treatment of parasites decreases the labeling efficiency of IAA, which labels free cysteines. Parasites are treated with DMSO, 50 μM Mz, or 500 μM Mz, and lysates prepared. Equal lysates are labeled with IAA as indicated, followed by CuAAC click to rhodamine-azide, and SDS-PAGE. As observed, on in-gel imaging, 50 μM Mz decreased IAA labeling two-fold and 500 μM Mz further decreased IAA labeling. Decreased labeling suggests that Mz reduces free cysteines, likely through binding to them. (B) There is even loading of protein samples, as observed on Coomassie staining, indicating that the observation of decreased IAA labeling in Mz-treated lysates is not due to protein loading differences. (C) Lane intensities were quantified with ImageJ and plotted relative to maximal IAA labeling, DMSO:100 μM IAA. Labels = Mz treatment:IAA concentration.

A

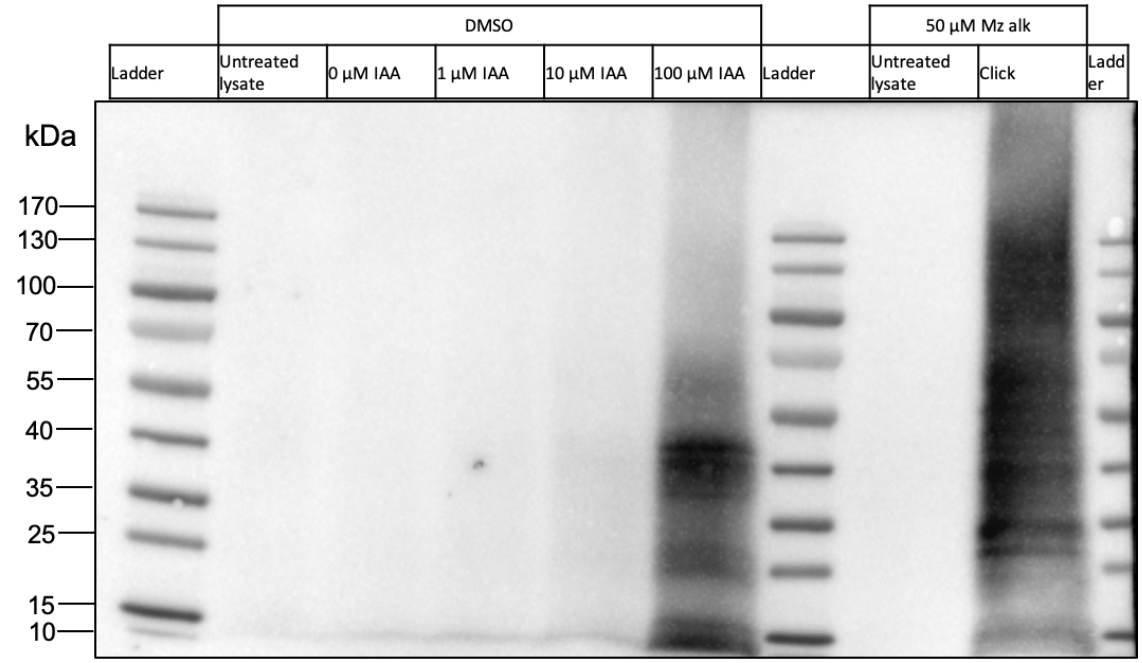

B

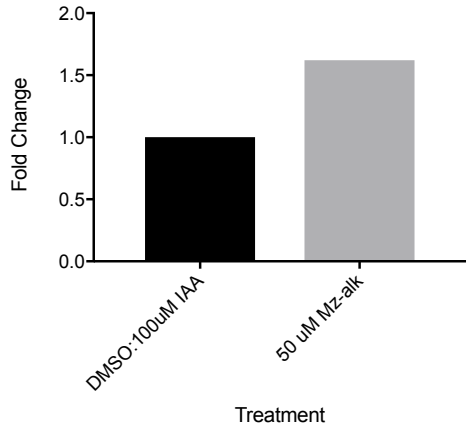

Figure 2-5. Mz-alkyne efficiently labels cysteine residues and allows for identification for drug-adduction sites. (A) 50 μM Mz-alkyne – treated lysate was CuAAC clicked to biotin-azide and compared to lysates from DMSO-treated parasites that were subsequently treated with different concentrations of IAA before CuAAC click to biotin-azide. 20 μg of each reaction was resolved by SDS-PAGE and streptavidin blotting was used to detect CuAAC biotin coupling. Compared to 100 μM IAA labeling of DMSO lysate, 50 μM Mz-alkyne labeled lysates are 1.6x more intense, as seen in (B).

UniProt	Gene names	Protein names[U]	Predicted Functional Group[U]	Length	Peptides identified (# correspond to first and last AA in peptide)	Residue
A2EC25	TVAG_137920	Profilin	Actin binding	123	92 – VVVISV**C**GGGKPQIEAKNQVFNVAK – 116	Cys98
A2DC34	TVAG_457100	Uncharacterized protein	Centrosome-associated	1051	878 – QLEIPITNFTSQKIVVDVE**C**LDGKH – 902	Cys897
A2DG76	TVAG_163990	Beige/BEACH domain containing protein	Unknown	1219	1020 – LVVCGSD**C**FIYLWNSMTS – 1037	Cys1027
A2FQA9	TVAG_186690	Dihydroorotate dehydrogenase family protein	Oxidoreductase	268	209 – QTKPPKVIEDNCVGCSQCELSC**C**YDAIKVVNAVAKVTPEKCFK – 251	Cys231
A2E6I9	TVAG_487960	AGC family protein kinase	Kinase	393	1 – MDDEEIT**C**IPIGNYILRQRIGEGAFSSVW – 29	Cys8
A2EWS6	TVAG_169080	Ankyrin repeat protein, putative	Unknown	745	286 – SAQMNVLHIASYYGNTDV**C**KIILNSSVDYHPLINAKGLYKQTPLHFASR – 334	Cys304
A2DUC4	TVAG_262120	ANK_REP_REGION domain-containing protein	Unknown	700	277 – GIITKQSFPSCDIYQYIIEKSYSKMALL**C**FKYFPDLEFTND – 317	Cys305
A2EPM0	TVAG_130970	WD_REPEATS_REGION domain-containing protein	Microtubule severing	550	270 – DL**C**VAQNEITIASTEK – 285	Cys272

Table 2-2. Peptides containing identified cysteine residues. To detect modified amino acid residues on Mz target proteins, lysates from Mz-alkyne were CuAAC clicked to biotin-azide and following established protocol[36], peptides were run on Thermo QExactive Hybrid Orbitrap Mass Spectrometer. Peptide search was performed with IP2 ProLuCID and searching for differential modification of 400.19978 Da on cysteine residues, here highlighted in red. Eight peptides were identified and correspond to eight previously unidentified target proteins. Adducted residues and peptides are shown. Protein names and predicted functional grouping are based on UniProt[20]. Of the eight proteins identified, only one protein highlighted in green is predicted to have hydrogenosomal localization, having MOT+ score of 0.9998 and MOT- score of 0.8886. The other seven proteins are predicted to be cytosolic proteins.

[U] Protein names and Predicted Functional Group from UniProt database: D506-D515. UniProt: a worldwide hub of protein knowledge The UniProt Consortium. *Nucleic Acids Res*. 2019;47. doi:10.1093/nar/gky1049

Supplementary figure and tables

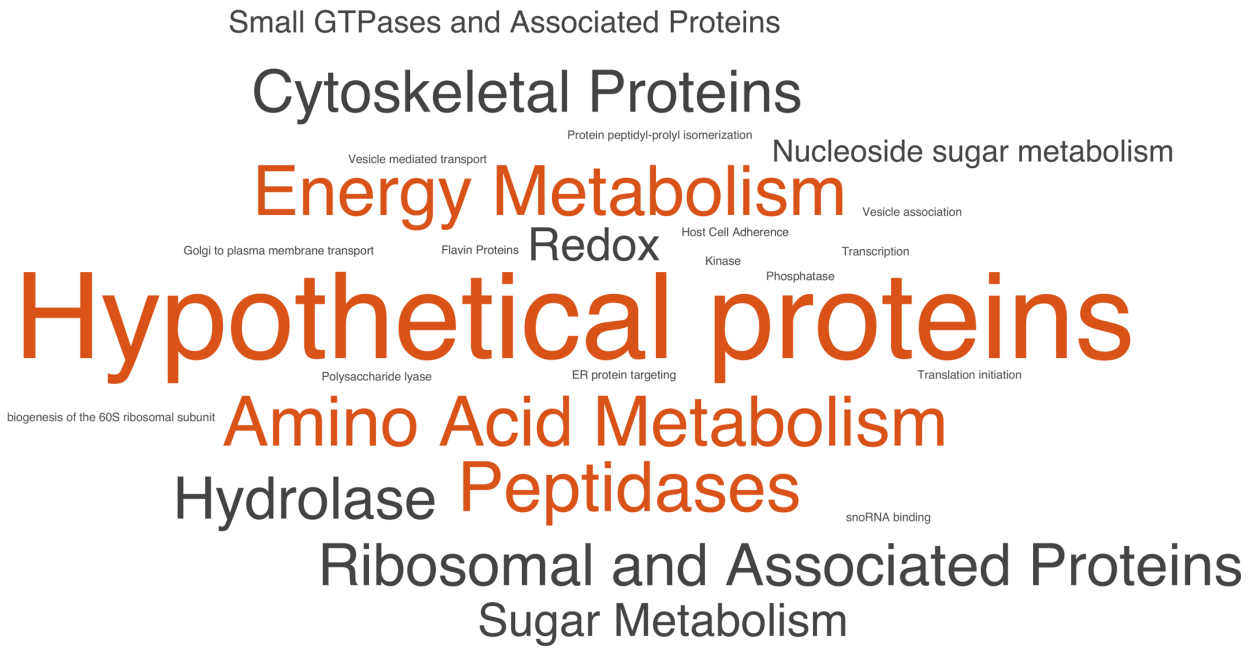

Supplementary Figure 2-1. Many cellular processes are affected by Mz-alkyne in both strains. Word cloud visualization of the functional group classification of all 61 target proteins shows that more proteins fall in the hypothetical proteins category than any other. Moreover, this suggests that trichomonocidal effect of metronidazole is likely secondary to failure of multiple pathways.

GENE PRODUCT ID	SYMBOL	GENE_PRODUCT_NAME	QUALIFIER	GO TERM	GO NAME
A2D7I8	TVAG_120430	4-alpha-glucanotransferase family protein	involved_in	GO:0005975	carbohydrate metabolic process
A2D7I8	TVAG_120430	4-alpha-glucanotransferase family protein	enables	GO:2001070	starch binding
A2D7I8	TVAG_120430	4-alpha-glucanotransferase family protein	enables	GO:0004134	4-alpha-glucanotransferase activity
A2D7I8	TVAG_120430	4-alpha-glucanotransferase family protein	enables	GO:0030246	carbohydrate binding
A2D7I8	TVAG_120430	4-alpha-glucanotransferase family protein	enables	GO:0016740	transferase activity
A2D7I8	TVAG_120430	4-alpha-glucanotransferase family protein	involved_in	GO:0005977	glycogen metabolic process
A2D900	TVAG_182620	TvhydB protein, putative	enables	GO:0051539	4 iron, 4 sulfur cluster binding
A2D900	TVAG_182620	TvhydB protein, putative	enables	GO:0005506	iron ion binding
A2D900	TVAG_182620	TvhydB protein, putative	involved_in	GO:0055114	oxidation-reduction process
A2D900	TVAG_182620	TvhydB protein, putative	enables	GO:0008901	ferredoxin hydrogenase activity
A2D900	TVAG_182620	TvhydB protein, putative	enables	GO:0051536	iron-sulfur cluster binding
A2D9B6	TVAG_183790	AP65-3 adhesin	enables	GO:0004473	malate dehydrogenase (decarboxylating) (NADP+) activity
A2D9B6	TVAG_183790	AP65-3 adhesin	enables	GO:0004470	malic enzyme activity
A2D9B6	TVAG_183790	AP65-3 adhesin	involved_in	GO:0006108	malate metabolic process
A2D9B6	TVAG_183790	AP65-3 adhesin	involved_in	GO:0006090	pyruvate metabolic process
A2D9B6	TVAG_183790	AP65-3 adhesin	enables	GO:0004470	malic enzyme activity
A2D9B6	TVAG_183790	AP65-3 adhesin	involved_in	GO:0055114	oxidation-reduction process
A2D9B6	TVAG_183790	AP65-3 adhesin	enables	GO:0004471	malate dehydrogenase (decarboxylating) (NAD+) activity
A2D9B6	TVAG_183790	AP65-3 adhesin	enables	GO:0051287	NAD binding
A2D9B6	TVAG_183790	AP65-3 adhesin	enables	GO:0046872	metal ion binding
A2DAX3	TVAG_377820	4Fe-4S binding domain containing protein	enables	GO:0009055	electron transfer activity
A2DAX3	TVAG_377820	4Fe-4S binding domain containing protein	enables	GO:0051536	iron-sulfur cluster binding
A2DAX3	TVAG_377820	4Fe-4S binding domain containing protein	involved_in	GO:0022900	electron transport chain
A2DCT5	TVAG_237350	KOG2701 domain-containing protein	involved_in	GO:0006893	Golgi to plasma membrane transport
A2DGQ3	TVAG_110520	40S ribosomal protein S27	involved_in	GO:0000028	ribosomal small subunit assembly
A2DGQ3	TVAG_110520	40S ribosomal protein S27	enables	GO:0003723	RNA binding
A2DGQ3	TVAG_110520	40S ribosomal protein S27	enables	GO:0003735	structural constituent of ribosome
A2DGQ3	TVAG_110520	40S ribosomal protein S27	part_of	GO:0022627	cytosolic small ribosomal subunit
A2DGQ3	TVAG_110520	40S ribosomal protein S27	part_of	GO:0005840	ribosome

A2DGQ3	TVAG_110520	40S ribosomal protein S27	involved_in	GO:0006412	translation
A2DGQ3	TVAG_110520	40S ribosomal protein S27	enables	GO:0003735	structural constituent of ribosome
A2DGQ3	TVAG_110520	40S ribosomal protein S27	part_of	GO:0005840	ribosome
A2DGQ3	TVAG_110520	40S ribosomal protein S27	enables	GO:0046872	metal ion binding
A2DKI5	TVAG_190580	Methionine aminopeptidase	enables	GO:0004177	aminopeptidase activity
A2DKI5	TVAG_190580	Methionine aminopeptidase	involved_in	GO:0006508	proteolysis
A2DKI5	TVAG_190580	Methionine aminopeptidase	enables	GO:0008235	metalloexopeptidase activity
A2DKI5	TVAG_190580	Methionine aminopeptidase	enables	GO:0004177	aminopeptidase activity
A2DKI5	TVAG_190580	Methionine aminopeptidase	enables	GO:0046872	metal ion binding
A2DKI5	TVAG_190580	Methionine aminopeptidase	enables	GO:0016787	hydrolase activity
A2DKI5	TVAG_190580	Methionine aminopeptidase	enables	GO:0008233	peptidase activity
A2DKI5	TVAG_190580	Methionine aminopeptidase	involved_in	GO:0006508	proteolysis
A2DKI5	TVAG_190580	Methionine aminopeptidase	part_of	GO:0005737	cytoplasm
A2DKI5	TVAG_190580	Methionine aminopeptidase	part_of	GO:0005737	cytoplasm
A2DKZ3	TVAG_146890	Serine/threonine-protein phosphatase	enables	GO:0004722	protein serine/threonine phosphatase activity
A2DKZ3	TVAG_146890	Serine/threonine-protein phosphatase	part_of	GO:0005634	nucleus
A2DKZ3	TVAG_146890	Serine/threonine-protein phosphatase	part_of	GO:0005737	cytoplasm
A2DKZ3	TVAG_146890	Serine/threonine-protein phosphatase	enables	GO:0016787	hydrolase activity
A2DKZ3	TVAG_146890	Serine/threonine-protein phosphatase	enables	GO:0016787	hydrolase activity
A2DKZ3	TVAG_146890	Serine/threonine-protein phosphatase	enables	GO:0004721	phosphoprotein phosphatase activity
A2DKZ3	TVAG_146890	Serine/threonine-protein phosphatase	enables	GO:0046872	metal ion binding
A2DKZ3	TVAG_146890	Serine/threonine-protein phosphatase	enables	GO:0004721	phosphoprotein phosphatase activity
A2DKZ3	TVAG_146890	Serine/threonine-protein phosphatase	involved_in	GO:0006470	protein dephosphorylation
A2DKZ3	TVAG_146890	Serine/threonine-protein phosphatase	involved_in	GO:0006470	protein dephosphorylation
A2DKZ3	TVAG_146890	Serine/threonine-protein phosphatase	involved_in	GO:0006470	protein dephosphorylation
A2DLA9	TVAG_267590	WASH_WAHD domain-containing protein	involved_in	GO:0034314	Arp2/3 complex-mediated actin nucleation
A2DLA9	TVAG_267590	WASH_WAHD domain-containing protein	part_of	GO:0071203	WASH complex
A2DLA9	TVAG_267590	WASH_WAHD domain-containing protein	part_of	GO:0005769	early endosome

A2DLA9	TVAG_267590	WASH_WAHD domain-containing protein	enables	GO:0043014	alpha-tubulin binding
A2DU34	TVAG_277930	Uncharacterized protein	part_of	GO:0016020	membrane
A2DU34	TVAG_277930	Uncharacterized protein	part_of	GO:0016021	integral component of membrane
A2DY82	TVAG_461080	Nucleolar GTP-binding protein 1	enables	GO:0005525	GTP binding
A2DY82	TVAG_461080	Nucleolar GTP-binding protein 1	part_of	GO:0005730	nucleolus
A2DY82	TVAG_461080	Nucleolar GTP-binding protein 1	involved_in	GO:0042254	ribosome biogenesis
A2DY82	TVAG_461080	Nucleolar GTP-binding protein 1	part_of	GO:0005634	nucleus
A2DY82	TVAG_461080	Nucleolar GTP-binding protein 1	part_of	GO:0005730	nucleolus
A2E134	TVAG_388070	Zinc finger, C2H2 type family protein	part_of	GO:0030687	preribosome, large subunit precursor
A2E134	TVAG_388070	Zinc finger, C2H2 type family protein	involved_in	GO:0042273	ribosomal large subunit biogenesis
A2E222	TVAG_463690	Haloacid dehalogenase-like hydrolase family protein	enables	GO:0016791	phosphatase activity
A2E222	TVAG_463690	Haloacid dehalogenase-like hydrolase family protein	enables	GO:0016787	hydrolase activity
A2E222	TVAG_463690	Haloacid dehalogenase-like hydrolase family protein	enables	GO:0016787	hydrolase activity
A2E222	TVAG_463690	Haloacid dehalogenase-like hydrolase family protein	involved_in	GO:0016311	dephosphorylation
A2E2S0	TVAG_212800	Clan MG, familly M24, aminopeptidase P-like metallopeptidase	enables	GO:0042393	histone binding
A2E2S0	TVAG_212800	Clan MG, familly M24, aminopeptidase P-like metallopeptidase	part_of	GO:0035101	FACT complex
A2E2S0	TVAG_212800	Clan MG, familly M24, aminopeptidase P-like metallopeptidase	involved_in	GO:0032968	positive regulation of transcription elongation from RNA polymerase II promoter
A2E2S0	TVAG_212800	Clan MG, familly M24, aminopeptidase P-like metallopeptidase	involved_in	GO:0034724	DNA replication-independent nucleosome organization
A2E2S0	TVAG_212800	Clan MG, familly M24, aminopeptidase P-like metallopeptidase	enables	GO:0031491	nucleosome binding
A2E2S0	TVAG_212800	Clan MG, familly M24, aminopeptidase P-like metallopeptidase	involved_in	GO:0006368	transcription elongation from RNA polymerase II promoter
A2E2S0	TVAG_212800	Clan MG, familly M24, aminopeptidase P-like metallopeptidase	part_of	GO:0035101	FACT complex
A2E2S0	TVAG_212800	Clan MG, familly M24, aminopeptidase P-like metallopeptidase	enables	GO:0004177	aminopeptidase activity

A2E2S0	TVAG_212800	Clan MG, familly M24, aminopeptidase P-like metallopeptidase	involved_in	GO:0006281	DNA repair
A2E2S0	TVAG_212800	Clan MG, familly M24, aminopeptidase P-like metallopeptidase	part_of	GO:0035101	FACT complex
A2E2S0	TVAG_212800	Clan MG, familly M24, aminopeptidase P-like metallopeptidase	involved_in	GO:0006508	proteolysis
A2E347	TVAG_405290	Dentin sialophosphoprotein, putative	part_of	GO:0016021	integral component of membrane
A2E347	TVAG_405290	Dentin sialophosphoprotein, putative	part_of	GO:0016020	membrane
A2E3S6	TVAG_117360	Haloacid dehalogenase-like hydrolase family protein	enables	GO:0016791	phosphatase activity
A2E3S6	TVAG_117360	Haloacid dehalogenase-like hydrolase family protein	enables	GO:0016787	hydrolase activity
A2E3S6	TVAG_117360	Haloacid dehalogenase-like hydrolase family protein	enables	GO:0016787	hydrolase activity
A2E3S6	TVAG_117360	Haloacid dehalogenase-like hydrolase family protein	involved_in	GO:0016311	dephosphorylation
A2E3T7	TVAG_117470	Thioredoxin domain-containing protein	part_of	GO:0005783	endoplasmic reticulum
A2E3T7	TVAG_117470	Thioredoxin domain-containing protein	involved_in	GO:0045454	cell redox homeostasis
A2E414	TVAG_074970	Hydrolase_4 domain-containing protein	enables	GO:0016298	lipase activity
A2E414	TVAG_074970	Hydrolase_4 domain-containing protein	part_of	GO:0016020	membrane
A2E4D0	TVAG_128790	Ribos_L4_asso_C domain-containing protein	part_of	GO:0022625	cytosolic large ribosomal subunit
A2E4D0	TVAG_128790	Ribos_L4_asso_C domain-containing protein	enables	GO:0003735	structural constituent of ribosome
A2E4D0	TVAG_128790	Ribos_L4_asso_C domain-containing protein	enables	GO:0003723	RNA binding
A2E4D0	TVAG_128790	Ribos_L4_asso_C domain-containing protein	part_of	GO:0005840	ribosome
A2E4D0	TVAG_128790	Ribos_L4_asso_C domain-containing protein	involved_in	GO:0006412	translation
A2E4D0	TVAG_128790	Ribos_L4_asso_C domain-containing protein	enables	GO:0003735	structural constituent of ribosome
A2E4D0	TVAG_128790	Ribos_L4_asso_C domain-containing protein	part_of	GO:0005840	ribosome
A2E5L3	TVAG_039020	Signal recognition particle subunit SRP72	contributes_to	GO:0043022	ribosome binding
A2E5L3	TVAG_039020	Signal recognition particle subunit SRP72	enables	GO:0008312	7S RNA binding
A2E5L3	TVAG_039020	Signal recognition particle subunit SRP72	involved_in	GO:0006614	SRP-dependent cotranslational protein targeting to membrane

A2E5L3	TVAG_039020	Signal recognition particle subunit SRP72	part_of	GO:0005786	signal recognition particle, endoplasmic reticulum targeting
A2E5L3	TVAG_039020	Signal recognition particle subunit SRP72	involved_in	GO:0006614	SRP-dependent cotranslational protein targeting to membrane
A2E5L3	TVAG_039020	Signal recognition particle subunit SRP72	enables	GO:0008312	7S RNA binding
A2E5L3	TVAG_039020	Signal recognition particle subunit SRP72	part_of	GO:0048500	signal recognition particle
A2E5L3	TVAG_039020	Signal recognition particle subunit SRP72	part_of	GO:0005786	signal recognition particle, endoplasmic reticulum targeting
A2E5L3	TVAG_039020	Signal recognition particle subunit SRP72	part_of	GO:0005737	cytoplasm
A2E5L3	TVAG_039020	Signal recognition particle subunit SRP72	part_of	GO:0005737	cytoplasm
A2E6A2	TVAG_458970	SUI1 domain-containing protein	involved_in	GO:0001731	formation of translation preinitiation complex
A2E6A2	TVAG_458970	SUI1 domain-containing protein	involved_in	GO:0002188	translation reinitiation
A2E6A2	TVAG_458970	SUI1 domain-containing protein	enables	GO:0003729	mRNA binding
A2E6A2	TVAG_458970	SUI1 domain-containing protein	enables	GO:0003743	translation initiation factor activity
A2E6A2	TVAG_458970	SUI1 domain-containing protein	involved_in	GO:0006413	translational initiation
A2E6A2	TVAG_458970	SUI1 domain-containing protein	enables	GO:0003743	translation initiation factor activity
A2E6A2	TVAG_458970	SUI1 domain-containing protein	involved_in	GO:0006413	translational initiation
A2E6B9	TVAG_459140	Nop domain-containing protein	part_of	GO:0031428	box C/D snoRNP complex
A2E6B9	TVAG_459140	Nop domain-containing protein	part_of	GO:0032040	small-subunit processome
A2E6B9	TVAG_459140	Nop domain-containing protein	enables	GO:0030515	snoRNA binding
A2E7M9	TVAG_344080	AP-1 complex subunit gamma	enables	GO:0035615	clathrin adaptor activity
A2E7M9	TVAG_344080	AP-1 complex subunit gamma	enables	GO:0140312	cargo adaptor activity
A2E7M9	TVAG_344080	AP-1 complex subunit gamma	part_of	GO:0030121	AP-1 adaptor complex
A2E7M9	TVAG_344080	AP-1 complex subunit gamma	involved_in	GO:0006898	receptor-mediated endocytosis
A2E7M9	TVAG_344080	AP-1 complex subunit gamma	involved_in	GO:0006896	Golgi to vacuole transport
A2E7M9	TVAG_344080	AP-1 complex subunit gamma	part_of	GO:0005794	Golgi apparatus
A2E7M9	TVAG_344080	AP-1 complex subunit gamma	involved_in	GO:0016192	vesicle-mediated transport
A2E7M9	TVAG_344080	AP-1 complex subunit gamma	involved_in	GO:0006886	intracellular protein transport
A2E7M9	TVAG_344080	AP-1 complex subunit gamma	part_of	GO:0030117	membrane coat
A2E7M9	TVAG_344080	AP-1 complex subunit gamma	part_of	GO:0030121	AP-1 adaptor complex

A2E7M9	TVAG_344080	AP-1 complex subunit gamma	part_of	GO:0005794	Golgi apparatus
A2E7M9	TVAG_344080	AP-1 complex subunit gamma	part_of	GO:0031410	cytoplasmic vesicle
A2E7M9	TVAG_344080	AP-1 complex subunit gamma	part_of	GO:0016020	membrane
A2E7M9	TVAG_344080	AP-1 complex subunit gamma	involved_in	GO:0015031	protein transport
A2E7M9	TVAG_344080	AP-1 complex subunit gamma	part_of	GO:0005737	cytoplasm
A2E7M9	TVAG_344080	AP-1 complex subunit gamma	involved_in	GO:0006886	intracellular protein transport
A2E8E3	TVAG_044950	Uncharacterized protein	part_of	GO:0016021	integral component of membrane
A2E8E3	TVAG_044950	Uncharacterized protein	part_of	GO:0016020	membrane
A2EC21	TVAG_137880	Peptidyl-prolyl cis-trans isomerase	part_of	GO:0005737	cytoplasm
A2EC21	TVAG_137880	Peptidyl-prolyl cis-trans isomerase	involved_in	GO:0000413	protein peptidyl-prolyl isomerization
A2EC21	TVAG_137880	Peptidyl-prolyl cis-trans isomerase	enables	GO:0003755	peptidyl-prolyl cis-trans isomerase activity
A2EC21	TVAG_137880	Peptidyl-prolyl cis-trans isomerase	involved_in	GO:0006457	protein folding
A2EC21	TVAG_137880	Peptidyl-prolyl cis-trans isomerase	enables	GO:0016018	cyclosporin A binding
A2EC21	TVAG_137880	Peptidyl-prolyl cis-trans isomerase	involved_in	GO:0000413	protein peptidyl-prolyl isomerization
A2EC21	TVAG_137880	Peptidyl-prolyl cis-trans isomerase	enables	GO:0003755	peptidyl-prolyl cis-trans isomerase activity
A2EC21	TVAG_137880	Peptidyl-prolyl cis-trans isomerase	involved_in	GO:0006457	protein folding
A2EC21	TVAG_137880	Peptidyl-prolyl cis-trans isomerase	enables	GO:0003755	peptidyl-prolyl cis-trans isomerase activity
A2EC21	TVAG_137880	Peptidyl-prolyl cis-trans isomerase	enables	GO:0016853	isomerase activity
A2EC21	TVAG_137880	Peptidyl-prolyl cis-trans isomerase	enables	GO:0003755	peptidyl-prolyl cis-trans isomerase activity
A2EC21	TVAG_137880	Peptidyl-prolyl cis-trans isomerase	enables	GO:0003755	peptidyl-prolyl cis-trans isomerase activity
A2EC78	TVAG_414060	Glucose-6-phosphate 1-dehydrogenase	involved_in	GO:0005975	carbohydrate metabolic process
A2EC78	TVAG_414060	Glucose-6-phosphate 1-dehydrogenase	involved_in	GO:0006006	glucose metabolic process
A2EC78	TVAG_414060	Glucose-6-phosphate 1-dehydrogenase	involved_in	GO:0006098	pentose-phosphate shunt
A2EC78	TVAG_414060	Glucose-6-phosphate 1-dehydrogenase	enables	GO:0017057	6-phosphogluconolactonase activity
A2EC78	TVAG_414060	Glucose-6-phosphate 1-dehydrogenase	enables	GO:0050661	NADP binding
A2EC78	TVAG_414060	Glucose-6-phosphate 1-dehydrogenase	involved_in	GO:0055114	oxidation-reduction process
A2EC78	TVAG_414060	Glucose-6-phosphate 1-dehydrogenase	enables	GO:0004345	glucose-6-phosphate dehydrogenase activity

A2EC78	TVAG_414060	Glucose-6-phosphate 1-dehydrogenase	enables	GO:0016614	oxidoreductase activity, acting on CH-OH group of donors
A2EC78	TVAG_414060	Glucose-6-phosphate 1-dehydrogenase	involved_in	GO:0005975	carbohydrate metabolic process
A2EC78	TVAG_414060	Glucose-6-phosphate 1-dehydrogenase	involved_in	GO:0055114	oxidation-reduction process
A2EC78	TVAG_414060	Glucose-6-phosphate 1-dehydrogenase	involved_in	GO:0006006	glucose metabolic process
A2EC78	TVAG_414060	Glucose-6-phosphate 1-dehydrogenase	enables	GO:0016491	oxidoreductase activity
A2EC78	TVAG_414060	Glucose-6-phosphate 1-dehydrogenase	enables	GO:0004345	glucose-6-phosphate dehydrogenase activity
A2EC78	TVAG_414060	Glucose-6-phosphate 1-dehydrogenase	involved_in	GO:0006098	pentose-phosphate shunt
A2ECT4	TVAG_276530	PALP domain-containing protein	enables	GO:0004124	cysteine synthase activity
A2ECT4	TVAG_276530	PALP domain-containing protein	enables	GO:0030170	pyridoxal phosphate binding
A2ECT4	TVAG_276530	PALP domain-containing protein	part_of	GO:0005737	cytoplasm
A2ECT4	TVAG_276530	PALP domain-containing protein	involved_in	GO:0006535	cysteine biosynthetic process from serine
A2EF89	TVAG_079570	Small GTP-binding protein, putative	involved_in	GO:0006886	intracellular protein transport
A2EF89	TVAG_079570	Small GTP-binding protein, putative	enables	GO:0003924	GTPase activity
A2EF89	TVAG_079570	Small GTP-binding protein, putative	part_of	GO:0012505	endomembrane system
A2EF89	TVAG_079570	Small GTP-binding protein, putative	enables	GO:0003924	GTPase activity
A2EF89	TVAG_079570	Small GTP-binding protein, putative	enables	GO:0005525	GTP binding
A2EGV2	TVAG_497090	Eukaryotic translation initiation factor, putative	enables	GO:0003729	mRNA binding
A2EGV2	TVAG_497090	Eukaryotic translation initiation factor, putative	part_of	GO:0005730	nucleolus
A2EGV2	TVAG_497090	Eukaryotic translation initiation factor, putative	part_of	GO:0071013	catalytic step 2 spliceosome
A2EGV2	TVAG_497090	Eukaryotic translation initiation factor, putative	enables	GO:0003723	RNA binding
A2EGV2	TVAG_497090	Eukaryotic translation initiation factor, putative	enables	GO:0003724	RNA helicase activity
A2EGV2	TVAG_497090	Eukaryotic translation initiation factor, putative	enables	GO:0003676	nucleic acid binding
A2EGV2	TVAG_497090	Eukaryotic translation initiation factor, putative	enables	GO:0005524	ATP binding
A2EGV2	TVAG_497090	Eukaryotic translation initiation factor, putative	enables	GO:0003743	translation initiation factor activity

A2EGV2	TVAG_497090	Eukaryotic translation initiation factor, putative	involved_in	GO:0006413	translational initiation
A2EIU6	TVAG_419720	Aminotran_1_2 domain-containing protein	involved_in	GO:0009058	biosynthetic process
A2EIU6	TVAG_419720	Aminotran_1_2 domain-containing protein	enables	GO:0030170	pyridoxal phosphate binding
A2EIU6	TVAG_419720	Aminotran_1_2 domain-containing protein	enables	GO:0003824	catalytic activity
A2EIU6	TVAG_419720	Aminotran_1_2 domain-containing protein	enables	GO:0016740	transferase activity
A2EIU6	TVAG_419720	Aminotran_1_2 domain-containing protein	enables	GO:0008483	transaminase activity
A2ER03	TVAG_016650	RPOLD domain-containing protein	part_of	GO:0005736	RNA polymerase I complex
A2ER03	TVAG_016650	RPOLD domain-containing protein	contributes_to	GO:0001054	RNA polymerase I activity
A2ER03	TVAG_016650	RPOLD domain-containing protein	part_of	GO:0005666	RNA polymerase III complex
A2ER03	TVAG_016650	RPOLD domain-containing protein	contributes_to	GO:0003899	DNA-directed 5'-3' RNA polymerase activity
A2ER03	TVAG_016650	RPOLD domain-containing protein	contributes_to	GO:0001056	RNA polymerase III activity
A2ER03	TVAG_016650	RPOLD domain-containing protein	enables	GO:0003899	DNA-directed 5'-3' RNA polymerase activity
A2ER03	TVAG_016650	RPOLD domain-containing protein	involved_in	GO:0006351	transcription, DNA-templated
A2ER03	TVAG_016650	RPOLD domain-containing protein	enables	GO:0046983	protein dimerization activity
A2ER03	TVAG_016650	RPOLD domain-containing protein	involved_in	GO:0006383	transcription by RNA polymerase III
A2ER03	TVAG_016650	RPOLD domain-containing protein	involved_in	GO:0006360	transcription by RNA polymerase I
A2ESH7	TVAG_417190	Haloacid dehalogenase-like hydrolase family protein	enables	GO:0016791	phosphatase activity
A2ESH7	TVAG_417190	Haloacid dehalogenase-like hydrolase family protein	enables	GO:0016787	hydrolase activity
A2ESH7	TVAG_417190	Haloacid dehalogenase-like hydrolase family protein	enables	GO:0016787	hydrolase activity
A2ESH7	TVAG_417190	Haloacid dehalogenase-like hydrolase family protein	involved_in	GO:0016311	dephosphorylation
A2EVS2	TVAG_299450	AA_TRNA_LIGASE_II_ALA domain-containing protein	enables	GO:0002161	aminoacyl-tRNA editing activity
A2EVS2	TVAG_299450	AA_TRNA_LIGASE_II_ALA domain-containing protein	enables	GO:0004813	alanine-tRNA ligase activity
A2EVS2	TVAG_299450	AA_TRNA_LIGASE_II_ALA domain-containing protein	enables	GO:0016597	amino acid binding
A2EVS2	TVAG_299450	AA_TRNA_LIGASE_II_ALA domain-containing protein	enables	GO:0005524	ATP binding

A2EVS2	TVAG_299450	AA_TRNA_LIGASE_II_ALA domain-containing protein	involved_in	GO:0006400	tRNA modification
A2EVS2	TVAG_299450	AA_TRNA_LIGASE_II_ALA domain-containing protein	involved_in	GO:0006419	alanyl-tRNA aminoacylation
A2EVS2	TVAG_299450	AA_TRNA_LIGASE_II_ALA domain-containing protein	enables	GO:0004812	aminoacyl-tRNA ligase activity
A2EVS2	TVAG_299450	AA_TRNA_LIGASE_II_ALA domain-containing protein	enables	GO:0004813	alanine-tRNA ligase activity
A2EVS2	TVAG_299450	AA_TRNA_LIGASE_II_ALA domain-containing protein	involved_in	GO:0043039	tRNA aminoacylation
A2EVS2	TVAG_299450	AA_TRNA_LIGASE_II_ALA domain-containing protein	enables	GO:0000166	nucleotide binding
A2EVS2	TVAG_299450	AA_TRNA_LIGASE_II_ALA domain-containing protein	enables	GO:0003676	nucleic acid binding
A2EVS2	TVAG_299450	AA_TRNA_LIGASE_II_ALA domain-containing protein	enables	GO:0005524	ATP binding
A2EVS2	TVAG_299450	AA_TRNA_LIGASE_II_ALA domain-containing protein	part_of	GO:0005737	cytoplasm
A2EVS2	TVAG_299450	AA_TRNA_LIGASE_II_ALA domain-containing protein	involved_in	GO:0006419	alanyl-tRNA aminoacylation
A2EVS2	TVAG_299450	AA_TRNA_LIGASE_II_ALA domain-containing protein	enables	GO:0004812	aminoacyl-tRNA ligase activity
A2EVS2	TVAG_299450	AA_TRNA_LIGASE_II_ALA domain-containing protein	involved_in	GO:0106074	aminoacyl-tRNA metabolism involved in translational fidelity
A2EVX8	TVAG_049830	Pyridine nucleotide-disulphide oxidoreductase family protein	enables	GO:0005506	iron ion binding
A2EVX8	TVAG_049830	Pyridine nucleotide-disulphide oxidoreductase family protein	enables	GO:0010181	FMN binding
A2EVX8	TVAG_049830	Pyridine nucleotide-disulphide oxidoreductase family protein	involved_in	GO:0055114	oxidation-reduction process
A2EVX8	TVAG_049830	Pyridine nucleotide-disulphide oxidoreductase family protein	enables	GO:0016491	oxidoreductase activity
A2EXK6	TVAG_260830	Uncharacterized protein	involved_in	GO:0006511	ubiquitin-dependent protein catabolic process
A2EXK6	TVAG_260830	Uncharacterized protein	involved_in	GO:0016567	protein ubiquitination
A2EXK6	TVAG_260830	Uncharacterized protein	involved_in	GO:0042981	regulation of apoptotic process
A2EZW3	TVAG_273370	Haloacid dehalogenase-like hydrolase family protein	enables	GO:0016791	phosphatase activity
A2EZW3	TVAG_273370	Haloacid dehalogenase-like hydrolase family protein	enables	GO:0016787	hydrolase activity
A2EZW3	TVAG_273370	Haloacid dehalogenase-like hydrolase family protein	enables	GO:0016787	hydrolase activity
A2EZW3	TVAG_273370	Haloacid dehalogenase-like hydrolase family protein	involved_in	GO:0016311	dephosphorylation
A2EZW4	TVAG_273380	6-phosphogluconate dehydrogenase, decarboxylating	part_of	GO:0005829	cytosol

A2EZW4	TVAG_273380	6-phosphogluconate dehydrogenase, decarboxylating	involved_in	GO:0009051	pentose-phosphate shunt, oxidative branch
A2EZW4	TVAG_273380	6-phosphogluconate dehydrogenase, decarboxylating	involved_in	GO:0046177	D-gluconate catabolic process
A2EZW4	TVAG_273380	6-phosphogluconate dehydrogenase, decarboxylating	enables	GO:0050661	NADP binding
A2EZW4	TVAG_273380	6-phosphogluconate dehydrogenase, decarboxylating	enables	GO:0004616	phosphogluconate dehydrogenase (decarboxylating) activity
A2EZW4	TVAG_273380	6-phosphogluconate dehydrogenase, decarboxylating	involved_in	GO:0006098	pentose-phosphate shunt
A2EZW4	TVAG_273380	6-phosphogluconate dehydrogenase, decarboxylating	enables	GO:0050661	NADP binding
A2EZW4	TVAG_273380	6-phosphogluconate dehydrogenase, decarboxylating	involved_in	GO:0055114	oxidation-reduction process
A2EZW4	TVAG_273380	6-phosphogluconate dehydrogenase, decarboxylating	enables	GO:0004616	phosphogluconate dehydrogenase (decarboxylating) activity
A2EZW4	TVAG_273380	6-phosphogluconate dehydrogenase, decarboxylating	enables	GO:0016491	oxidoreductase activity
A2EZW4	TVAG_273380	6-phosphogluconate dehydrogenase, decarboxylating	involved_in	GO:0055114	oxidation-reduction process
A2EZW4	TVAG_273380	6-phosphogluconate dehydrogenase, decarboxylating	involved_in	GO:0006098	pentose-phosphate shunt
A2EZW4	TVAG_273380	6-phosphogluconate dehydrogenase, decarboxylating	involved_in	GO:0019521	D-gluconate metabolic process
A2EZW4	TVAG_273380	6-phosphogluconate dehydrogenase, decarboxylating	enables	GO:0016491	oxidoreductase activity
A2EZW4	TVAG_273380	6-phosphogluconate dehydrogenase, decarboxylating	enables	GO:0004616	phosphogluconate dehydrogenase (decarboxylating) activity
A2EZW4	TVAG_273380	6-phosphogluconate dehydrogenase, decarboxylating	involved_in	GO:0006098	pentose-phosphate shunt
A2F0F6	TVAG_272760	Dihydrolipoyl dehydrogenase	involved_in	GO:0055114	oxidation-reduction process
A2F0F6	TVAG_272760	Dihydrolipoyl dehydrogenase	enables	GO:0050660	flavin adenine dinucleotide binding
A2F0F6	TVAG_272760	Dihydrolipoyl dehydrogenase	part_of	GO:0045252	oxoglutarate dehydrogenase complex
A2F0F6	TVAG_272760	Dihydrolipoyl dehydrogenase	part_of	GO:0005739	mitochondrion
A2F0F6	TVAG_272760	Dihydrolipoyl dehydrogenase	enables	GO:0004148	dihydrolipoyl dehydrogenase activity
A2F0F6	TVAG_272760	Dihydrolipoyl dehydrogenase	enables	GO:0016668	oxidoreductase activity, acting on a sulfur group of donors, NAD(P) as acceptor

A2F0F6	TVAG_272760	Dihydrolipoyl dehydrogenase	enables	GO:0050660	flavin adenine dinucleotide binding
A2F0F6	TVAG_272760	Dihydrolipoyl dehydrogenase	involved_in	GO:0055114	oxidation-reduction process
A2F0F6	TVAG_272760	Dihydrolipoyl dehydrogenase	enables	GO:0004148	dihydrolipoyl dehydrogenase activity
A2F0F6	TVAG_272760	Dihydrolipoyl dehydrogenase	enables	GO:0016491	oxidoreductase activity
A2F0F6	TVAG_272760	Dihydrolipoyl dehydrogenase	involved_in	GO:0045454	cell redox homeostasis
A2F0F6	TVAG_272760	Dihydrolipoyl dehydrogenase	involved_in	GO:0055114	oxidation-reduction process
A2F0F6	TVAG_272760	Dihydrolipoyl dehydrogenase	enables	GO:0000166	nucleotide binding
A2F0F6	TVAG_272760	Dihydrolipoyl dehydrogenase	enables	GO:0016491	oxidoreductase activity
A2F0F6	TVAG_272760	Dihydrolipoyl dehydrogenase	enables	GO:0004148	dihydrolipoyl dehydrogenase activity
A2F266	TVAG_154750	D-isomer specific 2-hydroxyacid dehydrogenase, putative	enables	GO:0004617	phosphoglycerate dehydrogenase activity
A2F266	TVAG_154750	D-isomer specific 2-hydroxyacid dehydrogenase, putative	involved_in	GO:0006520	cellular amino acid metabolic process
A2F266	TVAG_154750	D-isomer specific 2-hydroxyacid dehydrogenase, putative	involved_in	GO:0055114	oxidation-reduction process
A2F266	TVAG_154750	D-isomer specific 2-hydroxyacid dehydrogenase, putative	enables	GO:0016616	oxidoreductase activity, acting on the CH-OH group of donors, NAD or NADP as acceptor
A2F266	TVAG_154750	D-isomer specific 2-hydroxyacid dehydrogenase, putative	enables	GO:0051287	NAD binding
A2F266	TVAG_154750	D-isomer specific 2-hydroxyacid dehydrogenase, putative	involved_in	GO:0055114	oxidation-reduction process
A2F266	TVAG_154750	D-isomer specific 2-hydroxyacid dehydrogenase, putative	enables	GO:0016491	oxidoreductase activity
A2F507	TVAG_029150	Ubiquitin carboxyl-terminal hydrolase	involved_in	GO:0006511	ubiquitin-dependent protein catabolic process
A2F507	TVAG_029150	Ubiquitin carboxyl-terminal hydrolase	enables	GO:0008270	zinc ion binding
A2F507	TVAG_029150	Ubiquitin carboxyl-terminal hydrolase	involved_in	GO:0016579	protein deubiquitination
A2F507	TVAG_029150	Ubiquitin carboxyl-terminal hydrolase	enables	GO:0036459	thiol-dependent ubiquitinyl hydrolase activity
A2F507	TVAG_029150	Ubiquitin carboxyl-terminal hydrolase	enables	GO:0016787	hydrolase activity
A2F507	TVAG_029150	Ubiquitin carboxyl-terminal hydrolase	involved_in	GO:0006508	proteolysis
A2F507	TVAG_029150	Ubiquitin carboxyl-terminal hydrolase	enables	GO:0046872	metal ion binding
A2F507	TVAG_029150	Ubiquitin carboxyl-terminal hydrolase	enables	GO:0008233	peptidase activity
A2F507	TVAG_029150	Ubiquitin carboxyl-terminal hydrolase	enables	GO:0008234	cysteine-type peptidase activity

A2F507	TVAG_029150	Ubiquitin carboxyl-terminal hydrolase	enables	GO:0036459	thiol-dependent ubiquitinyl hydrolase activity
A2F507	TVAG_029150	Ubiquitin carboxyl-terminal hydrolase	involved_in	GO:0016579	protein deubiquitination
A2F9L1	TVAG_125360	Thioredoxin reductase	enables	GO:0004791	thioredoxin-disulfide reductase activity
A2F9L1	TVAG_125360	Thioredoxin reductase	involved_in	GO:0019430	removal of superoxide radicals
A2F9L1	TVAG_125360	Thioredoxin reductase	involved_in	GO:0055114	oxidation-reduction process
A2F9L1	TVAG_125360	Thioredoxin reductase	part_of	GO:0005737	cytoplasm
A2F9L1	TVAG_125360	Thioredoxin reductase	enables	GO:0016491	oxidoreductase activity
A2F9L1	TVAG_125360	Thioredoxin reductase	involved_in	GO:0055114	oxidation-reduction process
A2F9L1	TVAG_125360	Thioredoxin reductase	enables	GO:0016491	oxidoreductase activity
A2F9L1	TVAG_125360	Thioredoxin reductase	enables	GO:0004791	thioredoxin-disulfide reductase activity
A2F9L1	TVAG_125360	Thioredoxin reductase	involved_in	GO:0019430	removal of superoxide radicals
A2F9L1	TVAG_125360	Thioredoxin reductase	enables	GO:0004791	thioredoxin-disulfide reductase activity
A2FCW4	TVAG_037570	64kDa iron hydrogenase, putative	enables	GO:0051539	4 iron, 4 sulfur cluster binding
A2FCW4	TVAG_037570	64kDa iron hydrogenase, putative	enables	GO:0005506	iron ion binding
A2FCW4	TVAG_037570	64kDa iron hydrogenase, putative	involved_in	GO:0055114	oxidation-reduction process
A2FCW4	TVAG_037570	64kDa iron hydrogenase, putative	enables	GO:0008901	ferredoxin hydrogenase activity
A2FCW4	TVAG_037570	64kDa iron hydrogenase, putative	enables	GO:0009055	electron transfer activity
A2FCW4	TVAG_037570	64kDa iron hydrogenase, putative	enables	GO:0051536	iron-sulfur cluster binding
A2FCW4	TVAG_037570	64kDa iron hydrogenase, putative	involved_in	GO:0022900	electron transport chain
A2FDI8	TVAG_315190	Protein kinase domain-containing protein	involved_in	GO:0035556	intracellular signal transduction
A2FDI8	TVAG_315190	Protein kinase domain-containing protein	involved_in	GO:0006468	protein phosphorylation
A2FDI8	TVAG_315190	Protein kinase domain-containing protein	part_of	GO:0005737	cytoplasm
A2FDI8	TVAG_315190	Protein kinase domain-containing protein	part_of	GO:0005634	nucleus
A2FDI8	TVAG_315190	Protein kinase domain-containing protein	enables	GO:0004674	protein serine/threonine kinase activity
A2FDI8	TVAG_315190	Protein kinase domain-containing protein	enables	GO:0004672	protein kinase activity
A2FDI8	TVAG_315190	Protein kinase domain-containing protein	enables	GO:0005524	ATP binding
A2FDI8	TVAG_315190	Protein kinase domain-containing protein	involved_in	GO:0006468	protein phosphorylation

A2FDI8	TVAG_315190	Protein kinase domain-containing protein	enables	GO:0016301	kinase activity
A2FDI8	TVAG_315190	Protein kinase domain-containing protein	involved_in	GO:0016310	phosphorylation
A2FKA7	TVAG_293770	PFK domain-containing protein	involved_in	GO:0006007	glucose catabolic process
A2FKA7	TVAG_293770	PFK domain-containing protein	involved_in	GO:0051289	protein homotetramerization
A2FKA7	TVAG_293770	PFK domain-containing protein	enables	GO:0070095	fructose-6-phosphate binding
A2FKA7	TVAG_293770	PFK domain-containing protein	enables	GO:0003872	6-phosphofructokinase activity
A2FKA7	TVAG_293770	PFK domain-containing protein	enables	GO:0005524	ATP binding
A2FKA7	TVAG_293770	PFK domain-containing protein	part_of	GO:0005945	6-phosphofructokinase complex
A2FKA7	TVAG_293770	PFK domain-containing protein	involved_in	GO:0006002	fructose 6-phosphate metabolic process
A2FKA7	TVAG_293770	PFK domain-containing protein	enables	GO:0016208	AMP binding
A2FKA7	TVAG_293770	PFK domain-containing protein	involved_in	GO:0030388	fructose 1,6-bisphosphate metabolic process
A2FKA7	TVAG_293770	PFK domain-containing protein	enables	GO:0042802	identical protein binding
A2FKA7	TVAG_293770	PFK domain-containing protein	enables	GO:0048029	monosaccharide binding
A2FKA7	TVAG_293770	PFK domain-containing protein	involved_in	GO:0061621	canonical glycolysis
A2FKA7	TVAG_293770	PFK domain-containing protein	enables	GO:0003872	6-phosphofructokinase activity
A2FKA7	TVAG_293770	PFK domain-containing protein	enables	GO:0005524	ATP binding
A2FKA7	TVAG_293770	PFK domain-containing protein	involved_in	GO:0006002	fructose 6-phosphate metabolic process
A2FKA7	TVAG_293770	PFK domain-containing protein	involved_in	GO:0006096	glycolytic process
A2FKA7	TVAG_293770	PFK domain-containing protein	enables	GO:0008443	phosphofructokinase activity
A2FKA7	TVAG_293770	PFK domain-containing protein	enables	GO:0016301	kinase activity
A2FKA7	TVAG_293770	PFK domain-containing protein	involved_in	GO:0016310	phosphorylation
A2FKA7	TVAG_293770	PFK domain-containing protein	involved_in	GO:0046835	carbohydrate phosphorylation
A2FLD2	TVAG_057830	WD_REPEATS_REGION domain-containing protein	involved_in	GO:0006886	intracellular protein transport
A2FLD2	TVAG_057830	WD_REPEATS_REGION domain-containing protein	involved_in	GO:0006888	endoplasmic reticulum to Golgi vesicle-mediated transport

A2FLD2	TVAG_057830	WD_REPEATS_REGION domain-containing protein	involved_in	GO:0007029	endoplasmic reticulum organization
A2FLD2	TVAG_057830	WD_REPEATS_REGION domain-containing protein	part_of	GO:0030127	COPII vesicle coat
A2FLD2	TVAG_057830	WD_REPEATS_REGION domain-containing protein	part_of	GO:0070971	endoplasmic reticulum exit site
A2FLD2	TVAG_057830	WD_REPEATS_REGION domain-containing protein	enables	GO:0005198	structural molecule activity
A2FLD2	TVAG_057830	WD_REPEATS_REGION domain-containing protein	involved_in	GO:0090110	COPII-coated vesicle cargo loading
A2FLD2	TVAG_057830	WD_REPEATS_REGION domain-containing protein	involved_in	GO:0090114	COPII-coated vesicle budding
A2FLD2	TVAG_057830	WD_REPEATS_REGION domain-containing protein	involved_in	GO:0006888	endoplasmic reticulum to Golgi vesicle-mediated transport
A2FLD2	TVAG_057830	WD_REPEATS_REGION domain-containing protein	part_of	GO:0000139	Golgi membrane
A2FLD2	TVAG_057830	WD_REPEATS_REGION domain-containing protein	part_of	GO:0000139	Golgi membrane
A2FRN2	TVAG_327610	Cytidyltransferase-related domain containing protein	involved_in	GO:0009058	biosynthetic process
A2FRN2	TVAG_327610	Cytidyltransferase-related domain containing protein	enables	GO:0003824	catalytic activity
A2FRN2	TVAG_327610	Cytidyltransferase-related domain containing protein	enables	GO:0016740	transferase activity
A2G214	TVAG_181540	USP domain-containing protein	enables	GO:0004843	thiol-dependent ubiquitin-specific protease activity
A2G214	TVAG_181540	USP domain-containing protein	part_of	GO:0005829	cytosol
A2G214	TVAG_181540	USP domain-containing protein	enables	GO:0004197	cysteine-type endopeptidase activity
A2G214	TVAG_181540	USP domain-containing protein	part_of	GO:0005634	nucleus
A2G214	TVAG_181540	USP domain-containing protein	involved_in	GO:0016579	protein deubiquitination
A2G214	TVAG_181540	USP domain-containing protein	involved_in	GO:0006511	ubiquitin-dependent protein catabolic process
A2G214	TVAG_181540	USP domain-containing protein	involved_in	GO:0016579	protein deubiquitination
A2G214	TVAG_181540	USP domain-containing protein	enables	GO:0036459	thiol-dependent ubiquitinyl hydrolase activity
A2G214	TVAG_181540	USP domain-containing protein	enables	GO:0016787	hydrolase activity
A2G4A3	TVAG_374870	Doublecortin domain-containing protein	involved_in	GO:0035556	intracellular signal transduction
A2GEF2	TVAG_414560	NAD(P)-bd_dom domain-containing protein	enables	GO:0008460	dTDP-glucose 4,6-dehydratase activity
A2GEF2	TVAG_414560	NAD(P)-bd_dom domain-containing protein	involved_in	GO:0009225	nucleotide-sugar metabolic process

A2GLT5	TVAG_562550	Clathrin heavy chain-related protein	enables	GO:0032051	clathrin light chain binding
A2GLT5	TVAG_562550	Clathrin heavy chain-related protein	part_of	GO:0071439	clathrin complex
A2GLT5	TVAG_562550	Clathrin heavy chain-related protein	involved_in	GO:0006898	receptor-mediated endocytosis
A2GLT5	TVAG_562550	Clathrin heavy chain-related protein	enables	GO:0005198	structural molecule activity
A2GLT5	TVAG_562550	Clathrin heavy chain-related protein	involved_in	GO:0016192	vesicle-mediated transport
A2GLT5	TVAG_562550	Clathrin heavy chain-related protein	involved_in	GO:0006886	intracellular protein transport
A2GLT5	TVAG_562550	Clathrin heavy chain-related protein	part_of	GO:0030130	clathrin coat of trans-Golgi network vesicle
A2GLT5	TVAG_562550	Clathrin heavy chain-related protein	part_of	GO:0030132	clathrin coat of coated pit

Supplementary Table 2- 1. Available QuickGO analysis of target proteins
Of the 61 proteins found, only 50 had any GO annotation. All annotations are provided in the table. Where GO annotations were unified, the principal annotation was also used in Table 2-1 and subsequently in construction of the pie chart in Figure 2-3A.

Accession	Functional Group	TIGR Description	Contains import motif?	Class in training set	final MOT+ score	final MOT+ rank	final MOT- score	final MOT- rank
TVAG_272760	Amino Acid Metabolism	dihydrolipoamide dehydrogenase family protein	no		0.4350	1899	0.9999	46
TVAG_100550	Amino Acid Metabolism	Glycine cleavage H-protein	no		0.9996	97	0.9867	181
TVAG_056190	Amino Acid Metabolism	family M20, peptidase T-like metallopeptidase	no		0.3457	2186	0.9846	186
TVAG_054490	Amino Acid Metabolism	beta-eliminating lyase, putative	no		0.9993	123	0.9453	276
TVAG_109540	Amino Acid Metabolism	serine hydroxymethyltransferase family protein	no		0.8628	830	0.8307	414
TVAG_098820	Amino Acid Metabolism	aminotransferase, classes I and II family protein	no		0.0507	5093	0.3135	982
TVAG_183300	Amino Acid Metabolism	aminotransferase, class V family protein	no		0.0005	19880	0.3061	1000
TVAG_074600	Amino Acid Metabolism	aminotransferase, classes I and II family protein	no		0.1444	3369	0.2101	1220
TVAG_025980	Amino Acid Metabolism	glutamate dehydrogenase, putative	no		0.0373	5639	0.1533	1403
TVAG_268020	Amino Acid Metabolism	aminotransferase, classes I and II family protein	no		0.0573	4871	0.0736	1915
TVAG_147790	Amino Acid Metabolism	methionine gamma-lyase	no		0.0010	16653	0.0691	1999
TVAG_088220	Amino Acid Metabolism	aminotransferase, classes I and II family protein	no		0.0291	6143	0.0311	2781
TVAG_177600	Amino Acid Metabolism	Glycine cleavage H-protein	no		0.6079	1439	0.0222	3253
TVAG_419720	Amino Acid Metabolism	aminotransferase, classes I and II family protein	no		0.0410	5480	0.0217	3321
TVAG_208470	Amino Acid Metabolism	threonyl-tRNA synthetase family protein	no		0.0233	6610	0.0063	5597
TVAG_547520	Amino Acid Metabolism	cysteine synthases family protein	no		0.0079	9211	0.0061	5676
TVAG_267950	Amino Acid Metabolism	hypothetical protein	no		0.0001	31361	0.0056	5892
TVAG_379550	Amino Acid Metabolism	aminotransferase, classes I and II family protein	yes		0.8885	763	0.0018	9574
TVAG_081640	Amino Acid Metabolism	conserved hypothetical protein	no		0.9877	320	0.0005	14666
TVAG_344520	Amino Acid Metabolism	Amidinotransferase family protein	no		0.0000	33724	0.0005	15455
TVAG_152430	Amino Acid Metabolism	lysyl-tRNA synthetase family protein	no		0.0000	33999	0.0001	26838
TVAG_183850	Amino Acid Metabolism	Amidinotransferase family protein	no		0.0079	9205	0.0000	54681
TVAG_479760	ATPases	hypothetical protein	no		0.0000	46486	0.0002	22297
TVAG_075320	ATPases	V-type ATPase 116kDa subunit family protein	no		0.0697	4500	0.0001	29584
TVAG_277590	ATPases	calcium-translocating P-type ATPase	no		0.0046	10923	0.0000	31044
TVAG_420260	ATPases	hypothetical protein	no		0.0000	39288	0.0000	37299
TVAG_262750	ATPases	hypothetical protein	no		0.0008	17874	0.0000	42536
TVAG_006020	ATPases	hypothetical protein	no		0.0000	39375	0.0000	46589
TVAG_178030	ATPases	calcium-translocating P-type ATPase	no		0.0000	37639	0.0000	48758
TVAG_324980	ATPases	adenosinetriphosphatase, putative	no		0.0000	48392	0.0000	54617

TVAG_234160	Cytoskeletal Proteins	actin related protein, putative	no		0.0122	8052	0.1149	1593
TVAG_087140	Cytoskeletal Proteins	Arp2/3 complex, 34kD subunit p34-Arc family	no		0.0096	8729	0.0008	12524
TVAG_376130	Cytoskeletal Proteins	actin-binding protein, putative	no		0.0353	5730	0.0008	12955
TVAG_239310	Cytoskeletal Proteins	actinin, putative	no		0.0035	11827	0.0003	17285
TVAG_381030	Cytoskeletal Proteins	hypothetical protein	no		0.0004	22089	0.0001	24413
TVAG_351310	Cytoskeletal Proteins	fimbrin, putative	no		0.0008	17967	0.0000	37951
TVAG_190450	Cytoskeletal Proteins	alpha-actinin, putative	no		0.0000	44256	0.0000	49232
TVAG_354020	Cytoskeletal Proteins	Actin family protein	no		0.0000	58953	0.0000	53074
TVAG_192620	Cytoskeletal Proteins	Cofilin/tropomyosin-type actin-binding protein	no	negative	0.0000	58876	0.0000	56645
TVAG_008680	Cytoskeletal Proteins	beta-tubulin, putative	no	negative	0.0000	59513	0.0000	59449
TVAG_149090	Cytoskeletal Proteins	actin	no	negative	0.0000	59575	0.0000	59505
TVAG_292580	Cytosolic Chaperones	peptidyl-prolyl cis-trans isomerase, FKBP-type	no		0.1362	3468	0.5788	657
TVAG_381290	Cytosolic Chaperones	Hsp20/alpha crystallin family protein	no		0.6341	1378	0.1130	1603
TVAG_182370	Cytosolic Chaperones	chaperonin subunit eta CCTeta, putative	no		0.0231	6638	0.0464	2388
TVAG_435000	Cytosolic Chaperones	peptidyl-prolyl cis-trans isomerase, FKBP-type	no		0.0002	25231	0.0063	5603
TVAG_139320	Cytosolic Chaperones	dnaK protein	no		0.0000	40637	0.0002	18933
TVAG_153560	Cytosolic Chaperones	heat shock protein, putative	no		0.0000	50328	0.0001	25001
TVAG_277390	Cytosolic Chaperones	cytosolic cyclophilin, putative	no		0.0001	29975	0.0000	30711
TVAG_044510	Cytosolic Chaperones	cytoplasmic heat shock protein 70, putative	no		0.0000	47545	0.0000	32547
TVAG_267870	Energy Metabolism	malate dehydrogenase:SUBUNIT=A	yes		1.0000	2	1.0000	1
TVAG_340290	Energy Metabolism	adhesin AP65-1 precursor	yes	positive	1.0000	4	1.0000	2
TVAG_412220	Energy Metabolism	malate dehydrogenase:SUBUNIT=A	yes	positive	1.0000	5	1.0000	3
TVAG_183790	Energy Metabolism	AP65-3 adhesin	yes	positive	1.0000	6	1.0000	5
TVAG_416100	Energy Metabolism	malate dehydrogenase:SUBUNIT=A	yes	positive	1.0000	9	1.0000	7
TVAG_068130	Energy Metabolism	malate dehydrogenase:SUBUNIT=A	no	positive	1.0000	23	1.0000	8
TVAG_238830	Energy Metabolism	malate dehydrogenase:SUBUNIT=B	yes	positive	1.0000	3	1.0000	9
TVAG_144730	Energy Metabolism	adhesin protein AP51-2, putative	yes	positive	1.0000	7	1.0000	21
TVAG_296220	Energy Metabolism	Respiratory-chain NADH dehydrogenase 24 Kd	yes	positive	1.0000	20	1.0000	25
TVAG_047890	Energy Metabolism	hypothetical protein	yes	positive	1.0000	13	1.0000	27
TVAG_259190	Energy Metabolism	Succinyl-CoA ligase beta-chain, hydrogenosomal	yes	positive	1.0000	17	1.0000	29
TVAG_318670	Energy Metabolism	adhesin protein AP33-1	yes	positive	1.0000	12	1.0000	30
TVAG_165340	Energy Metabolism	hypothetical protein	yes	positive	1.0000	11	0.9999	37
TVAG_183500	Energy Metabolism	adhesin protein AP51-3, putative	yes	positive	1.0000	18	0.9999	38
TVAG_182620	Energy Metabolism	TvhydB protein, putative	no	positive	1.0000	35	0.9999	41

TVAG_310050	Energy Metabolism	TvhydB protein, putative	no		0.9856	346	0.9999	47
TVAG_198110	Energy Metabolism	pyruvate:ferredoxin oxidoreductase A	yes	positive	1.0000	24	0.9998	50
TVAG_230580	Energy Metabolism	pyruvate:ferredoxin oxidoreductase BI	yes		1.0000	19	0.9998	54
TVAG_395550	Energy Metabolism	hypothetical protein	no	positive	1.0000	28	0.9997	59
TVAG_254890	Energy Metabolism	pyruvate:ferredoxin oxidoreductase E	yes		1.0000	34	0.9995	70
TVAG_242960	Energy Metabolism	pyruvate:ferredoxin oxidoreductase BII	yes		1.0000	51	0.9959	116
TVAG_113870	Energy Metabolism	hypothetical protein	no		0.9998	86	0.9837	188
TVAG_489800	Energy Metabolism	adenylate kinase	yes	positive	1.0000	32	0.9815	192
TVAG_328940	Energy Metabolism	alcohol dehydrogenase, iron-containing	no		0.2360	2711	0.9502	266
TVAG_466790	Energy Metabolism	pyruvate:ferredoxin oxidoreductase F	no		0.9971	193	0.9387	287
TVAG_133030	Energy Metabolism	hydrogenase chain, putative	yes		0.9895	307	0.9319	300
TVAG_164890	Energy Metabolism	hypothetical protein	no		0.9911	291	0.9034	343
TVAG_105770	Energy Metabolism	pyruvate:ferredoxin oxidoreductase C	no		0.9326	615	0.8792	367
TVAG_228780	Energy Metabolism	alcohol dehydrogenase 1, putative	no		0.7502	1113	0.7622	479
TVAG_003900	Energy Metabolism	Ferredoxin 1	yes		0.0953	3998	0.6835	547
TVAG_399860	Energy Metabolism	Ferredoxin 2	yes		0.0124	8015	0.0630	2110
TVAG_361590	Energy Metabolism	64kDa iron hydrogenase, putative	yes		0.9980	164	0.0155	3852
TVAG_292710	Energy Metabolism	Ferredoxin 4	no		0.5173	1639	0.0125	4231
TVAG_037570	Energy Metabolism	64kDa iron hydrogenase, putative	yes		0.4551	1806	0.0091	4819
TVAG_327470	Energy Metabolism	alcohol dehydrogenase	no		0.9803	397	0.0081	5042
TVAG_160930	Energy Metabolism	Iron only hydrogenase large subunit, C-terminal	yes		0.4645	1768	0.0006	14196
TVAG_255980	Energy Metabolism	hypothetical protein	yes		0.4476	1825	0.0001	27557
TVAG_091590	ER	hypothetical protein	no		0.0001	29004	0.0182	3553
TVAG_150170	ER	ORMDL family protein	no		0.0107	8390	0.0034	7490
TVAG_318870	ER	spermatogenesis associated factor, putative	no		0.0001	32534	0.0026	8292
TVAG_092490	ER	endoplasmic reticulum heat shock protein 70, put.	no		0.0000	46669	0.0007	13419
TVAG_379250	ER	conserved hypothetical protein	no		0.2793	2494	0.0001	27521
TVAG_039020	ER	conserved hypothetical protein	no		0.0000	42846	0.0000	42943
TVAG_361540	Fe-S Cluster Assembly Proteins	HesB-like domain containing protein	yes	positive	1.0000	14	1.0000	10
TVAG_456770	Fe-S Cluster Assembly Proteins	HesB-like domain containing protein	yes	positive	1.0000	15	1.0000	11
TVAG_257780	Fe-S Cluster Assembly Proteins	Fe-hydrogenase assembly protein, putative	no	positive	1.0000	10	1.0000	14
TVAG_432650	Fe-S Cluster Assembly Proteins	NifU-like protein, putative	no		0.3337	2248	0.9921	143
TVAG_239660	Fe-S Cluster Assembly Proteins	IscS/NifS-like protein	no		0.0017	14522	0.6351	590

TVAG_422630	Fe-S Cluster Assembly Proteins	co-chaperone Hsc20 family protein	no		0.1543	3287	0.1466	1430
TVAG_032090	Fe-S Cluster Assembly Proteins	co-chaperone Hsc20 family protein	no		0.5431	1584	0.1081	1623
TVAG_342900	Flavin Proteins	Isoflavone reductase, putative	no		0.6110	1429	0.9487	269
TVAG_152690	Flavin Proteins	oxidoreductase, FAD/FMN-binding family protein	no		0.9978	174	0.9013	345
TVAG_040030	Flavin Proteins	conserved hypothetical protein	yes		0.9710	460	0.6777	554
TVAG_036010	Flavin Proteins	Hydrogenosomal oxygen reductase	yes		0.9999	60	0.4543	777
TVAG_154730	Flavin Proteins	iron-sulfur flavoprotein, putative	yes		0.9987	152	0.2227	1190
TVAG_127520	Flavin Proteins	NADH:flavin oxidoreductase	no		0.8768	800	0.0808	1825
TVAG_356810	Flavin Proteins	nitroimidazole resistance protein, putative	yes		0.4459	1875	0.0787	1843
TVAG_327760	Flavin Proteins	iron-sulfur flavoprotein, putative	no		0.0483	5178	0.0235	3166
TVAG_351540	Flavin Proteins	oxidoreductase, FAD/FMN-binding family protein	no		0.0010	16813	0.0080	5073
TVAG_049830	Flavin Proteins	Pyridine nucleotide-disulphide oxidoreductase family protein	no		0.0087	8944	0.0049	6246
TVAG_265760	Flavin Proteins	oxidoreductase, FAD/FMN-binding family protein	no		0.0369	5655	0.0003	17884
TVAG_445730	Hydrogenosomal Chaperones	chaperonin, 10 kDa family protein	yes		0.9995	112	1.0000	28
TVAG_392320	Hydrogenosomal Chaperones	chaperonin, 10 kDa family protein	yes		0.9912	288	0.9999	44
TVAG_088050	Hydrogenosomal Chaperones	chaperonin 60, putative	yes	positive	1.0000	29	0.9691	234
TVAG_297650	Hydrogenosomal Chaperones	co-chaperone GrpE family protein	yes		0.6775	1284	0.8099	441
TVAG_191660	Hydrogenosomal Chaperones	hypothetical protein	yes		0.4248	1930	0.6093	616
TVAG_041340	Hydrogenosomal Chaperones	chaperonin, 10 kDa family protein	yes		0.9999	65	0.3019	1007
TVAG_203620	Hydrogenosomal Chaperones	chaperonin 60, putative	yes		0.9999	75	0.2146	1207
TVAG_167250	Hydrogenosomal Chaperones	chaperonin, putative	yes		0.9851	356	0.0027	8226
TVAG_340390	Hydrogenosomal Chaperones	mitochondrial-type HSP70, putative	yes		0.0461	5252	0.0019	9525
TVAG_019190	Hydrogenosomal Chaperones	DnaJ domain containing protein	yes		0.8964	737	0.0006	14138
TVAG_237140	Hydrogenosomal Chaperones	mitochondrial-type HSP70, putative	yes		0.0166	7338	0.0000	32834
TVAG_433130	Hydrogenosomal Chaperones	Heat shock 70 kDa protein, putative	yes		0.0052	10459	0.0000	42800
TVAG_498620	Hypothetical proteins	hypothetical protein	no		0.0002	24650	0.7158	515
TVAG_057110	Hypothetical proteins	methylesterase-like serine peptidase	no		0.1443	3372	0.3461	915
TVAG_423530	Hypothetical proteins	hypothetical protein	no		0.0358	5712	0.0576	2183

TVAG_277930	Hypothetical proteins	hypothetical protein	no		0.0081	9171	0.0496	2332
TVAG_077910	Hypothetical proteins	hypothetical protein	no		0.0816	4208	0.0438	2437
TVAG_440200	Hypothetical proteins	hypothetical protein	no		0.1769	3078	0.0253	3031
TVAG_455090	Hypothetical proteins	hypothetical protein	no		0.0215	6799	0.0252	3045
TVAG_146920	Hypothetical proteins	hypothetical protein	no		0.5271	1620	0.0092	4810
TVAG_377380	Hypothetical proteins	hypothetical protein	no		0.0109	8351	0.0091	4825
TVAG_425470	Hypothetical proteins	hypothetical protein	no		0.0032	12126	0.0087	4918
TVAG_177910	Hypothetical proteins	hypothetical protein	no		0.0012	15824	0.0058	5830
TVAG_311860	Hypothetical proteins	hypothetical protein	no		0.0001	30137	0.0052	6107
TVAG_284380	Hypothetical proteins	hypothetical protein	no		0.0000	52998	0.0042	6834
TVAG_332970	Hypothetical proteins	hypothetical protein	no		0.0001	29639	0.0042	6847
TVAG_468220	Hypothetical proteins	conserved hypothetical protein	no		0.3944	2035	0.0038	7204
TVAG_393390	Hypothetical proteins	hypothetical protein	no		0.0034	11951	0.0029	8057
TVAG_198090	Hypothetical proteins	hypothetical protein	no		0.8419	879	0.0028	8123
TVAG_026100	Hypothetical proteins	hypothetical protein	no		0.0231	6633	0.0021	8882
TVAG_115470	Hypothetical proteins	hypothetical protein	no		0.0044	11025	0.0019	9415
TVAG_123850	Hypothetical proteins	hypothetical protein	no		0.0179	7151	0.0014	10498
TVAG_237550	Hypothetical proteins	hypothetical protein	no		0.0405	5501	0.0009	12028
TVAG_117090	Hypothetical proteins	hypothetical protein	no		0.0000	41586	0.0009	12238
TVAG_028050	Hypothetical proteins	hypothetical protein	no		0.0218	6783	0.0008	12376
TVAG_437350	Hypothetical proteins	hypothetical protein	no		0.0001	27118	0.0008	12641
TVAG_264120	Hypothetical proteins	hypothetical protein	no		0.0002	24038	0.0008	12954
TVAG_137270	Hypothetical proteins	hypothetical protein	no		0.0000	45226	0.0007	13756
TVAG_416710	Hypothetical proteins	hypothetical protein	no		0.0001	29848	0.0006	14127
TVAG_038870	Hypothetical proteins	hypothetical protein	no		0.0367	5665	0.0005	14905
TVAG_399830	Hypothetical proteins	hypothetical protein	no		0.0000	40367	0.0005	15388
TVAG_234150	Hypothetical proteins	FHA domain containing protein	no		0.0001	29109	0.0005	15490
TVAG_122960	Hypothetical proteins	hypothetical protein	no		0.0011	16256	0.0004	15621
TVAG_067030	Hypothetical proteins	hypothetical protein	no		0.0002	24609	0.0004	16109
TVAG_167240	Hypothetical proteins	hypothetical protein	no		0.0907	4060	0.0004	16209
TVAG_209310	Hypothetical proteins	hypothetical protein	no		0.0000	54929	0.0004	16942
TVAG_056920	Hypothetical proteins	hypothetical protein	no		0.0013	15586	0.0003	17311
TVAG_001130	Hypothetical proteins	hypothetical protein	no		0.0000	45405	0.0003	17756
TVAG_139550	Hypothetical proteins	hypothetical protein	no		0.0000	49791	0.0003	18384
TVAG_260830	Hypothetical proteins	hypothetical protein	no		0.0020	14013	0.0002	19847
TVAG_447580	Hypothetical proteins	hypothetical protein	no		0.0001	32843	0.0002	19855
TVAG_416700	Hypothetical proteins	hypothetical protein	no		0.0043	11080	0.0002	19905

TVAG_369980	Hypothetical proteins	hypothetical protein	no		0.0000	48231	0.0002	20807
TVAG_337970	Hypothetical proteins	hypothetical protein	no		0.0433	5380	0.0002	21535
TVAG_185900	Hypothetical proteins	hypothetical protein	no		0.0000	39122	0.0002	21562
TVAG_195900	Hypothetical proteins	hypothetical protein	no		0.0001	31541	0.0002	21608
TVAG_217400	Hypothetical proteins	hypothetical protein	no		0.0000	51074	0.0002	22291
TVAG_249920	Hypothetical proteins	hypothetical protein	no		0.0009	17273	0.0001	22696
TVAG_174010	Hypothetical proteins	hypothetical protein	no		0.0001	31979	0.0001	23047
TVAG_539120	Hypothetical proteins	hypothetical protein	no		0.0000	36646	0.0001	23089
TVAG_132350	Hypothetical proteins	conserved hypothetical protein	no		0.0004	22085	0.0001	23167
TVAG_197670	Hypothetical proteins	hypothetical protein	no		0.0000	44838	0.0001	23304
TVAG_136450	Hypothetical proteins	hypothetical protein	no		0.1672	3167	0.0001	23516
TVAG_263350	Hypothetical proteins	conserved hypothetical protein	no		0.0019	14144	0.0001	23910
TVAG_226310	Hypothetical proteins	hypothetical protein	no		0.0032	12108	0.0001	24948
TVAG_342980	Hypothetical proteins	hypothetical protein	no		0.0058	10162	0.0001	26258
TVAG_493810	Hypothetical proteins	hypothetical protein	no		0.0015	14966	0.0001	26332
TVAG_185520	Hypothetical proteins	hypothetical protein	no		0.0001	30871	0.0001	26411
TVAG_247370	Hypothetical proteins	hypothetical protein	no		0.0003	23249	0.0001	26498
TVAG_495570	Hypothetical proteins	hypothetical protein	no		0.1265	3554	0.0001	26887
TVAG_083420	Hypothetical proteins	hypothetical protein	no		0.0001	27980	0.0001	27466
TVAG_450060	Hypothetical proteins	hypothetical protein	no		0.0003	23560	0.0001	27674
TVAG_046430	Hypothetical proteins	conserved hypothetical protein	no		0.0732	4414	0.0001	27879
TVAG_102740	Hypothetical proteins	hypothetical protein	no		0.0000	37391	0.0001	27988
TVAG_130330	Hypothetical proteins	hypothetical protein	no		0.0000	47886	0.0001	28678
TVAG_450220	Hypothetical proteins	hypothetical protein	no		0.0074	9403	0.0000	29850
TVAG_411140	Hypothetical proteins	hypothetical protein	no		0.0033	12106	0.0000	29865
TVAG_137750	Hypothetical proteins	hypothetical protein	no		0.0519	5053	0.0000	29907
TVAG_113880	Hypothetical proteins	hypothetical protein	no		0.0000	36420	0.0000	30362
TVAG_458060	Hypothetical proteins	hypothetical protein	no		0.0000	33406	0.0000	30785
TVAG_341190	Hypothetical proteins	hypothetical protein	no		0.0004	21415	0.0000	31565
TVAG_412480	Hypothetical proteins	hypothetical protein	no		0.0474	5201	0.0000	32251
TVAG_233680	Hypothetical proteins	hypothetical protein	no		0.0000	37409	0.0000	32758
TVAG_432870	Hypothetical proteins	hypothetical protein	no		0.0210	6863	0.0000	34699
TVAG_335500	Hypothetical proteins	hypothetical protein	no		0.0000	42484	0.0000	35512
TVAG_022530	Hypothetical proteins	hypothetical protein	no		0.0009	17550	0.0000	35898
TVAG_343040	Hypothetical proteins	hypothetical protein	no		0.0000	35910	0.0000	36736
TVAG_211970	Hypothetical proteins	hypothetical protein	no		0.0000	40825	0.0000	37312
TVAG_477200	Hypothetical proteins	hypothetical protein	no		0.0000	52830	0.0000	38673

TVAG_392650	Hypothetical proteins	hypothetical protein	no		0.0001	31852	0.0000	38770
TVAG_283120	Hypothetical proteins	hypothetical protein	no		0.0024	13283	0.0000	38840
TVAG_106710	Hypothetical proteins	hypothetical protein	no		0.0001	29709	0.0000	39496
TVAG_044000	Hypothetical proteins	hypothetical protein	no		0.1220	3598	0.0000	39930
TVAG_011550	Hypothetical proteins	hypothetical protein	no		0.0000	40968	0.0000	40371
TVAG_137760	Hypothetical proteins	hypothetical protein	no		0.0005	20491	0.0000	41338
TVAG_340380	Hypothetical proteins	hypothetical protein	no		0.0000	37602	0.0000	42651
TVAG_399510	Hypothetical proteins	hypothetical protein	no		0.0004	22038	0.0000	42679
TVAG_302380	Hypothetical proteins	hypothetical protein	no		0.0026	12892	0.0000	43745
TVAG_442170	Hypothetical proteins	hypothetical protein	no		0.0002	24093	0.0000	45156
TVAG_530140	Hypothetical proteins	hypothetical protein	no		0.0002	24245	0.0000	45280
TVAG_420200	Hypothetical proteins	hypothetical protein	no		0.0001	28224	0.0000	45339
TVAG_468600	Hypothetical proteins	hypothetical protein	no		0.0000	57076	0.0000	45843
TVAG_165270	Hypothetical proteins	hypothetical protein	no		0.0000	51885	0.0000	46202
TVAG_343980	Hypothetical proteins	hypothetical protein	no		0.0001	31593	0.0000	46546
TVAG_371800	Hypothetical proteins	hypothetical protein	no		0.0000	39529	0.0000	46807
TVAG_140620	Hypothetical proteins	hypothetical protein	no		0.0001	27977	0.0000	46843
TVAG_053070	Hypothetical proteins	hypothetical protein	no		0.0001	29489	0.0000	47140
TVAG_214300	Hypothetical proteins	hypothetical protein	no		0.0001	27759	0.0000	47164
TVAG_192370	Hypothetical proteins	hypothetical protein	no		0.0001	30811	0.0000	49146
TVAG_038850	Hypothetical proteins	hypothetical protein	no		0.0001	29759	0.0000	49736
TVAG_213670	Hypothetical proteins	hypothetical protein	yes		0.0556	4927	0.0000	50559
TVAG_006090	Hypothetical proteins	hypothetical protein	no		0.0004	22115	0.0000	53115
TVAG_272350	Hypothetical proteins	hypothetical protein	no		0.0000	41080	0.0000	53465
TVAG_281980	Hypothetical proteins	hypothetical protein	no		0.0000	58058	0.0000	53798
TVAG_271850	Hypothetical proteins	cec-1, putative	no		0.0000	33748	0.0000	55143
TVAG_238370	Hypothetical proteins	viral A-type inclusion protein, putative	no		0.0000	57670	0.0000	56372
TVAG_506640	Hypothetical proteins	conserved hypothetical protein	no		0.0000	53685	0.0000	57720
TVAG_167810	Hypothetical proteins	hypothetical protein	no		0.0000	39386	0.0000	58081
TVAG_019960	Hypothetical proteins	hypothetical protein	no		0.0000	57961	0.0000	58312
TVAG_298320	Hypothetical proteins	hypothetical protein	no		0.0000	52810	0.0000	58632
TVAG_187360	Hypothetical proteins	hypothetical protein	no		0.0000	59000	0.0000	59343
TVAG_043470	Nuclear Protein	hypothetical protein	no		0.0329	5886	0.0015	10221
TVAG_271570	Nuclear Protein	Nucleoside transporter family protein	no		0.0009	17391	0.0002	19734
TVAG_332540	Nuclear Protein	hypothetical protein	no		0.0000	49899	0.0000	46389
TVAG_158990	Nuclear Protein	RNA-binding protein, putative	no	negative	0.0000	53294	0.0000	46617
TVAG_026390	Nuclear Protein	Histone H2B, putative	no	negative	0.0000	59617	0.0000	59541

TVAG_021440	Nuclear Protein	Histone H2A-IV, putative	no	negative	0.0000	59660	0.0000	59620
TVAG_014920	Nuclear Protein	histone H4-3	no	negative	0.0000	59646	0.0000	59646
TVAG_270750	Other function	acetyltransferase, GNAT family protein	no		0.9958	220	0.9994	71
TVAG_321030	Other function	CoA binding domain containing protein	yes		1.0000	48	0.9706	230
TVAG_293370	Other function	Nucleoside diphosphate kinase family protein	no		0.9050	702	0.9475	272
TVAG_454490	Other function	purine nucleoside phosphorylase, putative	no		0.9992	132	0.7752	471
TVAG_256720	Other function	4-carboxymuconolactone decarboxylase family	no		0.8525	853	0.6234	604
TVAG_321010	Other function	AMP-binding enzyme family protein	no		0.9001	720	0.5644	676
TVAG_107080	Other function	4-carboxymuconolactone decarboxylase, putative	no		0.8299	918	0.1322	1486
TVAG_065750	Other function	Major Facilitator Superfamily protein	no		0.1264	3555	0.1216	1542
TVAG_076230	Other function	mrp, putative	yes		0.3040	2369	0.1178	1575
TVAG_047210	Other function	D-isomer 2-hydroxyacid dehydrogenase, put.	yes		0.8003	1003	0.0485	2343
TVAG_139300	Other function	phosphoenol pyruvate carboxykinase, putative	no		0.9433	578	0.0426	2454
TVAG_388650	Other function	aminotransferase, classes I and II family protein	no		0.0425	5414	0.0183	3532
TVAG_325080	Other function	metallo-beta-lactamase superfamily protein	no		0.1434	3390	0.0171	3635
TVAG_310250	Other function	phosphoenol pyruvate carboxykinase, putative	no		0.7289	1165	0.0114	4374
TVAG_225930	Other function	conserved hypothetical protein	no		0.9451	574	0.0093	4797
TVAG_277050	Other function	citrate lyase beta like, putative	no		0.0001	27618	0.0088	4894
TVAG_217870	Other function	mrp protein, putative	yes		0.3366	2236	0.0081	5043
TVAG_038530	Other function	carbamoyl transferase Z4209 , putative	no		0.6606	1313	0.0061	5651
TVAG_424580	Other function	mevalonate kinase family protein	no		0.0027	12760	0.0043	6815
TVAG_083440	Other function	conserved hypothetical protein	no		0.0000	34935	0.0023	8626
TVAG_461020	Other function	ABC transporter family protein	no		0.2462	2641	0.0013	10665
TVAG_180400	Other function	Endonuclease/Exonuclease/phosphatase family	no		0.0004	21957	0.0012	10983
TVAG_118780	Other function	EF hand family protein	no		0.3669	2117	0.0009	12148
TVAG_346230	Other function	haloacid dehalogenase-like hydrolase family	no		0.0150	7581	0.0006	13920
TVAG_060450	Other function	acetyltransferase, GNAT family protein	no		0.0033	12105	0.0005	15136
TVAG_351320	Other function	purine nucleoside phosphorylase, putative	no		0.0000	40573	0.0005	15264
TVAG_076510	Other function	serine palmitoyl transferase subunit, putative	no		0.0136	7796	0.0003	18316
TVAG_256470	Other function	Thiamin pyrophosphokinase, catalytic domain	no		0.0000	34447	0.0000	29690
TVAG_386000	Other function	TB2/DP1, HVA22 family protein	no		0.0000	55334	0.0000	35650
TVAG_198430	Other function	14-3-3 protein	no		0.0001	32343	0.0000	41653

TVAG_049690	Other function	Thiamin pyrophosphokinase, catalytic domain	no		0.0153	7539	0.0000	41765
TVAG_048135	Other function	P270 surface immunogen-like	no		0.0020	13868	0.0000	44072
TVAG_096630	Other function	Thiamin pyrophosphokinase, catalytic domain	no		0.0002	24543	0.0000	44337
TVAG_454570	Other function	erythrocyte binding protein, putative	no		0.0000	49835	0.0000	44669
TVAG_037530	Other function	EF hand family protein	no		0.0002	26530	0.0000	48462
TVAG_092170	Other function	preprotein translocase, SecY subunit, putative	no		0.0000	40725	0.0000	54127
TVAG_055200	Oxygen Stress Response	thioredoxin peroxidase	no	positive	1.0000	30	1.0000	4
TVAG_064490	Oxygen Stress Response	rubrerythrin, putative	no	positive	1.0000	27	1.0000	20
TVAG_336320	Oxygen Stress Response	hydroxylamine reductase, putative	no		0.9941	243	0.9912	147
TVAG_206500	Oxygen Stress Response	hybrid-cluster protein, putative	no		0.9678	477	0.9156	323
TVAG_410350	Oxygen Stress Response	hypothetical protein	no		0.0125	7989	0.0069	5421
TVAG_114310	Oxygen Stress Response	thioredoxin peroxidase	no		0.6582	1319	0.0030	7943
TVAG_049140	Oxygen Stress Response	chloroplastic iron superoxide dismutase	no		0.8205	951	0.0021	9020
TVAG_039980	Oxygen Stress Response	iron superoxide dismutase, putative	no		0.1061	3799	0.0011	11297
TVAG_385350	Oxygen Stress Response	Thioredoxin family protein	yes		0.0034	12005	0.0010	11779
TVAG_224980	Peptidases	peptidase T-like metallopeptidase	no		0.8507	858	0.9944	127
TVAG_386080	Peptidases	aminopeptidase P-like metallopeptidase	no		0.0006	19246	0.0547	2230
TVAG_233350	Peptidases	insulinase-like metallopeptidase	no		0.0922	4040	0.0013	10676
TVAG_119710	Peptidases	insulinase-like metallopeptidase	no		0.2700	2528	0.0003	18477
TVAG_082020	Peptidases	hypothetical protein	no		0.0000	40353	0.0000	41664
TVAG_190580	Peptidases	aminopeptidase P-like metallopeptidase	no		0.0000	46443	0.0000	54544
TVAG_371680	Proteasome Degradation	PCI domain containing protein	no		0.0000	34083	0.0000	35975
TVAG_184150	Proteome Degradation	polyubiquitin, putative	no		0.0021	13685	0.1027	1652
TVAG_112860	Proteome Degradation	Ubiquitin family protein	no		0.0004	21013	0.0006	13903
TVAG_237680	Putative Translocase and Carrier Proteins	hydrogenosomal membrane protein 31 precursor	no	positive	0.9999	71	0.9881	171
TVAG_104250	Putative Translocase and Carrier Proteins	hydrogenosomal membrane protein Hmp35	no	positive	1.0000	52	0.8476	406
TVAG_031860	Putative Translocase and Carrier Proteins	hypothetical protein	no		0.0002	24097	0.0060	5763
TVAG_198350	Putative Translocase and Carrier Proteins	Mitochondrial import Tim17 protein family	no		0.1041	3830	0.0015	10106
TVAG_178100	Putative Translocase and Carrier Proteins	hypothetical protein	no		0.1206	3611	0.0007	13290
TVAG_196220	Putative Translocase and Carrier Proteins	Mitochondrial carrier protein	no		0.0006	19283	0.0002	20615
TVAG_370860	Putative Translocase and Carrier Proteins	hypothetical protein	no		0.0774	4324	0.0001	25597
TVAG_164560	Putative Translocase and Carrier Proteins	Mitochondrial carrier protein	no		0.0001	32068	0.0001	29001

TVAG_216170	Putative Translocase and Carrier Proteins	hypothetical protein	no		0.0007	18489	0.0000	31128
TVAG_470110	Putative Translocase and Carrier Proteins	hypothetical protein	no		0.0003	22487	0.0000	38510
TVAG_008790	Putative Translocase and Carrier Proteins	hypothetical protein	no		0.0000	35801	0.0000	46595
TVAG_262210	Putative Translocase and Carrier Proteins	Mitochondrial carrier protein	no		0.0000	32982	0.0000	53333
TVAG_051820	Putative Translocase and Carrier Proteins	Mitochondrial carrier protein	no		0.0000	40206	0.0000	53519
TVAG_123100	Putative Translocase and Carrier Proteins	hypothetical protein	no		0.0000	33180	0.0000	55521
TVAG_110140	Ribosomal and Associated Proteins	ubiquitin, putative	no		0.0009	17212	0.0744	1895
TVAG_172530	Ribosomal and Associated Proteins	hypothetical protein	no		0.0307	6015	0.0617	2130
TVAG_119970	Ribosomal and Associated Proteins	hypothetical protein	no		0.0941	4013	0.0030	7805
TVAG_067400	Ribosomal and Associated Proteins	elongation factor 1 alpha, putative	no		0.0054	10355	0.0011	11365
TVAG_283020	Ribosomal and Associated Proteins	translation initiation factor eIF-5A family protein	no		0.0001	28339	0.0001	23537
TVAG_276410	Ribosomal and Associated Proteins	hypothetical protein	no		0.0000	48921	0.0001	24866
TVAG_045340	Ribosomal and Associated Proteins	hypothetical protein	no		0.0005	20315	0.0000	30998
TVAG_248450	Ribosomal and Associated Proteins	conserved hypothetical protein	no		0.0005	20890	0.0000	31512
TVAG_047460	Ribosomal and Associated Proteins	Ribosomal S3Ae, putative	no	negative	0.0000	58839	0.0000	51457
TVAG_061890	Ribosomal and Associated Proteins	ribosomal protein L18ae, putative	no	negative	0.0000	58334	0.0000	53011
TVAG_054130	Ribosomal and Associated Proteins	60S ribosomal protein L7-2, putative	no	negative	0.0000	59043	0.0000	54747
TVAG_380910	Ribosomal and Associated Proteins	eukaryotic translation initiation factor, putative	no	negative	0.0000	59138	0.0000	54929
TVAG_319220	Ribosomal and Associated Proteins	Ribosomal protein S24e, putative	no	negative	0.0000	58408	0.0000	56098
TVAG_178000	Ribosomal and Associated Proteins	ribosomal protein L23, putative	no	negative	0.0000	58705	0.0000	57034
TVAG_272970	Ribosomal and Associated Proteins	Ribosomal protein S24e, putative	no		0.0000	58747	0.0000	58431
TVAG_098450	Ribosomal and Associated Proteins	40S ribosomal protein S4-C, putative	no	negative	0.0000	59359	0.0000	58910
TVAG_020040	Ribosomal and Associated Proteins	40S ribosomal protein S16, putative	no	negative	0.0000	59461	0.0000	58946
TVAG_005910	Ribosomal and Associated Proteins	ribosomal protein L8, putative	no	negative	0.0000	59289	0.0000	59013

TVAG_064640	Ribosomal and Associated Proteins	ribosomal protein L5	no	negative	0.0000	59280	0.0000	59157
TVAG_265950	Ribosomal and Associated Proteins	Ribosomal protein L32, putative	no	negative	0.0000	59338	0.0000	59207
TVAG_142440	Ribosomal and Associated Proteins	hypothetical protein	no	negative	0.0000	59302	0.0000	59230
TVAG_074610	Ribosomal and Associated Proteins	ribosomal protein, putative	no	negative	0.0000	59301	0.0000	59239
TVAG_112230	Ribosomal and Associated Proteins	Ribosomal protein L13e, putative	no	negative	0.0000	59458	0.0000	59242
TVAG_044560	Ribosomal and Associated Proteins	60S ribosomal protein L11, putative	no	negative	0.0000	59400	0.0000	59263
TVAG_066030	Ribosomal and Associated Proteins	hypothetical protein	no	negative	0.0000	59506	0.0000	59290
TVAG_051160	Ribosomal and Associated Proteins	ribosomal protein L10, putative	no	negative	0.0000	59352	0.0000	59298
TVAG_240050	Ribosomal and Associated Proteins	ribosomal protein, putative	no	negative	0.0000	59351	0.0000	59316
TVAG_120180	Ribosomal and Associated Proteins	Plectin/S10 domain containing protein	no	negative	0.0000	59376	0.0000	59317
TVAG_074480	Ribosomal and Associated Proteins	ribosomal protein L10a	no	negative	0.0000	59394	0.0000	59324
TVAG_182520	Ribosomal and Associated Proteins	Ribosomal protein L13e, putative	no	negative	0.0000	59413	0.0000	59328
TVAG_423320	Ribosomal and Associated Proteins	Ribosomal protein L13e, putative	no	negative	0.0000	59483	0.0000	59328
TVAG_020480	Ribosomal and Associated Proteins	ribosomal protein S13p/S18e, putative	no	negative	0.0000	59454	0.0000	59334
TVAG_121550	Ribosomal and Associated Proteins	hypothetical protein	no	negative	0.0000	59521	0.0000	59340
TVAG_006250	Ribosomal and Associated Proteins	ribosomal protein S15a	no	negative	0.0000	59449	0.0000	59362
TVAG_128790	Ribosomal and Associated Proteins	ribosomal protein, putative	no	negative	0.0000	59419	0.0000	59372
TVAG_106800	Ribosomal and Associated Proteins	Ribosomal protein S3, putative	no	negative	0.0000	59460	0.0000	59383
TVAG_083260	Ribosomal and Associated Proteins	ribosomal protein L22, putative	no	negative	0.0000	59370	0.0000	59384
TVAG_101690	Ribosomal and Associated Proteins	Ribosomal protein L24e, putative	no	negative	0.0000	59294	0.0000	59390
TVAG_348090	Ribosomal and Associated Proteins	Ribosomal S3Ae, putative	no	negative	0.0000	59345	0.0000	59397
TVAG_152720	Ribosomal and Associated Proteins	40S ribosomal protein S14, putative	no	negative	0.0000	59263	0.0000	59433
TVAG_117480	Ribosomal and Associated Proteins	ribosomal protein S14	no	negative	0.0000	59355	0.0000	59435
TVAG_054500	Ribosomal and Associated Proteins	ribosomal protein L6, putative	no	negative	0.0000	59450	0.0000	59438

TVAG_121100	Ribosomal and Associated Proteins	60S ribosomal protein L18, putative	no	negative	0.0000	59505	0.0000	59441
TVAG_342830	Ribosomal and Associated Proteins	ribosomal protein S14, putative	no	negative	0.0000	59365	0.0000	59452
TVAG_119330	Ribosomal and Associated Proteins	ribosomal protein L21e, putative	no	negative	0.0000	59392	0.0000	59457
TVAG_370550	Ribosomal and Associated Proteins	Ribosomal protein S6e, putative	no	negative	0.0000	59444	0.0000	59466
TVAG_014160	Ribosomal and Associated Proteins	60S ribosomal protein L12, putative	no		0.0000	59520	0.0000	59468
TVAG_482430	Ribosomal and Associated Proteins	60S ribosomal protein L18, putative	no	negative	0.0000	59423	0.0000	59473
TVAG_015800	Ribosomal and Associated Proteins	60S ribosomal protein L23, putative	no	negative	0.0000	59308	0.0000	59477
TVAG_299380	Ribosomal and Associated Proteins	ribosomal protein S14, putative	no	negative	0.0000	59241	0.0000	59485
TVAG_148950	Ribosomal and Associated Proteins	60S ribosomal protein L15-1, putative	no	negative	0.0000	59427	0.0000	59486
TVAG_013060	Ribosomal and Associated Proteins	hypothetical protein	no	negative	0.0000	59503	0.0000	59489
TVAG_040820	Ribosomal and Associated Proteins	40S ribosomal protein S17-B, putative	no	negative	0.0000	59624	0.0000	59512
TVAG_033590	Ribosomal and Associated Proteins	Ribosomal protein S6e, putative	no	negative	0.0000	59474	0.0000	59527
TVAG_041350	Ribosomal and Associated Proteins	hypothetical protein	no	negative	0.0000	59426	0.0000	59529
TVAG_094720	Ribosomal and Associated Proteins	Ribosomal protein L34e, putative	no	negative	0.0000	59403	0.0000	59545
TVAG_006170	Ribosomal and Associated Proteins	60S ribosomal protein L19-3, putative	no	negative	0.0000	59360	0.0000	59593
TVAG_464120	Ribosomal and Associated Proteins	ribosomal protein S14, putative	no	negative	0.0000	59386	0.0000	59601
TVAG_038050	Ribosomal and Associated Proteins	hypothetical protein	no	negative	0.0000	59499	0.0000	59622
TVAG_071920	Ribosomal and Associated Proteins	40S ribosomal protein S23, putative	no	negative	0.0000	59608	0.0000	59653
TVAG_218150	Signaling	Adenylate and Guanylate cyclase catalytic domain containing protein	no		0.9515	558	0.3595	899
TVAG_169060	Signaling	Cdc42 homolog, putative	no		0.0002	24797	0.0002	18840
TVAG_026290	Signaling	hypothetical protein	no		0.0005	19877	0.0001	22834
TVAG_491610	Signaling	protein kinase, putative	no		0.0003	23677	0.0001	27794
TVAG_464010	Signaling	Calreticulin family protein	no		0.0000	41264	0.0001	28973
TVAG_204940	Signaling	Calreticulin family protein	no		0.0000	50569	0.0000	48144
TVAG_453070	Small GTPases and Associated Proteins	Ras-related protein R-Ras2, putative	no		0.0007	18158	0.1236	1528
TVAG_134510	Small GTPases and Associated Proteins	guanine nucleotide regulatory protein, putative	no		0.0287	6163	0.0774	1853

TVAG_446980	Small GTPases and Associated Proteins	GTP-binding protein, putative	no		0.0049	10636	0.0764	1872
TVAG_383350	Small GTPases and Associated Proteins	GTP-binding protein YPTM2, putative	no		0.7808	1049	0.0483	2348
TVAG_047800	Small GTPases and Associated Proteins	Ras-like GTP-binding protein YPT1, putative	no		0.4044	1994	0.0206	3375
TVAG_499340	Small GTPases and Associated Proteins	hypothetical protein	no		0.0031	12287	0.0124	4238
TVAG_362470	Small GTPases and Associated Proteins	small GTP-binding protein, putative	no		0.0002	25300	0.0050	6192
TVAG_390750	Small GTPases and Associated Proteins	small GTP-binding protein, putative	no		0.2865	2442	0.0047	6454
TVAG_220970	Small GTPases and Associated Proteins	small GTP-binding protein, putative	no		0.0444	5335	0.0044	6747
TVAG_415960	Small GTPases and Associated Proteins	small GTP-binding protein, putative	no		0.0030	12475	0.0041	6859
TVAG_395100	Small GTPases and Associated Proteins	small GTP-binding protein, putative	no		0.0238	6557	0.0024	8533
TVAG_106390	Small GTPases and Associated Proteins	small GTP-binding protein, putative	no		0.0000	35954	0.0018	9647
TVAG_121740	Small GTPases and Associated Proteins	Ras family protein	no		0.0045	10957	0.0017	9813
TVAG_393370	Small GTPases and Associated Proteins	small GTP-binding protein, putative	no		0.0093	8808	0.0015	10196
TVAG_185340	Small GTPases and Associated Proteins	Ras family protein	no		0.0165	7349	0.0015	10241
TVAG_070500	Small GTPases and Associated Proteins	hypothetical protein	no		0.0848	4167	0.0015	10253
TVAG_056480	Small GTPases and Associated Proteins	small GTP-binding protein, putative	no		0.0012	15816	0.0014	10366
TVAG_056930	Small GTPases and Associated Proteins	small GTP-binding protein, putative	no		0.0000	52441	0.0014	10394
TVAG_484100	Small GTPases and Associated Proteins	small GTP-binding protein, putative	no		0.0046	10892	0.0013	10748
TVAG_150540	Small GTPases and Associated Proteins	small GTP-binding protein, putative	no		0.0007	18227	0.0012	11080
TVAG_126970	Small GTPases and Associated Proteins	GDP dissociation inhibitor family protein	no		0.0008	18093	0.0010	11652
TVAG_128860	Small GTPases and Associated Proteins	Ras family protein	no		0.0694	4508	0.0009	12217
TVAG_379850	Small GTPases and Associated Proteins	GTP-binding protein YPTM1, putative	no		0.2422	2669	0.0007	13469
TVAG_261280	Small GTPases and Associated Proteins	small GTP-binding protein, putative	no		0.0110	8344	0.0007	13701
TVAG_383530	Small GTPases and Associated Proteins	small GTP-binding protein, putative	no		0.0001	27211	0.0006	14106
TVAG_081590	Small GTPases and Associated Proteins	small GTP-binding protein, putative	no		0.0427	5410	0.0006	14338

TVAG_136740	Small GTPases and Associated Proteins	small GTP-binding protein, putative	no		0.1249	3567	0.0006	14570
TVAG_211200	Small GTPases and Associated Proteins	small GTP-binding protein, putative	no		0.0013	15709	0.0005	15411
TVAG_159810	Small GTPases and Associated Proteins	small GTP-binding protein, putative	no		0.0001	30277	0.0004	15696
TVAG_192440	Small GTPases and Associated Proteins	small GTP-binding protein, putative	no		0.0160	7426	0.0004	15779
TVAG_416520	Small GTPases and Associated Proteins	hypothetical protein	no		0.0002	25596	0.0004	16210
TVAG_093060	Small GTPases and Associated Proteins	Ras family protein	no		0.0000	34336	0.0003	17145
TVAG_349870	Small GTPases and Associated Proteins	small GTP-binding protein, putative	no		0.0574	4868	0.0003	17450
TVAG_456910	Small GTPases and Associated Proteins	small GTP-binding protein, putative	no		0.0000	41033	0.0003	17517
TVAG_384490	Small GTPases and Associated Proteins	small GTP-binding protein, putative	no		0.0869	4135	0.0003	17928
TVAG_158270	Small GTPases and Associated Proteins	small GTP-binding protein, putative	no		0.0002	25943	0.0002	21058
TVAG_397350	Small GTPases and Associated Proteins	small GTP-binding protein, putative	no		0.0001	28662	0.0002	21387
TVAG_328110	Small GTPases and Associated Proteins	small GTP-binding protein, putative	no		0.0019	14195	0.0002	21420
TVAG_079570	Small GTPases and Associated Proteins	small GTP-binding protein, putative	no		0.0837	4183	0.0002	21523
TVAG_409800	Small GTPases and Associated Proteins	small GTP-binding protein, putative	no		0.0001	31270	0.0002	21756
TVAG_079630	Small GTPases and Associated Proteins	hypothetical protein	no		0.0011	16551	0.0002	22119
TVAG_044270	Small GTPases and Associated Proteins	small GTP-binding protein, putative	no		0.0011	16347	0.0002	22214
TVAG_404940	Small GTPases and Associated Proteins	small GTP-binding protein, putative	no		0.0001	27818	0.0002	22217
TVAG_104710	Small GTPases and Associated Proteins	small GTP-binding protein, putative	no		0.0005	20216	0.0001	22856
TVAG_498380	Small GTPases and Associated Proteins	small GTP-binding protein, putative	no		0.0249	6469	0.0001	23293
TVAG_462370	Small GTPases and Associated Proteins	small GTP-binding protein, putative	no		0.0209	6877	0.0001	23980
TVAG_216900	Small GTPases and Associated Proteins	Ras family protein	no		0.0000	44163	0.0001	24307
TVAG_169740	Small GTPases and Associated Proteins	Ras-related protein Rab11C, putative	no		0.0000	53701	0.0001	24832
TVAG_065320	Small GTPases and Associated Proteins	small GTP-binding protein, putative	no		0.0014	15452	0.0001	25535
TVAG_151010	Small GTPases and Associated Proteins	small GTP-binding protein, putative	no		0.0062	9911	0.0001	26201

TVAG_124590	Small GTPases and Associated Proteins	small GTP-binding protein, putative	no		0.0173	7245	0.0001	26427
TVAG_124540	Small GTPases and Associated Proteins	small GTP-binding protein, putative	no		0.0004	21323	0.0001	26686
TVAG_139270	Small GTPases and Associated Proteins	small GTP-binding protein, putative	no		0.0015	15079	0.0001	26818
TVAG_320200	Small GTPases and Associated Proteins	Ras family protein	no		0.0010	16979	0.0001	26827
TVAG_329350	Small GTPases and Associated Proteins	small GTP-binding protein, putative	no		0.0072	9481	0.0001	28365
TVAG_241150	Small GTPases and Associated Proteins	small GTP-binding protein, putative	no		0.0023	13431	0.0001	28536
TVAG_051830	Small GTPases and Associated Proteins	small GTP-binding protein, putative	no		0.0107	8395	0.0001	29096
TVAG_377960	Small GTPases and Associated Proteins	Ras family protein	no		0.0000	43178	0.0001	29113
TVAG_190510	Small GTPases and Associated Proteins	small GTP-binding protein, putative	no		0.0035	11899	0.0000	30826
TVAG_379590	Small GTPases and Associated Proteins	Ras family protein	no		0.0000	41085	0.0000	31036
TVAG_076670	Small GTPases and Associated Proteins	small GTP-binding protein, putative	no		0.0000	37333	0.0000	31136
TVAG_048600	Small GTPases and Associated Proteins	small GTP-binding protein, putative	no		0.0001	27458	0.0000	31516
TVAG_018050	Small GTPases and Associated Proteins	small GTP-binding protein, putative	no		0.0072	9480	0.0000	31540
TVAG_282070	Small GTPases and Associated Proteins	small GTP-binding protein, putative	no		0.0248	6487	0.0000	32133
TVAG_402160	Small GTPases and Associated Proteins	RasGEF domain containing protein	no		0.0059	10104	0.0000	32826
TVAG_371280	Small GTPases and Associated Proteins	small GTP-binding protein, putative	no		0.0024	13226	0.0000	33570
TVAG_249220	Small GTPases and Associated Proteins	small GTP-binding protein, putative	no		0.0012	15838	0.0000	33619
TVAG_122340	Small GTPases and Associated Proteins	small GTP-binding protein, putative	no		0.0002	26223	0.0000	34152
TVAG_430220	Small GTPases and Associated Proteins	small GTP-binding protein, putative	no		0.0000	40656	0.0000	34627
TVAG_112840	Small GTPases and Associated Proteins	small GTP-binding protein, putative	no		0.0003	23031	0.0000	35469
TVAG_178380	Small GTPases and Associated Proteins	XRP2, putative	no		0.0007	18546	0.0000	35594
TVAG_459470	Small GTPases and Associated Proteins	small GTP-binding protein, putative	no		0.0005	20763	0.0000	35737
TVAG_446610	Small GTPases and Associated Proteins	small GTP-binding protein, putative	no		0.0000	33398	0.0000	37363
TVAG_194760	Small GTPases and Associated Proteins	Kelch motif family protein	no		0.0001	31151	0.0000	37579

TVAG_101260	Small GTPases and Associated Proteins	Ras family protein	no		0.0000	34562	0.0000	37663
TVAG_373310	Small GTPases and Associated Proteins	small GTP-binding protein, putative	no		0.0061	9959	0.0000	37727
TVAG_446990	Small GTPases and Associated Proteins	hypothetical protein	no		0.0109	8357	0.0000	38419
TVAG_055550	Small GTPases and Associated Proteins	small GTP-binding protein, putative	no		0.0002	24237	0.0000	38441
TVAG_308190	Small GTPases and Associated Proteins	small GTP-binding protein, putative	no		0.0019	14116	0.0000	39506
TVAG_161280	Small GTPases and Associated Proteins	small GTP-binding protein, putative	no		0.0023	13329	0.0000	39548
TVAG_300910	Small GTPases and Associated Proteins	Ras family protein	no		0.0037	11570	0.0000	39816
TVAG_029020	Small GTPases and Associated Proteins	small GTP-binding protein, putative	no		0.0027	12759	0.0000	40025
TVAG_136260	Small GTPases and Associated Proteins	small GTP-binding protein, putative	no		0.0011	16421	0.0000	40282
TVAG_006260	Small GTPases and Associated Proteins	small GTP-binding protein, putative	no		0.0005	20361	0.0000	40646
TVAG_504530	Small GTPases and Associated Proteins	small GTP-binding protein, putative	no		0.0001	28213	0.0000	40807
TVAG_462450	Small GTPases and Associated Proteins	small GTP-binding protein, putative	no		0.0002	26504	0.0000	41567
TVAG_060820	Small GTPases and Associated Proteins	small GTP-binding protein, putative	no		0.0000	41304	0.0000	41851
TVAG_350580	Small GTPases and Associated Proteins	Ras family protein	no		0.0001	27355	0.0000	42474
TVAG_122270	Small GTPases and Associated Proteins	small GTP-binding protein, putative	no		0.0032	12118	0.0000	42533
TVAG_434770	Small GTPases and Associated Proteins	small GTP-binding protein, putative	no		0.0000	34865	0.0000	42703
TVAG_454230	Small GTPases and Associated Proteins	Ras family protein	no		0.0003	22496	0.0000	43030
TVAG_159730	Small GTPases and Associated Proteins	small GTP-binding protein, putative	no		0.0600	4768	0.0000	43220
TVAG_036230	Small GTPases and Associated Proteins	Ras family protein	no		0.0797	4250	0.0000	43281
TVAG_201980	Small GTPases and Associated Proteins	small GTP-binding protein, putative	no		0.0953	3999	0.0000	43771
TVAG_193770	Small GTPases and Associated Proteins	Ras family protein	no		0.0132	7863	0.0000	44877
TVAG_212310	Small GTPases and Associated Proteins	small GTP-binding protein, putative	no		0.0007	18328	0.0000	45711
TVAG_080400	Small GTPases and Associated Proteins	small GTP-binding protein, putative	no		0.0000	42174	0.0000	46292
TVAG_236570	Small GTPases and Associated Proteins	Ras family protein	no		0.0510	5080	0.0000	47789

TVAG_024790	Small GTPases and Associated Proteins	small GTP-binding protein, putative	no		0.0011	16359	0.0000	47873
TVAG_090060	Small GTPases and Associated Proteins	small GTP-binding protein, putative	no		0.0027	12850	0.0000	47997
TVAG_320300	Small GTPases and Associated Proteins	Ras family protein	no		0.0008	17816	0.0000	48424
TVAG_257310	Small GTPases and Associated Proteins	small GTP-binding protein, putative	no		0.0056	10221	0.0000	50133
TVAG_364210	Small GTPases and Associated Proteins	small GTP-binding protein, putative	no		0.0008	17965	0.0000	50169
TVAG_283380	Small GTPases and Associated Proteins	hypothetical protein	no		0.0000	56334	0.0000	50618
TVAG_422690	Small GTPases and Associated Proteins	small GTP-binding protein, putative	no		0.0000	46008	0.0000	50722
TVAG_527180	Small GTPases and Associated Proteins	small GTP-binding protein, putative	no		0.0000	39292	0.0000	52460
TVAG_038950	Small GTPases and Associated Proteins	Ras family protein	no		0.0029	12530	0.0000	53112
TVAG_180430	Small GTPases and Associated Proteins	small GTP-binding protein, putative	no		0.0000	44009	0.0000	53240
TVAG_405730	Small GTPases and Associated Proteins	small GTP-binding protein, putative	no		0.0036	11696	0.0000	53507
TVAG_181000	Small GTPases and Associated Proteins	small GTP-binding protein, putative	no		0.0100	8599	0.0000	53756
TVAG_424920	Small GTPases and Associated Proteins	small GTP-binding protein, putative	no		0.0223	6729	0.0000	53834
TVAG_391930	Small GTPases and Associated Proteins	Ras family protein	no		0.0007	18443	0.0000	54018
TVAG_440690	Small GTPases and Associated Proteins	small GTP-binding protein, putative	no		0.0001	29509	0.0000	54531
TVAG_015270	Small GTPases and Associated Proteins	small GTP-binding protein, putative	no		0.0013	15738	0.0000	54548
TVAG_348580	Small GTPases and Associated Proteins	small GTP-binding protein, putative	no		0.0001	31190	0.0000	54646
TVAG_092740	Small GTPases and Associated Proteins	small GTP-binding protein, putative	no		0.0000	38062	0.0000	54827
TVAG_020610	Small GTPases and Associated Proteins	small GTP-binding protein, putative	no		0.0002	26435	0.0000	54847
TVAG_157610	Small GTPases and Associated Proteins	small GTP-binding protein, putative	no		0.0004	21760	0.0000	55094
TVAG_038420	Small GTPases and Associated Proteins	hypothetical protein	no		0.0000	56806	0.0000	55227
TVAG_278280	Small GTPases and Associated Proteins	small GTP-binding protein, putative	no		0.0001	29583	0.0000	55230
TVAG_008100	Small GTPases and Associated Proteins	small GTP-binding protein, putative	no		0.0012	15793	0.0000	55250
TVAG_101480	Small GTPases and Associated Proteins	small GTP-binding protein, putative	no		0.0000	34318	0.0000	56225

TVAG_442270	Small GTPases and Associated Proteins	small GTP-binding protein, putative	no		0.0004	21356	0.0000	56634
TVAG_075460	Small GTPases and Associated Proteins	small GTP-binding protein, putative	no		0.0117	8159	0.0000	56702
TVAG_340860	Small GTPases and Associated Proteins	Ras family protein	no		0.0000	35875	0.0000	56911
TVAG_351500	Small GTPases and Associated Proteins	Ras-like GTP-binding protein RYL1, putative	no		0.0000	55787	0.0000	57053
TVAG_147840	Small GTPases and Associated Proteins	small GTP-binding protein, putative	no		0.0000	34349	0.0000	57112
TVAG_297320	Small GTPases and Associated Proteins	Ras family protein	no		0.0005	20308	0.0000	57589
TVAG_074410	Small GTPases and Associated Proteins	small GTP-binding protein, putative	no		0.0001	28148	0.0000	57623
TVAG_331490	Small GTPases and Associated Proteins	Ras family protein	no		0.0022	13618	0.0000	57715
TVAG_006280	Small GTPases and Associated Proteins	Ras family protein	no		0.0054	10340	0.0000	57859
TVAG_185300	Small GTPases and Associated Proteins	small GTP-binding protein, putative	no		0.0017	14573	0.0000	58084
TVAG_085320	Small GTPases and Associated Proteins	small GTP-binding protein, putative	no		0.0008	18056	0.0000	58265
TVAG_038250	Small GTPases and Associated Proteins	Ras family protein	no		0.0014	15389	0.0000	58309
TVAG_370000	Small GTPases and Associated Proteins	small GTP-binding protein, putative	no		0.0007	18677	0.0000	58376
TVAG_185080	Small GTPases and Associated Proteins	hypothetical protein	no		0.0005	20751	0.0000	58834
TVAG_259320	Small GTPases and Associated Proteins	small GTP-binding protein, putative	no		0.0008	17912	0.0000	58863
TVAG_038190	Small GTPases and Associated Proteins	small GTP-binding protein, putative	no		0.0003	22818	0.0000	59091
TVAG_528800	Small GTPases and Associated Proteins	small GTP-binding protein, putative	no		0.0043	11139	0.0000	59095
TVAG_286490	Small GTPases and Associated Proteins	small GTP-binding protein, putative	no		0.0000	45618	0.0000	59338
TVAG_099490	Sugar Metabolism	ROK family protein	yes		1.0000	46	1.0000	24
TVAG_442070	Sugar Metabolism	ROK family protein	no		0.9979	170	0.9996	63
TVAG_491670	Sugar Metabolism	malic enzyme, putative	no		0.1645	3191	0.9773	207
TVAG_054830	Sugar Metabolism	Phosphoglucomutase/phosphomannomutase	no		0.8349	899	0.9681	239
TVAG_293770	Sugar Metabolism	Phosphofructokinase family protein	no		0.4768	1739	0.9551	261
TVAG_462920	Sugar Metabolism	Phosphofructokinase family protein	no		0.0492	5140	0.8455	407
TVAG_496160	Sugar Metabolism	Phosphofructokinase family protein	no		0.0112	8287	0.8378	411
TVAG_391760	Sugar Metabolism	Phosphofructokinase family protein	no		0.9949	236	0.8229	424
TVAG_205910	Sugar Metabolism	Phosphoglucomutase/phosphomannomutase	no		0.8286	924	0.7084	522
TVAG_258220	Sugar Metabolism	glycosyl transferase, group 1 family protein	no		0.9987	153	0.6230	605

TVAG_073860	Sugar Metabolism	pyruvate, phosphate dikinase family protein	no		0.4316	1908	0.6168	609
TVAG_006140	Sugar Metabolism	6-phosphogluconate dehydrogenase, putative	no		0.6273	1395	0.5286	708
TVAG_263740	Sugar Metabolism	enolase family protein	no		0.0653	4624	0.2764	1054
TVAG_430830	Sugar Metabolism	pi-dependent fructose 6-P 1-phosphotransferase	no		0.1838	3025	0.1604	1375
TVAG_079260	Sugar Metabolism	Pi-dependent fructose 6-P 1-phosphotransferase	no		0.6325	1384	0.0977	1683
TVAG_212020	Sugar Metabolism	transketolase family protein	no		0.0079	9220	0.0883	1747
TVAG_253650	Sugar Metabolism	malate dehydrogenase, putative	no		0.8081	986	0.0490	2336
TVAG_276310	Sugar Metabolism	1,4-alpha-glucan branching enz. IIB, chloroplast put.	no		0.1371	3460	0.0322	2722
TVAG_154680	Sugar Metabolism	4-alpha-glucanotransferase family protein	no		0.0128	7946	0.0253	3044
TVAG_282580	Sugar Metabolism	phosphoglycerate mutase family protein	no		0.0000	46810	0.0096	4739
TVAG_464170	Sugar Metabolism	enolase 4, putative	no		0.9253	640	0.0077	5169
TVAG_373720	Sugar Metabolism	pyruvate kinase family protein	no		0.0270	6302	0.0053	6065
TVAG_045010	Sugar Metabolism	hypothetical protein	no		0.7728	1074	0.0032	7641
TVAG_043500	Sugar Metabolism	enolase 3, putative	no	negative	0.0000	34003	0.0031	7735
TVAG_222040	Sugar Metabolism	4-alpha-glucanotransferase family protein	no		0.8325	908	0.0030	7921
TVAG_204360	Sugar Metabolism	malate dehydrogenase, putative	no		0.8687	820	0.0029	7961
TVAG_226870	Sugar Metabolism	4-alpha-glucanotransferase family protein	no		0.0011	16578	0.0020	9294
TVAG_113710	Sugar Metabolism	phosphoglycerate mutase, putative	no		0.0011	16377	0.0015	10172
TVAG_329460	Sugar Metabolism	enolase 2, putative	no		0.0001	29225	0.0006	14342
TVAG_157940	Sugar Metabolism	4-alpha-glucanotransferase family protein	no		0.0019	14222	0.0003	17589
TVAG_348330	Sugar Metabolism	glycogen phosphorylase	no		0.0066	9740	0.0001	23690
TVAG_204370	Sugar Metabolism	hypothetical protein	no		0.0004	21928	0.0001	24539
TVAG_092750	Sugar Metabolism	hypothetical protein	no		0.0000	37900	0.0001	25490
TVAG_146910	Sugar Metabolism	hypothetical protein	no		0.0001	27095	0.0001	27744
TVAG_397250	Sugar Metabolism	hypothetical protein	no		0.0019	14217	0.0000	33752
TVAG_381690	Sugar Metabolism	AT5g28840/F7P1_20, putative	no		0.0002	24848	0.0000	35357
TVAG_336940	Sugar Metabolism	hypothetical protein	no		0.0001	30727	0.0000	35567
TVAG_191140	Sugar Metabolism	Starch binding domain containing protein	no		0.0598	4775	0.0000	37733
TVAG_268050	Sugar Metabolism	Phosphoglycerate kinase, putative	no	negative	0.0000	51404	0.0000	42928
TVAG_383940	Sugar Metabolism	Phosphoglycerate kinase, putative	no		0.0000	37238	0.0000	44491
TVAG_061930	Sugar Metabolism	glucose-6-phosphate isomerase family protein	no	negative	0.0000	46152	0.0000	49424
TVAG_360700	Sugar Metabolism	fructose-1,6-bisphosphate aldolase, putative	no		0.0000	57503	0.0000	53276
TVAG_043060	Sugar Metabolism	fructose-1,6-bisphosphate aldolase	no		0.0000	55620	0.0000	56270
TVAG_300000	Sugar Metabolism	fructose-1,6-bisphosphate aldolase, putative	no		0.0000	57896	0.0000	56380
TVAG_148040	Vesicle Association	ADP-ribosylation factor 1, putative	no		0.0000	34190	0.0009	12059

TVAG_369020	Vesicle Association	Region in Clathrin and VPS family protein	no		0.0010	16820	0.0009	12151
TVAG_249080	Vesicle Association	Synaptobrevin family protein	no		0.0449	5302	0.0004	15876
TVAG_450230	Vesicle Association	Adaptor complexes medium subunit family protein	no		0.0002	26274	0.0002	18908
TVAG_071140	Vesicle Association	Clathrin adaptor complex small chain family protein	no		0.0000	39920	0.0002	19793
TVAG_562550	Vesicle Association	clathrin heavy chain-related protein	no		0.0000	41156	0.0001	27539
TVAG_064150	Vesicle Association	ADP-ribosylation factor, putative	no		0.0000	34577	0.0000	30636
TVAG_547230	Vesicle Association	Adaptin N terminal region family protein	no		0.0000	40813	0.0000	31616
TVAG_369030	Vesicle Association	Clathrin and VPS domain-containing protein	no		0.0000	40440	0.0000	33621
TVAG_379690	Vesicle Association	Clathrin adaptor complex small chain family protein	no		0.0000	35510	0.0000	37967
TVAG_044240	Vesicle Association	Adaptin N terminal region family protein	no		0.0019	14100	0.0000	43636
TVAG_532880	Vesicle Association	Clathrin and VPS domain-containing protein	no		0.0006	19155	0.0000	57151

Supplementary Table 2- 2. Predicted MOT+ and MOT- scores of identified hydrogenosomal proteins. Predicted MOT+ and MOT- scores are assigned to proteins identified in the *T. vaginalis* hydrogenosome proteome (Schneider et al., 2011). Scores and ranks from Burstein et al., 2012 were matched to each protein. In addition, the presence or absence of recognized hydrogenosome targeting sequence (HTS) is indicated (yes or no). Burstein et al. used certain proteins as true positives, as they had been previously found to localize to the hydrogenosome. These are annotated as "positive" in the "Class in training set" column. Those indicated as "negative" are proteins believed to be strictly cytosolic based on TrichDB annotation and GO analysis. Ribosomal proteins were classified as negative, especially as protein synthesis does not happen in the hydrogenosome. Interestingly, some ribosomal proteins and few other "negative" proteins were found in this proteome, and indicated as "negative"; all other proteins that were not used in training the algorithm are blank.

References:

1. Schwebke JR, Burgess D. Trichomoniasis. *Clin Microbiol Rev*. 2004;17(4):794-803. doi:10.1128/CMR.17.4.794-803.2004

2. Newman L, Rowley J, Hoorn S Vander, et al. Global Estimates of the Prevalence and Incidence of Four Curable Sexually Transmitted Infections in 2012 Based on Systematic Review and Global Reporting. *PLoS One*. 2015;10(12). doi:10.1371/journal.pone.0143304

3. Meites E, Gaydos CA, Hobbs MM, et al. A Review of Evidence-Based Care of Symptomatic Trichomoniasis and Asymptomatic Trichomonas vaginalis Infections. *Clin Infect Dis*. 2015. doi:10.1093/cid/civ738

4. Workowski KA, Bolan GA. Sexually transmitted diseases treatment guidelines, 2015. *MMWR Recomm Reports*. 2015;64(3):1-138. doi:10.1016/j.annemergmed.2015.07.526

5. Muller M, Lindmark DG. Uptake of metronidazole and its effect on viability in trichomonads and Entamoeba invadens under anaerobic and aerobic conditions. *Antimicrob Agents Chemother*. 1976;9(4):696-700. doi:10.1128/AAC.9.4.696

6. Leitsch D, Kolarich D, Binder M, Stadlmann J, Altmann F, Duchêne M. Trichomonas vaginalis: Metronidazole and other nitroimidazole drugs are reduced by the flavin enzyme thioredoxin reductase and disrupt the cellular redox system. Implications for nitroimidazole toxicity and resistance. *Mol Microbiol*. 2009;72(2):518-536. doi:10.1111/j.1365-2958.2009.06675.x

7. Yarlett N, Gorrell TE, Marczak R, Müller M. Reduction of nitroimidazole derivatives by hydrogenosomal extracts of Trichomonas vaginalis. *Mol Biochem Parasitol*. 1985;14(1):29-40. doi:10.1016/0166-6851(85)90103-3

8. Jorgensen MA, Trend MA, Hazell SL, Mendz GL. Potential involvement of several nitroreductases in metronidazole resistance in Helicobacter pylori. *Arch Biochem Biophys*. 2001;392(2):180-191. doi:10.1006/abbi.2001.2427

9. Hrdý I, Cammack R, Stopka P, Kulda J, Tachezy J. Alternative pathway of metronidazole activation in Trichomonas vaginalis hydrogenosomes. *Antimicrob Agents Chemother*. 2005;49(12):5033-5036. doi:10.1128/AAC.49.12.5033-5036.2005

10. Leitsch D, Kolarich D, Wilson IBH, Altmann F, Duchêne M. Nitroimidazole action in Entamoeba histolytica: A central role for thioredoxin reductase. *PLoS Biol*. 2007;5(8):1820-1834. doi:10.1371/journal.pbio.0050211

11. Leitsch D, Schlosser S, Burgess A, Duchêne M. Nitroimidazole drugs vary in their mode of action in the human parasite Giardia lamblia. *Int J Parasitol Drugs Drug Resist*. 2012;2:166-170. doi:10.1016/j.ijpddr.2012.04.002

12. Shiflett AM, Johnson PJ. Mitochondrion-Related Organelles in Eukaryotic Protists. *Annu Rev Microbiol*. 2010;64(1):409-429. doi:10.1146/annurev.micro.62.081307.162826

13. Leitsch D, Kolarich D, Duchêne M. The flavin inhibitor diphenyleneiodonium renders Trichomonas vaginalis resistant to metronidazole, inhibits thioredoxin reductase and flavin reductase, and shuts off hydrogenosomal enzymatic pathways. *Mol Biochem Parasitol*. 2010;171(1):17-24. doi:10.1016/j.molbiopara.2010.01.001

14. Moreno SNJ, Mason RP, Docampo R. Distinct reduction of nitrofurans and metronidazole to free radical metabolites by Tritrichomonas foetus hydrogenosomal and cytosolic enzymes. *J Biol Chem*. 1984.

15. Kolb HC, Finn MG, Sharpless KB. Click Chemistry: Diverse Chemical Function from a Few Good Reactions. *Angew Chemie Int Ed*. 2001;40(11):2004-2021. doi:10.1002/1521-3773(20010601)40:11<2004::AID-ANIE2004>3.0.CO;2-5

16. Carlton JM, Hirt RP, Silva JC, et al. Draft genome sequence of the sexually transmitted pathogen Trichomonas vaginalis. *Science (80-)*. 2007;315(5809):207-212. doi:10.1126/science.1132894

17. Leitsch D, Janssen BD, Kolarich D, Johnson PJ, Duchêne M. Trichomonas vaginalis flavin reductase 1 and its role in metronidazole resistance. *Mol Microbiol*.

2014;91(1):198-208. doi:10.1111/mmi.12455

18. West SB, Wislocki PG, Fiorentini KM, Alvaro R, Wolf FJ, Lu AYH. Drug residue formation from ronidazole, a 5-nitroimidazole. I. Characterization of in vitro protein alkylation. *Chem Biol Interact*. 1982;41(3):265-279. doi:10.1016/0009-2797(82)90105-3

19. Dunne RL, Dunn LA, Upcroft P, O'Donoghue PJ, Upcroft JA. Drug resistance in the sexually transmitted protozoan Trichomonas vaginalis. *Cell Res*. 2003;13(4):239-249. doi:10.1038/sj.cr.7290169

20. D506-D515. UniProt: a worldwide hub of protein knowledge The UniProt Consortium. *Nucleic Acids Res*. 2019;47. doi:10.1093/nar/gky1049

21. Mentel M, Zimorski V, Haferkamp P, Martin W, Henze K. Protein import into hydrogenosomes of Trichomonas vaginalis involves both N-terminal and internal targeting signals: A case study of thioredoxin reductases. *Eukaryot Cell*. 2008;7(10):1750-1757. doi:10.1128/EC.00206-08

22. Schneider RE, Brown MT, Shiflett AM, et al. The Trichomonas vaginalis hydrogenosome proteome is highly reduced relative to mitochondria, yet complex compared with mitosomes. *Int J Parasitol*. 2011;41(13-14):1421-1434. doi:10.1016/j.ijpara.2011.10.001

23. Aurrecoechea C, Brestelli J, Brunk BP, et al. GiardiaDB and TrichDB: integrated genomic resources for the eukaryotic protist pathogens Giardia lamblia and Trichomonas vaginalis. *Nucleic Acids Res*. 2009;37. doi:10.1093/nar/gkn631

24. Arese P, Cappuccinelli P. Glycolysis and pentose phosphate cycle in Trichomonas vaginalis: I. Enzyme activity pattern and the constant proportion quintet. *Int J Biochem*. 1974;5(11-12):859-865. doi:10.1016/0020-711X(74)90121-9

25. Binns D, Dimmer E, Huntley R, Barrell D, O'donovan C, Apweiler R. QuickGO: a web-based tool for Gene Ontology searching. *Bioinforma Appl NOTE*. 2009;25(22):3045-3046. doi:10.1093/bioinformatics/btp536

26. Kelley LA, Mezulis S, Yates CM, Wass MN, Sternberg MJE. The Phyre2 web portal for protein modeling, prediction and analysis. *Nat Protoc*. 2015;10(6):845-858. doi:10.1038/nprot.2015.053

27. Kulda J. Trichomonads, hydrogenosomes and drug resistance. *Int J Parasitol*. 1999;29(2):199-212. doi:10.1016/S0020-7519(98)00155-6

28. Burstein D, Gould SB, Zimorski V, et al. A machine learning approach to identify hydrogenosomal proteins in trichomonas vaginalis. *Eukaryot Cell*. 2012;11(2):217-228. doi:10.1128/EC.05225-11

29. Debard S, Bader G, De Craene JO, et al. Nonconventional localizations of cytosolic aminoacyl-tRNA synthetases in yeast and human cells. *Methods*. 2017;113:91-104. doi:10.1016/j.ymeth.2016.09.017

30. Backus KM. Applications of reactive cysteine profiling. In: *Current Topics in Microbiology and Immunology*. Vol 420. Springer Verlag; 2019:375-417. doi:10.1007/82_2018_120

31. Leitsch D. Drug susceptibility testing in microaerophilic parasites: Cysteine strongly affects the effectivities of metronidazole and auranofin, a novel and promising antimicrobial. *Int J Parasitol Drugs Drug Resist*. 2017;7(3):321-327. doi:10.1016/j.ijpddr.2017.09.001

32. Alderete JF. Antigen analysis of several pathogenic strains of Trichomonas vaginalis. *Infect Immun*. 1983;39(3):1041-1047.

33. Backus KM, Correia BE, Lum KM, et al. Proteome-wide covalent ligand discovery in native biological systems. *Nature*. 2016;534(7608):570-574. doi:10.1038/nature18002

34. Abo M, Li C, Weerapana E. Isotopically-Labeled Iodoacetamide-Alkyne Probes for Quantitative Cysteine-Reactivity Profiling. *Mol Pharm*. 2018;15(3):743-749. doi:10.1021/acs.molpharmaceut.7b00832

35. Xu JH, Eberhardt J, Hill-Payne B, et al. Integrative X-ray Structure and Molecular Modeling for the Rationalization of Procaspase-8 Inhibitor Potency and Selectivity. *ACS Chem Biol*. 2020;15(2):575-586. doi:10.1021/acschembio.0c00019

36. Cao J, Armenta E, Boatner L, et al. Suzuki–Miyaura cross-coupling for chemoproteomic applications. April 2020. doi:10.26434/CHEMRXIV.12055218.V1

37. Hughes CS, Moggridge S, Müller T, Sorensen PH, Morin GB, Krijgsveld J. Single-pot, solid-phase-enhanced sample preparation for proteomics experiments. *Nat Protoc*. 2019;14(1):68-85. doi:10.1038/s41596-018-0082-x

38. Girard M, Clairmont F, Maneckjee A, Mousseau N, Dawson BA, Whitehouse LW. 5-Nitroimidazoles. II: Unexpected reactivity of ronidazole and dimetridazole with thiols. *Can J Chem*. 1993;71(9):1349-1352. doi:10.1139/v93-174

39. Nagy M, Lacroute F, Thomas D. Divergent evolution of pyrimidine biosynthesis between anaerobic and aerobic yeasts. *Proc Natl Acad Sci U S A*. 1992;89(19):8966-8970. doi:10.1073/pnas.89.19.8966

40. Heyworth PG, Gutteridge WE, Ginger CD. Pyrimidine metabolism in *Trichomonas vaginalis*. *FEBS Lett*. 1984;176(1):55-60. doi:10.1016/0014-5793(84)80910-2

41. Yang Y, Yang X, Verhelst SHL. Comparative analysis of click chemistry mediated activity-based protein profiling in cell lysates. *Molecules*. 2013;18(10):12599-12608. doi:10.3390/molecules181012599

42. Ings RMJ, McFadzean JA, Ormerod WE. The mode of action of metronidazole in Trichomonas vaginalis and other micro-organisms. *Biochem Pharmacol*. 1974;23(9):1421-1429. doi:10.1016/0006-2952(74)90362-1

43. De Miguel N, Lustig G, Twu O, Chattopadhyay A, Wohlschlegel JA, Johnson PJ. Proteome analysis of the surface of trichomonas vaginalis reveals novel proteins and strain-dependent differential expression. *Mol Cell Proteomics*. 2010;9(7):1554-1566. doi:10.1074/mcp.M000022-MCP201

44. Clark CG, Diamond LS. Methods for cultivation of luminal parasitic protists of clinical importance. *Clin Microbiol Rev*. 2002;15(3):329-341. doi:10.1128/CMR.15.3.329-341.2002

45. Cox J, Mann M. MaxQuant enables high peptide identification rates, individualized p.p.b.-range mass accuracies and proteome-wide protein quantification. *Nat Biotechnol*. 2008;26(12):1367-1372. doi:10.1038/nbt.1511

46. Cox J, Neuhauser N, Michalski A, Scheltema RA, Olsen J V., Mann M. Andromeda: A peptide search engine integrated into the MaxQuant environment. *J Proteome Res*. 2011;10(4):1794-1805. doi:10.1021/pr101065j

47. ME R, B P, D W, et al. Limma powers differential expression analyses for RNA-sequencing and microarray studies. *Nucleic Acids Res*. 2015;43(7):e47. https://www.ncbi.nlm.nih.gov/pmc/articles/PMC4402510/. Accessed April 14, 2020.

48. Fischer S, Brunk BP, Chen F, et al. Using OrthoMCL to Assign Proteins to OrthoMCL-DB Groups or to Cluster Proteomes Into New Ortholog Groups. In: *Current Protocols in Bioinformatics*. Vol 35. Hoboken, NJ, USA: John Wiley & Sons, Inc.; 2011:6.12.1-6.12.19. doi:10.1002/0471250953.bi0612s35

Chapter 3 : Leukocyte lysis and cytokine induction by the human sexually transmitted parasite *Trichomonas vaginalis*

RESEARCH ARTICLE

Leukocyte Lysis and Cytokine Induction by the Human Sexually Transmitted Parasite *Trichomonas vaginalis*

Frances Mercer[1], Fitz Gerald I. Diala[1,2], Yi-Pei Chen[1,2], Brenda M. Molgora[1,2], Shek Hang Ng[1], Patricia J. Johnson[1,2]*

1 Department of Microbiology, Immunology & Molecular Genetics, University of California, Los Angeles, Los Angeles, California, United States of America, **2** Molecular Biology Institute, University of California, Los Angeles, Los Angeles, California, United States of America

* johnsonp@ucla.edu

OPEN ACCESS

Citation: Mercer F, Diala FGI, Chen Y-P, Molgora BM, Ng SH, Johnson PJ (2016) Leukocyte Lysis and Cytokine Induction by the Human Sexually Transmitted Parasite *Trichomonas vaginalis*. PLoS Negl Trop Dis 10(8): e0004913. doi:10.1371/journal.pntd.0004913

Editor: Elodie Ghedin, New York University, UNITED STATES

Received: May 10, 2016

Accepted: July 19, 2016

Published: August 16, 2016

Data Availability Statement: All relevant data are within the paper and its Supporting Information files.

Funding: This work was supported by National Institutes of Health Grant R01AI103182 (PJJ) and F32AI122643 (FM). FGID and YPC were supported by the Microbial Pathogenesis Training Grant (T32-AI07323), and BMM was supported by the Cellular & Molecular Training Grant (T32GM007185). The funders had no role in study design, data collection and analysis, decision to publish, or preparation of the manuscript.

Abstract

Trichomonas vaginalis (Tv) is an extracellular protozoan parasite that causes the most common non-viral sexually transmitted infection: trichomoniasis. While acute symptoms in women may include vaginitis, infections are often asymptomatic, but can persist and are associated with medical complications including increased HIV susceptibility, infertility, preterm labor, and higher incidence of cervical cancer. Heightened inflammation resulting from *Tv* infection could account for these complications. Effective cellular immune responses to *Tv* have not been characterized, and re-infection is common, suggesting a dysfunctional adaptive immune response. Using primary human leukocyte components, we have established an *in vitro* co-culture system to assess the interaction between *Tv* and the cells of the human immune system. We determined that *in vitro*, *Tv* is able to lyse T-cells and B-cells, showing a preference for B-cells. We also found that *Tv* lysis of lymphocytes was mediated by contact-dependent and soluble factors. *Tv* lysis of monocytes is far less efficient, and almost entirely contact-dependent. Interestingly, a common symbiont of *Tv*, *Mycoplasma hominis*, did not affect cytolytic activity of the parasite, but had a major impact on cytokine responses. *M. hominis* enabled more diverse inflammatory cytokine secretion in response to *Tv* and, of the cytokines tested, *Tv* strains cleared of *M. hominis* induced only IL-8 secretion from monocytes. The quality of the adaptive immune response to *Tv* is therefore likely influenced by *Tv* symbionts, commensals, and concomitant infections, and may be further complicated by direct parasite lysis of effector immune cells.

Author Summary

The unicellular parasite *Trichomonas vaginalis* (*Tv*) causes the most common non-viral sexually transmitted infection worldwide, with approximately one quarter of a billion people infected annually. *Tv* infections are linked to pre-term and low-weight infant birth, increased susceptibility to and transmission of HIV infection, and increased aggressiveness

Competing Interests: The authors have declared that no competing interests exist.

of urogenital tract cancers. How the immune system responds to *Tv*, and how the parasite persists in the presence of the immune system, is not well understood. We show that *Tv* can kill human immune cells. We found that a clinical isolate of *Tv* is more efficient at killing immune cells than a laboratory-adapted strain, and that *Tv* preferentially targets B-cells. This killing activity is mediated by both contact-dependent and soluble factors. Killing immune cells could allow *Tv* to subvert or disable the immune system. Conversely, we found that cells of the immune system respond to *Tv* by secreting soluble inflammatory mediators called cytokines, mainly interleukin-8. However, these cells secrete greater amounts, and a broader profile of inflammatory cytokines when they encounter *Tv* harboring its symbiont bacterium, *Mycoplasma hominis*. We conclude that *Tv* may interact with immune cells in different ways, depending on the strain of *Tv* and the symbiont it harbors.

Introduction

Trichomonas vaginalis (*Tv*) is a unicellular, aerotolerant, flagellated protozoan parasite that is an obligate extracellular pathogen, restricted to humans [1]. *Tv* adheres to and lyses host epithelial cells [2], followed by phagocytosis of cellular contents [3]. *Tv* destruction of the epithelial layer in the female reproductive tract (FRT) is apparent in the clinical presentation of "strawberry cervix," in which red lesions are visible on the external surface of the cervix of infected women [1]. Once thought to be a commensal member of the vaginal microflora, *Tv* is now known to be pathogenic and is responsible for the most common non-viral sexually transmitted infection (STI) in the United States and worldwide: trichomoniasis [4]. The WHO reports ~275 million cases annually [1], but this number is likely a gross underestimation, as the CDC estimates that at least 50% percent of cases are asymptomatic. In the United States, an estimated 8–10 million new infections occur annually [5]. Alarmingly, trichomoniasis is on the rise in adolescents [6], and in dense urban areas prevalence can be as high as 50% [7]. Because *Tv* responds well to metronidazole, an antibiotic that specifically kills anaerobic cells [1], most symptomatic cases are successfully treated. However, emergence of metronidazole-resistant strains continues to increase [4,8–12], and metronidazole treatment may not efficacious for preventing pregnancy-related *Tv* complications [13,14]. Moreover, the association of subclinical infection with complications affecting women's reproductive health [6,15] necessitates a better understanding of how *Tv* causes disease, and how the immune system responds to the parasite.

Trichomoniasis is associated with increased susceptibility to HIV, HSV-2, pelvic inflammatory disorder, pre-term and low-weight infant birth, infertility, and endometritis [15]. *Tv* infection is also associated with bacterial vaginosis, suggesting a disruption of the microflora [6]. In addition, *Tv* infection or serostatus has been correlated with an increased incidence of cervical cancer [16,17], especially invasive types [18–20]. Although *Tv* is typically asymptomatic in men [21], they are commonly infected and trichomonads can be detected in prostate tissue [22]. *Tv* infection in men has been linked to invasive forms of prostate cancer [23], and infertility [24]. It is thought that *Tv*- induced inflammation can exacerbate existing neoplastic lesions, increasing chances of malignancy [25,26].

Tv often co-exists with a symbiont bacterium, *Mycoplasma hominis* [27]. Otherwise axenic cultures of clinical isolates and lab strains of *Tv* often contain *M. hominis*, growing both externally to and within *Tv* [28,29]. This is unlikely to be an artifact of laboratory-introduced contamination, as a recent study of clinical isolates found the prevalence of *M. hominis* in *Tv*

isolates to be 56% [30]. The prevalence of the biological association of *Tv* and *M. hominis* underscores the epidemiological relevance of studying *Tv* strains containing *M. hominis*.

Despite the association of *Tv* with numerous complications of a putative inflammatory etiology, how the immune system responds to and clears *Tv* is not well understood. Neutrophils are usually abundant during acute infection [31,32]. Antibodies can be detected in sera of infected persons [1,33,34], and after experimental challenge in a mouse model [35]. Peripheral blood mononuclear cells (PBMC) from infected persons proliferate *in vitro* in response to recall antigen [36], and CD4+T cells were shown to be present after experimental mouse infection [35]. However, partner re-infection is common [1], indicating that there may be inadequate formation of immunological memory, or that *Tv* subverts effective adaptive immune responses. *Tv* has also been shown to induce IL-8 secretion from primary human monocytes [37]. In addition, the *Tv* symbiont *Mycoplasma hominis* has been shown to enable induction of an array of inflammatory cytokines in a macrophage cell line following *Tv* encounter [38]. However, studies examining the cytokine profile following *Tv* encounter with primary human monocytes have yet to be performed.

Tv shares a niche with numerous other commensal microorganisms in the FRT [39], and infection is often concomitant with other STIs [1,5]. Leukocytes populate mucosal tissues of the FRT [40], where they manage responses to commensals and other STIs. Leukocytes are predominant in the lamina propria, but may also follow trans-epithelial chemokine signals to home to the luminal side of the mucosa [41]. *Tv* may therefore encounter leukocytes while adhering to epithelial cells on the luminal side of the FRT, or approaching the lamina propria as the epithelial layer is breached by *Tv* cytolysis of epithelial cells. *Tv* has been demonstrated to phagocytose human leukocytes [42], indicating that direct leukocyte killing could contribute to *Tv* immune subversion; however, the efficiency, kinetics, and cell-specificity of this process is unknown.

Characterizing the type of immune response that *Tv* stimulates and determining whether *Tv* cytotoxic activity can kill leukocytes will be important to understanding why *Tv* is often persistent, how *Tv* infection may lead to inflammatory sequelae, and how *Tv* infection may affect the microbiome in the FRT. *Tv* is a human-specific pathogen, and most attempts at experimental mouse infection have failed to sustain adequate parasite titers, with the exception of a model using pre-treatment with estrogen and dexamethasone [43], both of which are immunosuppressive and therefore undesirable for analysis of immune function. In addition, specific host-surface proteins are implicated in pathogenesis [44], so using cells of the natural host for these studies is optimal. Using primary human leukocytes, here we show that *Tv* is able to kill immune effector cells, showing a preference for B-cells, and that cytokine responses induced by the parasite are largely dependent on the symbiont *M. hominis*.

Methods

Ethics statement

All work with cells from human blood donation was done in compliance with the UCLA School of Medicine IRB Committee.

Trichomonas vaginalis strains and culture

Tv strains G3 (Beckenham, UK 1973, ATCC-PRA-98), and MSA1132 (Mt. Dora, Fla, USA 2008) were grown in TYM medium supplemented with 10% horse serum (Sigma), 10 U/ml penicillin (Invitrogen), 10 μg/ml streptomycin (Invitrogen), 180 μM ferrous ammonium sulfate, and 28 μM sulfosalicylic acid [45] at 37°C. Strains were passaged daily and maintained at an approximate concentration of 1 x 10^5–2 x 10^6 cells/ mL. To generate *M. hominis* free strains,

Tv was grown in the presence of 50 μg/ml chloramphenicol and 5 μg/ml tetracycline (Sigma-Aldrich), supplemented daily for at least 5 days and *M. hominis* clearance was confirmed by PCR as described below. To generate dead, intact controls, *Tv* was counted, and then reconstituted in complete RPMI media, and rendered dead—but intact—by treatment at 65°C for 1 hour, followed by 3 freeze-thaw cycles [46]. Trichomonads were confirmed by microscopy to be immobile and intact and flow cytometry analysis using Zombie Red dead-cell exclusion dye (Biolegend) confirmed that trichomonads were not viable after this treatment.

Primary human cell acquisition and culture

Primary human peripheral blood mononuclear cells (PBMC) were isolated from leukopacks or trima filters using Ficoll gradient. Blood was obtained from 32 de-identified, healthy donors from the UCLA Virology Core using a UCLA Institutional Review Board approved protocol. Monocytes were isolated based on adherence to plastic (for monocytes used in cytotoxicity experiments) or by Rosette Sep © negative isolation (Stem Cell technologies) (for monocytes used in cytokine secretion experiments). PBMC and monocytes were frozen directly after purification and used the day they were thawed. All experiments with PBMC and monocytes were done using RPMI 1640 media supplemented with 10% Fetal Bovine Serum, Pen/Strep, GlutaMAX, and MEM non-essential amino acids, (Life Technologies), and incubated at 37°C with 5% CO_2.

In vitro differentiation of human monocyte-derived macrophages (HMDM)

Primary human PBMC were isolated from a trima filters using Ficoll gradient using blood from donors at the UCLA Virology Core. Monocytes were separated based on adherence to plastic and were plated at 2.7 x 10^5 cells/ml. 20 ng/ml of GM-CSF (Biolegend) was added for 4 days to induce macrophage differentiation. The differentiation was verified by staining with anti- CD14-PE (Invitrogen- MHCD14014) and an increase in forward scatter (size).

Flow-Cytometry based cytotoxicity assay

Brooks et al. demonstrated that *Tv*- host cell co-cultures are suitable for flow cytometry analysis [47]. As the similar size of *Tv* and leukocytes confounds cell discernment via size and scatter properties alone, we utilized differential dye staining. PBMC were labeled with Carboxyfluorescein succinimidyl ester (CFSE) (Biolegend) at 1:2000 for 3 minutes according to the manufacturer's instructions and then washed and plated at 2.5 x 10^5 cells/well in 100 μl in u-bottom 96 well plates. *Tv* was labeled with Cell Tracker Blue © (Molecular Probes), according to the manufacturer's instructions, and then allowed to recover in complete TYM media for 45 minutes- 2 hours. *Tv* was then reconstituted in complete RPMI media and added directly to wells containing PBMC at the indicated multiplicities of infection (MOI) for the indicated period of time. After incubation, cells were stained with anti-CD3 APC clone HIT3a and anti-CD19 PeCy7 clone HIN19 (both from Biolegend) at 1 μg/ml in FACS buffer (PBS with 5% FBS and 0.1% sodium azide) on ice for 30 minutes. Cells were then washed and resuspended in FACS buffer and analyzed within 2 hours on an LSR Fortessa © (Becton-Dickinson) at the UCLA Broad Stem Cell Research Center Flow Cytometry core facility. Directly before sample acquisition, 5 μl of Bright Count © counting beads (Life Technologies) was added to each sample. Data were analyzed using FlowJo (Treestar), and counts of each population (*Tv*, T-cell or B-cell) were determined according to the gating strategy is shown in S1 Fig. Cell counts were uniformly normalized to 2,000 beads, and percent death was calculated as ((# of B-cells in PBMC alone condition—# of B-cells in co-culture condition) / # of B-cells in PBMC alone condition)

100, for B-cells (same analysis was done for T-cells) or as ((# of parasites in parasites alone condition—# of parasites in co-culture condition) / # of parasites in parasites alone condition) 100 for *Tv*. Zombie Red dead-cell exclusion dye (Biolegend) was added to preliminary cytotoxicity experiments to assure that live cell gates based on forward and side scatter did not include dead cells (S2 Fig), and then found to be redundant since dead cells disappear from the live cell scatter plot completely. Zombie Red staining was therefore excluded in subsequent experiments for simplicity. For transwell cytotoxicity experiments, an HTS Transwell—96 well plate (Corning) with 0.4 μm polycarbonate membrane was used. PBMC were placed in the bottom, receiver plate, which was spun down and processed as described above after the co-culture. Two-tailed, unpaired student's T-test was done to determine statistical significance between conditions, when relevant.

Lactate dehydrogenase-based cytotoxicity assay

Monocytes isolated based on plastic adherence as described above were plated at 5 x 10^5 cells/well in 96-well flat-bottom plates. *Tv* was reconstituted in complete RPMI media as described above and added at the indicated MOI for the indicated period of time. After the co-culture, monocyte death was measured by determining mammalian-specific lactate dehydrogenase (LDH) release using the CytoTox-One © homogeneous membrane integrity assay (Promega) according to the manufacturer's instructions. Samples were read on a Victor^3 1420 plate reader (Perkin-Elmer) to generate mean fluorescence intensity (MFI) values correlating with LDH presence in the supernatants. Percent death was calculated as (MFI from co-culture supernatants- MFI from live monocytes alone supernatants)/ (MFI from detergent solubilized monocytes alone supernatants–MFI from live monocytes alone supernatants) *100. Transwell cytotoxicity experiments were conducted as described above.

Cytokine analysis

Human monocytes isolated by Rosette Sep © negative selection were plated at 5 x 10^4 cells/well in 96-well u-bottom plates. *Tv* was counted, and then reconstituted in complete RPMI media, and rendered dead, but intact as described above. Dead, intact *Tv* were then added to monocytes, or human monocyte derived macrophages (HMDM) at an MOI (multiplicity of infection) of 1, and allowed to incubate overnight (16 hours). Positive controls were 100 ng/ml LPS (sigma) 10 μg/ml poly (I:C) (Tocris) or 1000 U/ml IFN gamma (Biolegend). Subsequently plates were centrifuged and supernatants were harvested and frozen at -80°C. Supernatants were then thawed on ice and analyzed using Cytometric Bead Array (Becton-Dickenson) for IL-8, IL-6, IL-1β, TNFα, and IL-12 according to the manufacturer's instructions. IL-6, IL-1β, and IL-12 were multiplexed, and IL-8 was measured separately on supernatants diluted 1:100. Data were analyzed using FlowJo (Treestar) to determine MFI, which was normalized to absolute concentrations according to a standard curve generated using lyophilized protein provided with the kit. IL-23 was measured using Legend Max Human IL-23 (p19/p40) ELISA kit with pre-coated wells (Biolegend) according to the manufacturer's instructions. Wells were read using a Victor^3 1420 plate reader (Perkin-Elmer), and MFI was normalized as described above.

M. hominis analysis in *T. vaginalis* strains

Dense 15ml cultures of *Tv* were lysed using a solution of 8M urea, 2% sarkosyl, 0.15M NaCl, 0.001M EDTA, and 0.1M Tris HCL pH7.5, and DNA was extracted using phenol: chloroform: ISA (Amresco), precipitated with isopropanol, and reconstituted in 10mM Tris pH8+ RNase. Then PCR was performed on *Tv* DNA using the following primer pairs: (1) *M. hominis* specific primers: 5' CAA TGG CTA ATG CCG GAT ACG C 3' and 5' GGT ACC GTC AGT CTG

CAA T 3' [48] and (2) universal 16S rDNA primers: 5' AGA GTT TGA TCC TGG CTC AG 3' and 5' GGA CTA CCA GGG TAT CTA AT 3' (Greg James, PCR for Clinical Microbiology, 2010). PCR products were sequenced (Genewiz), and resultant sequences were aligned using NCBI nucleotide BLAST and ApE software and confidence peaks were examined in comparison to *M. hominis* sequence. These analysis were done on non-clonal *Tv* strains G3 and MSA1132 either cured of resident *M. hominis* strains or prior to curing with antibiotic treatment. Identical *M. hominis* sequences were derived using uncured strains in replicate experiments.

Results

Trichomonas vaginalis (*Tv*) is known to lyse cervical and prostate epithelial cells [2]. Since leukocytes are present in the genital mucosa [40], and in the lamina propria directly beneath the epithelial layer [41], we asked whether *Tv* is able to kill leukocytes. To assess this, we set up an *in vitro* co-culture system of *Tv* with primary human peripheral blood mononuclear cells (PBMC), and then determined numbers of surviving cells using flow cytometry following the co-culture. Prior to the co-culture, *Tv* were labeled with Cell Tracker Blue © (CTB), and PBMC were labeled with carboxyfluorescein succinimidyl ester (CFSE). After co-culture, wells were stained with anti-CD3 and anti-CD19 to identify T-cells and B-cells, respectively. Directly before flow cytometry analysis, counting beads were added to wells for sample-to-sample volume normalization. Counts of live CTB+ CFSE- (*Tv*), CFSE+CD3+ (T-cells) and CFSE+CD19 + (B-cells) events were then determined and normalized to PBMC alone, or *Tv* alone controls to calculate percent death of each population. Using this system, we first tested a common laboratory adapted strain of *Tv* (G3) [49] compared to a relatively recent clinical isolate of *Tv* (MSA1132) [2]. We observed that clinical strain MSA1132 was able to kill ~30% of T cells and ~70% of B-cells in the co-culture, using a multiplicity of infection (MOI) of 0.5 (1:2 *Tv*: host cell ratio). On the other hand, *Tv* lab strain G3 did not kill T-cells under these conditions and demonstrated only minimal killing of B-cells (Fig 1A).

Having determined that *Tv*MSA1132 is cytotoxic towards lymphocytes, we next addressed the efficiency and kinetics of *Tv* lymphotoxic activity. The amount of *Tv* needed to lyse lymphocytes was determined by performing the cytotoxicity assay at various MOI. We found moderate levels of lymphocyte death occurring at MOI of 0.25 (1:4, *Tv*: host cells), whereas at MOI 2 (2:1, *Tv*: host cell), we found almost complete killing of B-cells and ~75% killing of T-cells (Fig 1B). Lymphocyte killing requires live parasites, as co-cultures containing dead, intact *Tv* at the same MOI did not result in any lymphocyte death (S3 Fig). Next, we determined how fast *Tv* killing of lymphocytes occurs by performing cytotoxicity assays at an intermediate MOI (0.5), and assessing lymphocyte death at various time points during the co-culture. We found that lymphocyte death was not rapid, and required 2 hours to achieve low levels, and 5–6 hours to achieve relatively high levels of death (Fig 1C). Using *Tv*MSA1132 as a model clinical strain, these data indicate that some clinical strains of *Tv* possess lymphotoxic activity and require several hours and high parasite titers to achieve maximal killing; nevertheless moderate lymphotoxic effects are observed at shorter time points and lower parasite titers. Also, while there was some donor-to-donor variability in susceptibility to *Tv* cytotoxicity, B-cells were significantly more susceptible (S4A Fig).

Tv likely comes into direct contact with lymphocytes at the luminal side of the vaginal mucosa and also in the lamina propria after tissue invasion associated with lysis of the epithelial layer. However, *Tv* killing of lymphocytes could have an extended effect in tissues if it were mediated by soluble factors. We therefore asked whether *Tv* lymphotoxic activity was contact-dependent, or mediated by soluble factors by performing our cytotoxicity assays utilizing a trans-well insert system with a 0.4 μm porous membrane. As *Tv* is 7–10 μm in diameter, the

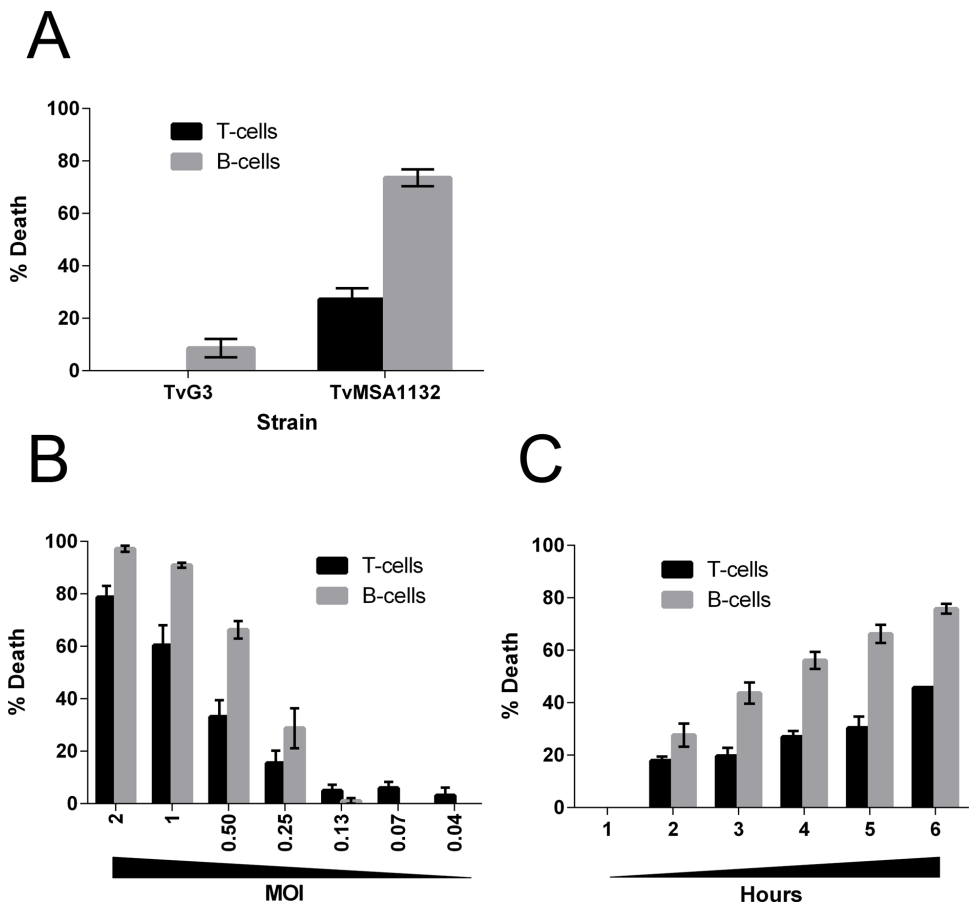

Fig 1. Lymphotoxic activity of *Tv*. (A) PBMC and *Tv* strains *Tv*G3 (laboratory adapted) or *Tv*MSA1132 (clinical isolate) were differentially labeled with CFSE or Cell Tracker Blue, respectively and co-cultured at an MOI of 0.5 for 4 hours. Cells were then stained with anti-CD3 and anti-CD19 to detect T-cells or B-cells, respectively, and lymphocyte death was assessed with flow cytometry analysis. **(B)** Killing of lymphocytes by *Tv*MSA1132 was assessed as in **(A)** at the indicated MOI for 4 hours. **(C)** Killing of lymphocytes by *Tv*MSA1132 was assessed as in **(A)** at an MOI 0.5 for the indicated period of time. All data in **(A-C)** are averages with standard deviation of triplicate wells and representative of at least 3 donors/ independent experiments.

doi:10.1371/journal.pntd.0004913.g001

parasite cannot pass through [2]. In conditions where PBMC and *Tv* were cultured together, death of T-cells and B-cells was observed at levels similar to that shown in Fig 1. However, when *Tv* and PBMC were placed in separate chambers there was an approximately 2-fold decrease in death of T-cells and B-cells (Fig 2A and 2B). The significant difference in lymphotoxic activity observed when parasite and lymphocytes were in the same chamber or separated by a membrane indicates that killing of B-cells and T-cells by *Tv* is mediated by both contact dependent and soluble factors.

We next asked whether *Tv* can lyse monocytes. To avoid variability arising from adherence of activated monocytes to plastic, we measured levels of lactate dehydrogenase (LDH) released in the culture supernatants upon lysis of monocytes, instead of using flow cytometry. *Tv* killing

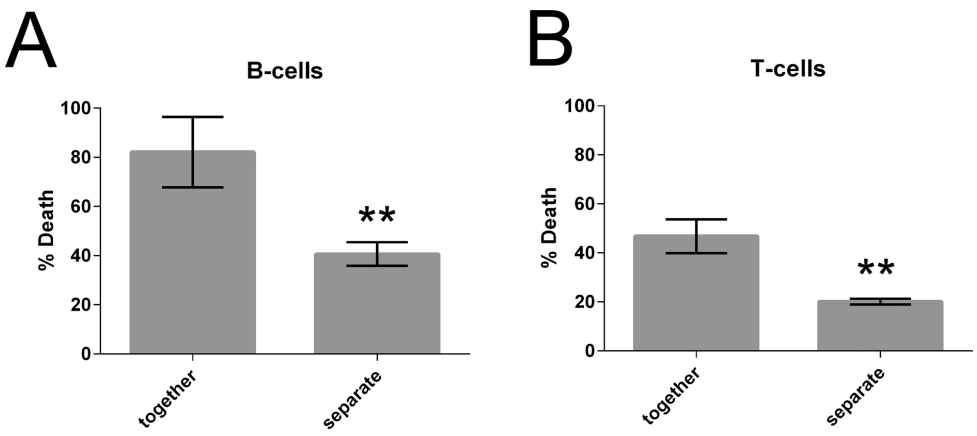

Fig 2. *Tv* lymphotoxic activity is mediated by contact dependent and soluble factors. PBMC and *Tv*MSA1132 were co-cultured and lymphocyte death was assessed as described in Fig 1 at an MOI of 0.5 for 4 hours in a transwell apparatus. PBMC were placed in the bottom chamber and *Tv*MSA1132 were placed either with PBMC in the bottom chamber (together) or in a top chamber with shared media, but separated by a 0.4 μm porous membrane (separate). Percent death in the bottom chamber was then assessed for B-cells **(A)** and T-cells **(B)**. Data shown are averages of triplicate wells with standard deviation, and are representative of 4 donors and 2 independent experiments.

doi:10.1371/journal.pntd.0004913.g002

of monocytes was found to be inefficient, with only ~20% death of monocytes observed at an MOI of 2 (2 *Tv*:1 monocyte) (Fig 3A). A 1–6 hour time course was used to assess the kinetics of killing, and death was found to be linear over 6 hours (Fig 3B). It is notable that prolonged co-incubation did not significantly increase monocyte death even after 24 hour. While there was some donor-to-donor variability, *Tv* killing of monocytes was always less efficient than that of lymphocytes (S4B Fig). To determine whether *Tv* lysis of monocytes is contact-dependent, cytotoxicity assays were performed using the transwell system. We found that unlike that observed for killing of lymphocytes (Fig 2), separation of *Tv* from monocytes almost completely abolished cytotoxic activity (Fig 3C). Together these data indicate that *Tv* killing of monocytes is inefficient and primarily contact-dependent.

Since symbionts often increase fitness of their hosts, we next asked whether a common symbiont of Tv, *M. hominis*, affects the ability of *Tv* to kill leukocytes. *Tv*MSA1132 naturally contains *M. hominis*, thus to generate isogenic strains that either harbor the symbiont or not, we cultured *Tv*MSA1132 for 1 week either untreated, or in the presence of chloramphenicol and tetracycline. PCR using *M. hominis*-specific primers was then conducted to confirm that *M. hominis* was undetectable in the culture treated with additional antibiotics (S5 Fig). Furthermore, sequencing the products generated by PCR using universal 16S bacterial primers on our untreated cultures confirmed that *M. hominis* is the only bacterial species present in the untreated culture. We then used the untreated (*M. hominis*+) and antibiotic treated (*M. hominis*-) strains side-by-side in leukocyte cytotoxicity assays. We found that the ability to kill T-cells, B-cells or monocytes was not significantly different, indicating that *M. hominis* does not confer greater leukotoxic activity to *Tv* (Fig 4A–4C).

Having observed that *Tv* is potentially able to modulate immune responses by killing lymphocytes, we next asked the converse question: what type of immune response is mounted against *Tv*? To address this, we assayed for the presence of several cytokines secreted from primary human monocytes after overnight exposure to *Tv*. To prevent *Tv* killing of monocytes from affecting the results, we made dead, intact preparations of *Tv* before co-culture and

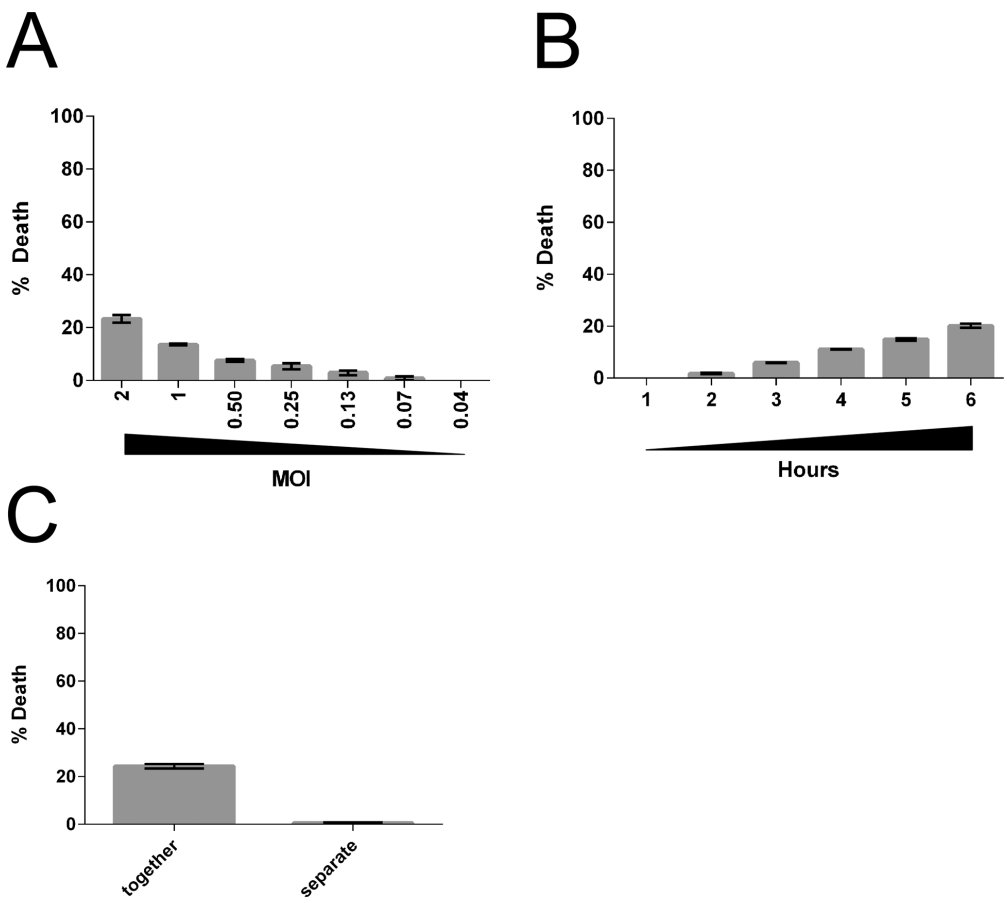

Fig 3. *Tv* cytotoxicity towards monocytes is inefficient and contact-dependent. (A) Primary human monocytes were co-cultured with *Tv*MSA1132 at the indicated MOI. Monocyte death was assessed by detecting the release of mammalian lactate dehydrogenase (LDH) into culture supernatants after 4 hours. **(B)** Primary human monocytes were co-cultured with *Tv*MSA1132 at MOI 0.5 for the indicated times and percent death was determined. **(C)** Killing of monocytes by *Tv*MSA1132 at an MOI of 2 was determined using a transwell apparatus as described in Figure legend 2, except monocytes were used instead of lymphocytes. LDH was measured in culture supernatants after 4 hours. All data in shown **(A-C)** are averages of triplicate wells with standard deviation, and are representative of at least 3 donors/independent experiments.

doi:10.1371/journal.pntd.0004913.g003

confirmed that no monocyte death occurred after incubation with dead *Tv*. Fiori and colleagues recently showed that *M*. *hominis* dramatically increased the amount of pro-inflammatory cytokine induced from a human macrophage-like cell line [38]. We were able to reproduce these results using primary human monocyte derived macrophages (HMDM) (S6 Fig). We therefore compared cytokine responses induced from untreated (*M*. *hominis*+) or additional antibiotic treated (*M*. *hominis*-) strains using fresh, naïve human monocytes. We also compared the responses against the laboratory adapted (*Tv*G3) versus the clinical (*Tv*MSA1132) strain. Levels of cytokines known to support Th1 responses (IL-12) and Th17 responses (IL-6, IL-1β, and IL-23) were assessed. IL-8, a broadly inflammatory, neutrophil-

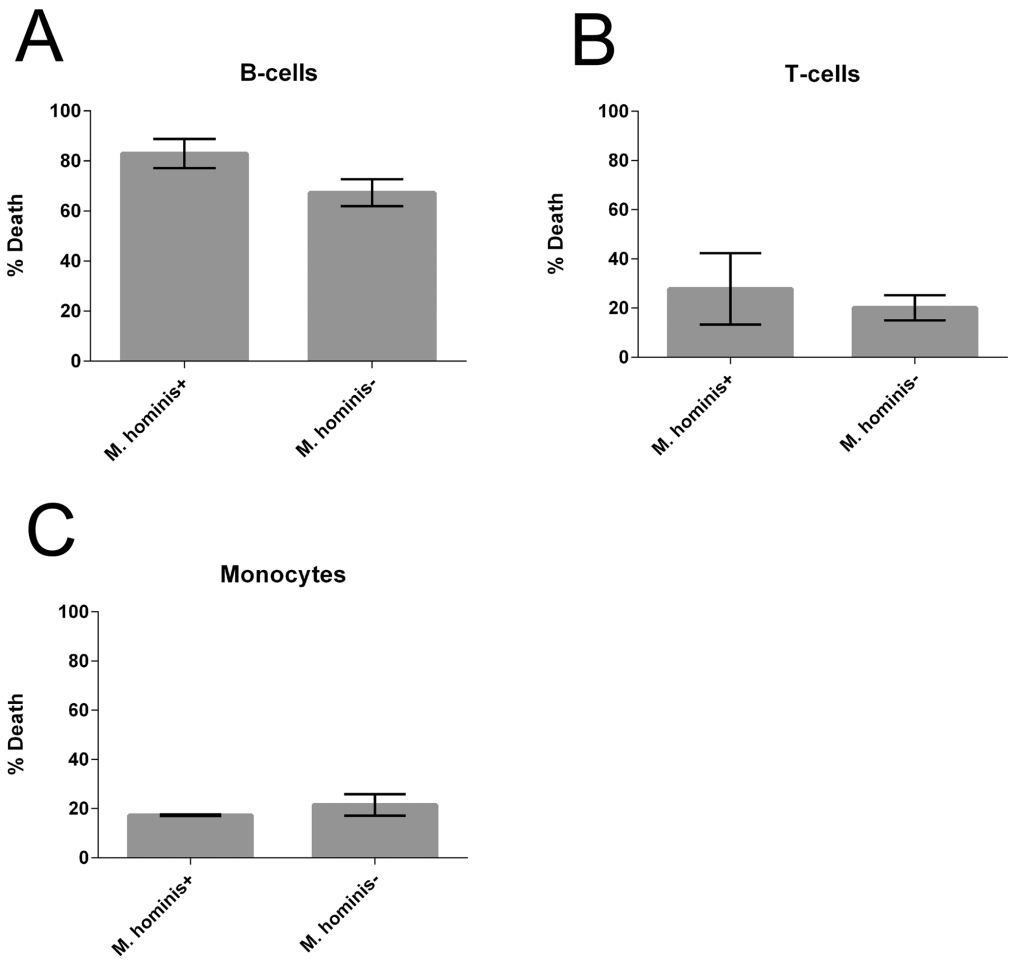

Fig 4. *Tv* symbiont *Mycoplasma hominis* does not affect *Tv* leukotoxic activity. Killing of B-cells **(A)**, T-cells **(B)**, or monocytes **(C)** by *Tv*MSA1132 was determined at an MOI 0.5 for 4 hours. Prior to the cytotoxicity assay, *Tv*MSA1132 was either cultured in the presence (*M. hominis* -) or absence (*M. hominis* +) of additional antibiotics. Data shown are average of triplicate wells with standard deviation, and are representative of 3 donors/ independent experiments.

doi:10.1371/journal.pntd.0004913.g004

recruiting chemokine previously reported to be highly secreted following *Tv* encounter [31,32,37] was also measured. All strains of *Tv* tested induced IL-8 secretion over background (Fig 5A). Notably, the presence of *M. hominis* greatly increased IL-8 induction, relative to isogenic strains lacking *M. hominis* (Fig 5A), and enabled induction of IL-6 and IL-1β which were otherwise not detectable in response to *Tv* alone (Fig 5B and 5C). In contrast, neither *M. hominis* positive nor negative parasites induced detectable IL-23 or IL-12 secretion (Fig 5D and 5E). No difference was observed in the immunogenicity of laboratory-adapted strain *Tv*G3 compared to clinical strain *Tv*MSA1132 (Fig 5A–5E). Together these analyses indicate that IL-8 is the dominant cytokine response to *Tv*, both in the presence and absence of *M. hominis*. The

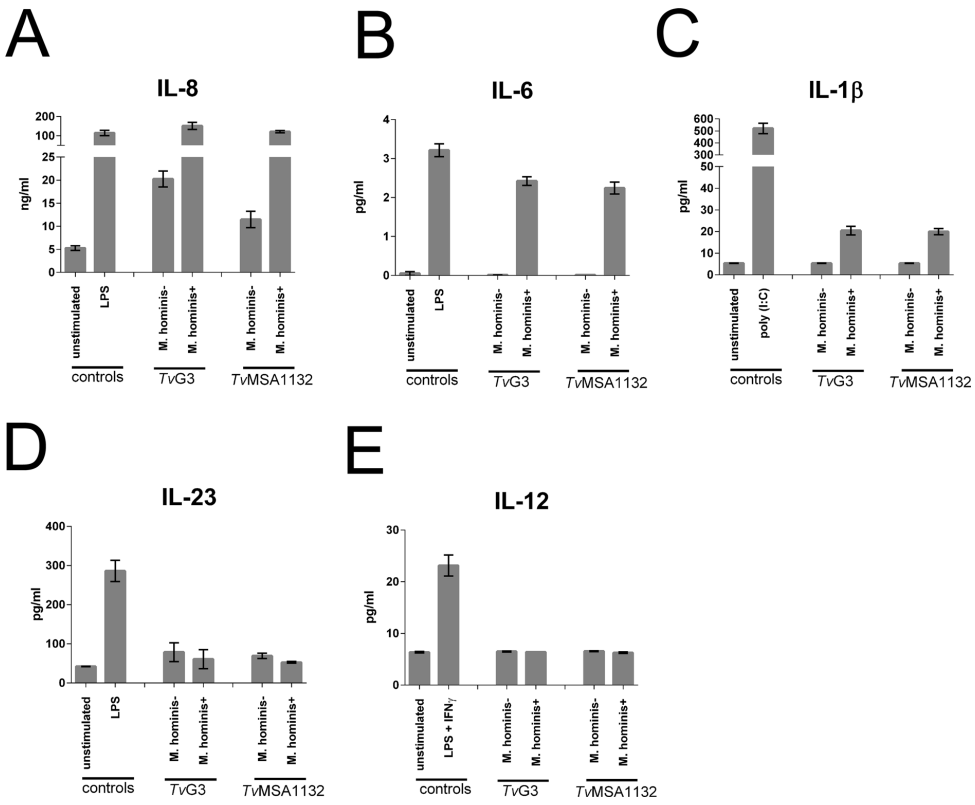

Fig 5. Induction of cytokine secretion from human monocytes by *Tv* is largely dependent on the presence of *Mycoplasma hominis* and is dominated by IL-8 secretion. Primary human monocytes were cultured with either dead intact *Tv*G3, *Tv*MSA1132, unstimulated, or treated with LPS (**A, B, D**) or poly (I:C) **(C)** or LPS and IFNγ **(E)** for 16 hours. Prior to killing, *Tv* strains were either untreated (*M. hominis*+) or treated with additional antibiotic to clear the symbiont (*M. hominis*-). Supernatants were collected and the indicated cytokines were measured using Cytometric Bead Array (CBA) or ELISA. Data shown are average of triplicate wells with standard deviation, and are representative of 3 donors/ independent experiments.

doi:10.1371/journal.pntd.0004913.g005

data also show that the symbiont *M. hominis* greatly increases the induction of inflammatory cytokines IL-6 and IL-1β, in addition to IL-8. This increased immunogenicity may be instrumental in triggering adaptive immune responses that would not normally be mounted against *Tv* in the absence of the symbiont.

Discussion

Despite the numerous inflammatory complications associated with *Tv* infection, how *Tv* interacts with the cells of the host immune system is not well characterized. Furthermore, partner re-infection after treatment for trichomoniasis indicates a lack of effective adaptive immunity to *Tv*. Using primary human leukocytes, we have demonstrated that *Tv* has leukotoxic activity, that IL-8 secretion dominates the primary cytokine response to *Tv* infection, and that the *M. hominis* symbiont is likely to play a major role in shaping more robust and diverse inflammatory responses to *Tv*. These results form a foundation for the dissection of interactions between

Tv and the cells of the human immune system. These studies are the first to examine how primary human leukocytes respond to *Tv*, and to assess *Tv* leukotoxic activity, with attention to strain specificity, host cell-preference, timing, and dosage. These analyses have also interrogated the contribution of the symbiont *M*. *hominis* to the pathogenesis and immunogenicity of *Tv* using primary immune cells. We found that immune responses against *Tv* may be modulated by leukotoxic activity of the parasite as well as the presence of *M*. *hominis*. These results suggest potential explanations for the considerable variability in *Tv* clinical presentation, pathogenicity, and inflammatory sequelae.

The leukotoxic activity of *Tv* reported here may be important in subverting immune responses, or in modulating the leukocyte repertoire in the vaginal mucosa, where leukocytes may control concomitant STIs and commensal micro-organisms [41]. We sought to determine which cells among PBMC are primary targets of the parasite and found that *Tv* demonstrates a preference for killing B-cells, followed by T-cells, and is very inefficient at killing monocytes. Interestingly, while the cell-type preference was maintained in all donors tested, there was some variability in overall susceptibility of leukocytes to *Tv*- mediated killing (S4 Fig), which could account for variation in symptoms and sequelae in the clinic. It is interesting that B-cells are the most vulnerable leukocyte in the presence of *Tv*, as humoral immunity is likely to be important in host defense against *Tv*: a large extracellular eukaryotic pathogen. Antibodies against *Tv* can be detected in sera and vaginal washes of infected individuals [1,34,50], indicating that humoral immunity is formed against the parasite. Furthermore, *Tv* strains that do not harbor the symbiont *M*. *hominis* do not induce detectable levels of IL-1β, IL-6 or IL-12 secretion from monocytes (Fig 5B, 5C and 5E), suggesting formation of default Th2 responses to *Tv*, at least in the absence of symbiont *M*. *hominis*. Since ~50% *Tv* clinical isolates lack *M*. *hominis* [27,30], Th2 responses could predominate in these cases. Killing of antibody-producing B-cells (such as those at the mucosa secreting IgA [51] could therefore be a way for the parasite to subvert immune clearance. Interestingly, *Tv* proteases are reported to cleave IgG and secretory IgA [52] and Tv exhibits antigenic variation [53], both consistent with a model of humoral immunity subversion as an evolved behavior of *Tv* to survive in its host. We also found that approximately 50% of *Tv* leukotoxic activity against B-cells was mediated by soluble factors, indicating that the parasite may kill B-cells even if it does not come into direct contact with them, potentially allowing for a broader effect of this anti-B cell activity. Contact dependent killing was also observed, consistent with previous work showing that human PBMC can be phagocytosed by *Tv* [54].

Moderate cytotoxic activity of *Tv* against T-cells was also detected, albeit lower than that exhibited towards B-cells, again mediated by both contact-dependent and soluble factors (Figs 1 and 2). *Tv*-antigen-induced proliferation of PBMC from infected women [36] indicates that T-cell responses are formed against *Tv in vivo*. *Tv* killing of T-cells could therefore potentially subvert anti-*Tv* immune responses as well as affect the T-cell repertoire in the such that control of concomitant STIs or commensals is dysregulated. Indeed, Tv infection is associated with dysbiosis of microbiota in the FRT and bacterial vaginosis [55–57]. Since T-cell polarization is a delicate and multi-factorial process involving both positive and negative feedback, *Tv* killing of T-cells could have more complex downstream implications in anti-*Tv* immunity, on other vaginal microflora, and on mucosal inflammation.

We observed both contact-dependent and contact-independent leukotoxic activity for the clinical isolate *Tv*MSA1132. Previously demonstrated phagocytosis of leukocytes [42] could account for or contribute to the contact-dependent leukotoxic activity observed. Alternatively, the cytotoxicity could be mediated almost entirely by soluble factors, but require close proximity; concentrations of pH and secreted effectors being effectively higher in such a microenvironment. Contact-independent killing of leukocytes by *Tv* has not been previously described.

However soluble, extracellular *Tv* cysteine proteases have been isolated [58,59] and several studies implicate them in *Tv* cytolytic mechanisms [60–63]. In addition, several genes with homology to known pore-forming toxins are present in the *Tv* genome [49]. Future work to determine the identity of soluble factors involved in *Tv* contact-independent killing of lymphocytes will be important to understand the mechanism underlying this mode of host cell cytotoxicity.

The observation that the recent clinical isolate *Tv*MSA1132 demonstrated dramatically enhanced lymphotoxic activity compared to the common laboratory adapted strain *Tv*G3 (Fig 1A) is notable. We have previously shown that *Tv* lysis of prostate and vaginal epithelial cells, which is strictly contact-dependent, is highly variable among different *Tv* strains [2]. Strain differences in contact-independent modes of lysis, as demonstrated here, reveal an added layer of strain variation in pathogenic behavior, underscoring the value of using clinical strains for studies of *Tv* molecular pathogenesis, and highlighting a likely reason for the considerable clinical variability in trichomoniasis presentation and outcomes. Unfortunately, the clinical symptoms of the patient from which *Tv*MSA1132 was isolated are not available to allow direct comparison of host cell toxicity *in vitro* with clinical outcomes. Variability between *Tv* and *M. hominis* strains and their host cell-specific interactions may also explain why in this study we did not find differences between *M. hominis* positive and negative *Tv* cultures in their ability to kill leukocytes (Fig 4), in contrast to the enhancement of epithelial cell lysis conferred to *Tv* by *M. hominis* observed by Vancini and colleagues [64]. This further supports a model of diverse mechanisms underlying *Tv* cytotoxicity that may be strain and host cell type dependent.

In contrast to the efficient killing of lymphocytes by *Tv*MSA1132, monocytes were refractory to killing and the cytotoxicity that was observed was almost exclusively contact-dependent (Fig 3). Variation in the ability of *Tv* to kill host cells may be dependent on specific host-cell factors that are enriched on epithelial cells [2] and B-cells, and are present at lower levels on T-cells and monocytes. Only one host-cell receptor for mediating *Tv* interaction with host cells, galectin-1, has been identified. However, knock-down of galectin-1 expression in epithelial cells abrogated only ~20% of *Tv* adherence, indicating that adherence and contact-dependent cytolysis is a multi-factorial process [44]. Future studies aimed at identifying novel host molecules that confer vulnerability to contact-independent *Tv* killing will be important to understanding mechanisms of *Tv* leukotoxic activity.

A lack of robust cytotoxic activity towards monocytes (Fig 3) indicates that *Tv* does not subvert cytokine secretion from myeloid cells by killing the producers. Rather, cytokine secretion by monocytes is likely to proceed even in the presence of live, active parasites. In agreement with Fiori and colleagues [38] we found cytokine secretion by monocytes to be remarkably affected by the presence of the symbiont *M. hominis* (Fig 5). The absence of inflammatory cytokine production stimulated from monocytes in the presence of *M. hominis*-free *Tv* strains suggests that Th2 responses may be formed in cases where *Tv* strains are *M. hominis* negative. As *Tv* is an extracellular pathogen, and no IL-12 was induced in response to any *Tv* strain tested, it seems unlikely that Th1 responses are formed against the parasite. However, in the presence of *M. hominis* or other bacterial or viral antigens to provide co-stimulation in the milieu *in vivo*, Th17 responses specific to *Tv* may form. In humans, IL-1β, IL-6, and IL-23 support the formation or persistence of Th17 cells [65]. We saw that IL-1β and IL-6 were stimulated by *M. hominis*-infected *Tv*. In contrast to that observed by Fiori et al., we did not detect significantly high amounts of IL-23 in response to *M. hominis* + *Tv*, which potentially highlights a difference between the THP-1 macrophage cell line that Fiori et al. used and our primary human monocyte system, or that Fiori et al. used live trichomonads as opposed to our use of dead-intact trichomonads as stimulant. Regardless, IL-23 could be present in *in vivo* milieus as a result of other commensals or concomitant STIs. Indeed, IL-17 has been shown to be a major player in

the immune response against the related parasite *Giardia lamblia* [66–68], and IL-22, a common cytokine associated with Th17 responses has been detected in vaginal secretions from *Tv* infected patients [69]. Th17 responses are common in the mucosa, where they respond to extracellular pathogens by recruiting neutrophils and repairing damaged epithelia [70,71], consistent with FRT neutrophilia and epithelial damage associated with *Tv* infection.

The commensal lactobacilli, dominant in ~75% of women's vaginal microbiomes, have been shown to modulate *Tv* pathogenic properties *in vitro* [72]; it is conceivable that moieties present on commensal bacteria sharing a niche with *Tv* could additionally affect cytokine responses during *Tv* infection. Recently, additional *Mycoplasma* species associated with clinical strains of *Tv* have been discovered [73]. Known symbionts, commensals, and concomitant STIs are likely only the "tip-of-the-iceberg;" many other yet undefined organisms may contribute to the complex ecosystem with which *Tv* co-operates and contends. Meta-analysis of the FRT microbiome in the context of *Tv* infection, as well as development of suitable *in vivo* models will be instrumental to more fully appreciate this diversity and test hypotheses about *Tv* clearance and inflammation with a more holistic approach.

We found that both *Tv* strains examined, regardless of *M. hominis* status, induce IL-8 secretion (Fig 5) [1,31,32,37]. IL-8 is a pleiotropic cytokine [74], with a main function of recruiting neutrophils, consistent with that observed in trichomoniasis in the clinic. Furthermore, work in mouse models has shown that prevention of neutrophil influx is needed to establish infection [43], and primary human neutrophils were shown to swarm and attack *Tv in vitro* [32] suggesting that neutrophils are crucial for control of *Tv* infection. However, the molecular determinants of neutrophil-*Tv* interactions are not characterized. Neutrophils have a range of highly inflammatory and destructive behaviors [75], and can even contribute to cancer microenvironments [74]. It is possible that neutrophils may contribute to the associations of reproductive complications, inflammatory pathologies, and cancers of the reproductive tract with *Tv*.

These studies shed light on potential reasons for variability in *Tv* clinical presentation and associated complications, suggest potential immune subversion strategies of the parasite, and may help to inform future immunotherapy interventions. A better understanding of how *Tv* interacts with the immune system will also potentiate the design of immunotherapies to aid in scenarios of antibiotic resistance or to mitigate damaging inflammatory processes induced by *Tv* infections.

Supporting Information

S1 Fig. Gating strategy used for flow cytometry- based cytotoxicity assays. (Top panels) Total wells were analyzed for forward scatter vs. side scatter and beads, and live cells were gated on. Beads were further gated based on A-405 positivity to more accurately ensure their identity. (Middle panels) Live cells were further sub-gated based on CFSE+ to gate on leukocytes only (*Tv* excluded). (Bottom panels) Leukocytes were then further gated based on CD19 and CD3 positivity to identity B-cells and T-cells, respectively.
(TIF)

S2 Fig. Viability analysis of leukocytes after *Tv* co-culture. Total PBMC from live cell gates (shown in S1 Fig) were analysed for Zombie Red expression to rule out that significant T-cells or B-cells occurring in live cell gates had compromised membranes.
(TIF)

S3 Fig. Dead trichomonads do not cause death of PBMC. To assure that PBMC death observed after co-cultures with *Tv* was specific to live Tv-mediated mechanisms, we co-

cultured PBMC with dead, intact *Tv* as a control. We did not observe any decrease in counts of viable PBMC after co-culture with dead, intact *Tv*. Data shown are from *Tv* co-culture with PBMC at MOI 0.5 for 4 hours and representative of multiple experiments.
(TIF)

S4 Fig. Donor variation in susceptibility to *Tv*- mediated killing. % death is shown for all donors used in the study, at MOI 0.5 *Tv*MSA1132 for 4 hours. B-cell versus T-cell susceptibility was compared using paired (donor-matched), student's T-test.
(TIF)

S5 Fig. *Mycoplasma hominis* is undetectable in *Tv*MSA1132 treated with antibiotics and is the only bacteria present in untreated *Tv*MSA1132 cultures. Chloramphenicol/ tetracycline treated (*Tv*MSA1132 Cm/Tet) parasites were analyzed for the presence of bacterial symbionts using universal 16S primers designed to amplify a conserved region of bacterial 16S rDNA. The designed primers amplify a fragment of 834 bp. (Cm: chloramphenicol; Tet: tetracycline) specifically in *Tv*MSA1132 untreated parasites. DNA sequencing of the uncloned, amplified 16S bacterial rDNA fragment from untreated *Tv*MSA1132 was analyzed by BLAST analyses of Genbank. Only one sequence, with 100% homology to 16S region of *M. hominis* was detected. The sequence matched the following accession numbers with 100% identity: (all strains of *M. hominis*) CP009652.1, JN935871.1, NR113679.1, NR041881.1, FP236530.1, AF443616.3, AF443617.3, AJ002268.1, AJ002267.1, AJ002266.1, and AJ002265.1.
(TIF)

S6 Fig. *M. hominis*+, but not *M. hominis*- strains stimulate cytokine release from human monocyte- derived macrophages. (A) Differentiation of human monocytes to macrophages (HMDM) was verified by the expression of CD14 and the increase in size. **(B)** HMDM were either unstimulated, treated with LPS, or cultured with heat-inactivated *Tv*G3 for 16 hours. Supernatants were collected and the indicated cytokines were measured using CBA. Data shown are average of triplicate wells with standard deviation, and are representative of 3 donors/ independent experiments.
(TIF)

Acknowledgments

We would like to thank Deborah Anisman-Posner and Irene Kim at the UCLA virology core for recruiting blood donors and processing buffy coats. We also thank Felicia Codrea and Jessica Scholes at the Eli and Edith Broad Flow Cytometry Core facility at UCLA for training and technical expertise. We thank our colleagues Drs. Brian Janssen, Angelica Riestra, Olivia Twu, and Sharon Alterzon for helpful comments and discussions, Drs. Melissa Conrad and Jane Carlton for sharing information about *Mycoplasma hominis* status of their *T. vaginalis* isolates and Drs. Linda Baum and Dusan Bogunovic for advice on HMDM differentiation. We also thank Dr. Stephen Rawlings for comments on the manuscript.

Author Contributions

Conceptualization: FM PJJ.

Formal analysis: FM FGID YC BMM PJJ.

Funding acquisition: FM PJJ.

Investigation: FM FGID YC BMM SHN.

Methodology: FM FGID YC BMM PJJ.

Project administration: FM PJJ.

Supervision: FM PJJ.

Validation: FM FGID YC BMM SHN PJJ.

Visualization: FM FGID YC BMM.

Writing - original draft: FM PJJ.

Writing - review & editing: FM FGID YC BMM SHN PJJ.

References

1. Schwebke JR, Burgess D (2004) Trichomoniasis. Clin Microbiol Rev 17: 794–803, table of contents. PMID: 15489349
2. Lustig G, Ryan CM, Secor WE, Johnson PJ (2013) Trichomonas vaginalis contact-dependent cytolysis of epithelial cells. Infect Immun 81: 1411–1419. doi: 10.1128/IAI.01244-12 PMID: 23429535
3. Midlej V, Benchimol M (2010) Trichomonas vaginalis kills and eats—evidence for phagocytic activity as a cytopathic effect. Parasitology 137: 65–76. doi: 10.1017/S0031182009991041 PMID: 19723359
4. Meade JC, Carlton JM (2013) Genetic diversity in Trichomonas vaginalis. Sex Transm Infect 89: 444–448. doi: 10.1136/sextrans-2013-051098 PMID: 23702460
5. McClelland RS (2008) Trichomonas vaginalis infection: can we afford to do nothing? J Infect Dis 197: 487–489. doi: 10.1086/526498 PMID: 18275270
6. Fichorova RN (2009) Impact of T. vaginalis infection on innate immune responses and reproductive outcome. J Reprod Immunol 83: 185–189. doi: 10.1016/j.jri.2009.08.007 PMID: 19850356
7. Shafir SC, Sorvillo FJ, Smith L (2009) Current issues and considerations regarding trichomoniasis and human immunodeficiency virus in African-Americans. Clin Microbiol Rev 22: 37–45, Table of Contents. doi: 10.1128/CMR.00002-08 PMID: 19136432
8. Grossman JH 3rd, Galask RP (1990) Persistent vaginitis caused by metronidazole-resistant trichomonas. Obstet Gynecol 76: 521–522. PMID: 2381638
9. Dunne RL, Dunn LA, Upcroft P, O'Donoghue PJ, Upcroft JA (2003) Drug resistance in the sexually transmitted protozoan Trichomonas vaginalis. Cell Res 13: 239–249. PMID: 12974614
10. Land KM, Johnson PJ (1999) Molecular basis of metronidazole resistance in pathogenic bacteria and protozoa. Drug Resist Updat 2: 289–294. PMID: 11504503
11. Upcroft JA, Dunn LA, Wal T, Tabrizi S, Delgadillo-Correa MG, et al. (2009) Metronidazole resistance in Trichomonas vaginalis from highland women in Papua New Guinea. Sex Health 6: 334–338. doi: 10.1071/SH09011 PMID: 19917203
12. Leitsch D, Janssen BD, Kolarich D, Johnson PJ, Duchene M (2014) Trichomonas vaginalis flavin reductase 1 and its role in metronidazole resistance. Mol Microbiol 91: 198–208. doi: 10.1111/mmi.12455 PMID: 24256032
13. Gulmezoglu AM, Azhar M (2011) Interventions for trichomoniasis in pregnancy. Cochrane Database Syst Rev: CD000220. doi: 10.1002/14651858.CD000220.pub2 PMID: 21563127
14. Okun N, Gronau KA, Hannah ME (2005) Antibiotics for bacterial vaginosis or Trichomonas vaginalis in pregnancy: a systematic review. Obstet Gynecol 105: 857–868. PMID: 15802417
15. Hirt RP, Sherrard J (2015) Trichomonas vaginalis origins, molecular pathobiology and clinical considerations. Curr Opin Infect Dis 28: 72–79. doi: 10.1097/QCO.0000000000000128 PMID: 25485651
16. Gram IT, Macaluso M, Churchill J, Stalsberg H (1992) Trichomonas vaginalis (TV) and human papillomavirus (HPV) infection and the incidence of cervical intraepithelial neoplasia (CIN) grade III. Cancer Causes Control 3: 231–236. PMID: 1319218
17. Boyle DC, Smith JR (1999) Infection and cervical intraepithelial neoplasia. Int J Gynecol Cancer 9: 177–186. PMID: 11240764
18. Yap EH, Ho TH, Chan YC, Thong TW, Ng GC, et al. (1995) Serum antibodies to Trichomonas vaginalis in invasive cervical cancer patients. Genitourin Med 71: 402–404. PMID: 8566984
19. Sayed el-Ahl SA, el-Wakil HS, Kamel NM, Mahmoud MS (2002) A preliminary study on the relationship between Trichomonas vaginalis and cervical cancer in Egyptian women. J Egypt Soc Parasitol 32: 167–178. PMID: 12049252

20. Zhang ZF, Graham S, Yu SZ, Marshall J, Zielezny M, et al. (1995) Trichomonas vaginalis and cervical cancer. A prospective study in China. Ann Epidemiol 5: 325–332. PMID: 8520717

21. Sena AC, Miller WC, Hobbs MM, Schwebke JR, Leone PA, et al. (2007) Trichomonas vaginalis infection in male sexual partners: implications for diagnosis, treatment, and prevention. Clin Infect Dis 44: 13–22. PMID: 17143809

22. Mitteregger D, Aberle SW, Makristathis A, Walochnik J, Brozek W, et al. (2012) High detection rate of Trichomonas vaginalis in benign hyperplastic prostatic tissue. Med Microbiol Immunol 201: 113–116. doi: 10.1007/s00430-011-0205-2 PMID: 21660495

23. Stark JR, Judson G, Alderete JF, Mundodi V, Kucknoor AS, et al. (2009) Prospective study of Trichomonas vaginalis infection and prostate cancer incidence and mortality: Physicians' Health Study. J Natl Cancer Inst 101: 1406–1411. doi: 10.1093/jnci/djp306 PMID: 19741211

24. Benchimol M, Rosa ID, Fontes RD, Dias AJB (2008) Trichomonas adhere and phagocytose sperm cells: adhesion seems to be a prominent stage during interaction. Parasitology Research 102: 597–604. PMID: 18043945

25. Sutcliffe S, Neace C, Magnuson NS, Reeves R, Alderete JF (2012) Trichomonosis, a common curable STI, and prostate carcinogenesis—a proposed molecular mechanism. PLoS Pathog 8: e1002801. doi: 10.1371/journal.ppat.1002801 PMID: 22912571

26. Hanahan D, Weinberg RA (2011) Hallmarks of cancer: the next generation. Cell 144: 646–674. doi: 10.1016/j.cell.2011.02.013 PMID: 21376230

27. Rappelli P, Addis MF, Carta F, Fiori PL (1998) Mycoplasma hominis parasitism of Trichomonas vaginalis. Lancet 352: 1286. PMID: 9788469

28. Vancini RG, Benchimol M (2008) Entry and intracellular location of Mycoplasma hominis in Trichomonas vaginalis. Arch Microbiol 189: 7–18. PMID: 17710384

29. Dessi D, Delogu G, Emonte E, Catania MR, Fiori PL, et al. (2005) Long-term survival and intracellular replication of Mycoplasma hominis in Trichomonas vaginalis cells: potential role of the protozoon in transmitting bacterial infection. Infect Immun 73: 1180–1186. PMID: 15664961

30. da Luz Becker D, Dos Santos O, Frasson AP, de Vargas Rigo G, Macedo AJ, et al. (2015) High rates of double-stranded RNA viruses and Mycoplasma hominis in Trichomonas vaginalis clinical isolates in South Brazil. Infect Genet Evol 34: 181–187. doi: 10.1016/j.meegid.2015.07.005 PMID: 26160539

31. Shaio MF, Lin PR, Liu JY, Tang KD (1994) Monocyte-derived interleukin-8 involved in the recruitment of neutrophils induced by Trichomonas vaginalis infection. J Infect Dis 170: 1638–1640. PMID: 7996015

32. Rein MF, Sullivan JA, Mandell GL (1980) Trichomonacidal activity of human polymorphonuclear neutrophils: killing by disruption and fragmentation. J Infect Dis 142: 575–585. PMID: 7441017

33. Twu O, Dessi D, Vu A, Mercer F, Stevens GC, et al. (2014) Trichomonas vaginalis homolog of macrophage migration inhibitory factor induces prostate cell growth, invasiveness, and inflammatory responses. Proc Natl Acad Sci U S A 111: 8179–8184. doi: 10.1073/pnas.1321884111 PMID: 24843155

34. Ton Nu PA, Rappelli P, Dessi D, Nguyen VQ, Fiori PL (2015) Kinetics of circulating antibody response to Trichomonas vaginalis: clinical and diagnostic implications. Sex Transm Infect.

35. Smith JD, Garber GE (2015) Trichomonas vaginalis Infection Induces Vaginal CD4+ T-Cell Infiltration in a Mouse Model: A Vaccine Strategy to Reduce Vaginal Infection and HIV Transmission. J Infect Dis 212: 285–293. doi: 10.1093/infdis/jiv036 PMID: 25616405

36. Mason PR, Patterson BA (1985) Proliferative response of human lymphocytes to secretory and cellular antigens of Trichomonas vaginalis. J Parasitol 71: 265–268. PMID: 3874274

37. Shaio MF, Lin PR, Liu JY, Yang KD (1995) Generation of interleukin-8 from human monocytes in response to Trichomonas vaginalis stimulation. Infect Immun 63: 3864–3870. PMID: 7558293

38. Fiori PL, Diaz N, Cocco AR, Rappelli P, Dessi D (2013) Association of Trichomonas vaginalis with its symbiont Mycoplasma hominis synergistically upregulates the in vitro proinflammatory response of human monocytes. Sex Transm Infect 89: 449–454. doi: 10.1136/sextrans-2012-051006 PMID: 23633668

39. Brotman RM, Ravel J, Bavoil PM, Gravitt PE, Ghanem KG (2014) Microbiome, sex hormones, and immune responses in the reproductive tract: challenges for vaccine development against sexually transmitted infections. Vaccine 32: 1543–1552. doi: 10.1016/j.vaccine.2013.10.010 PMID: 24135572

40. Givan AL, White HD, Stern JE, Colby E, Gosselin EJ, et al. (1997) Flow cytometric analysis of leukocytes in the human female reproductive tract: comparison of fallopian tube, uterus, cervix, and vagina. Am J Reprod Immunol 38: 350–359. PMID: 9352027

41. Wira CR, Fahey JV, Sentman CL, Pioli PA, Shen L (2005) Innate and adaptive immunity in female genital tract: cellular responses and interactions. Immunol Rev 206: 306–335. PMID: 16048557

42. Rendon-Maldonado JG, Espinosa-Cantellano M, Gonzalez-Robles A, Martinez-Palomo A (1998) Trichomonas vaginalis: in vitro phagocytosis of lactobacilli, vaginal epithelial cells, leukocytes, and erythrocytes. Exp Parasitol 89: 241–250. PMID: 9635448

43. Cobo ER, Eckmann L, Corbeil LB (2011) Murine models of vaginal trichomonad infections. Am J Trop Med Hyg 85: 667–673. doi: 10.4269/ajtmh.2011.11-0123 PMID: 21976570

44. Okumura CY, Baum LG, Johnson PJ (2008) Galectin-1 on cervical epithelial cells is a receptor for the sexually transmitted human parasite Trichomonas vaginalis. Cell Microbiol 10: 2078–2090. doi: 10.1111/j.1462-5822.2008.01190.x PMID: 18637021

45. Clark CG, Diamond LS (2002) Methods for cultivation of luminal parasitic protists of clinical importance. Clin Microbiol Rev 15: 329–341. PMID: 12097242

46. Zielinski CE, Mele F, Aschenbrenner D, Jarrossay D, Ronchi F, et al. (2012) Pathogen-induced human TH17 cells produce IFN-gamma or IL-10 and are regulated by IL-1beta. Nature 484: 514–518. doi: 10.1038/nature10957 PMID: 22466287

47. Brooks AE, Parsamand T, Kelly RW, Simoes-Barbosa A (2013) An improved quantitative method to assess adhesive properties of Trichomonas vaginalis to host vaginal ectocervical cells using flow cytometry. J Microbiol Methods 92: 73–78. doi: 10.1016/j.mimet.2012.10.011 PMID: 23142340

48. Blanchard A, Yanez A, Dybvig K, Watson HL, Griffiths G, et al. (1993) Evaluation of intraspecies genetic variation within the 16S rRNA gene of Mycoplasma hominis and detection by polymerase chain reaction. J Clin Microbiol 31: 1358–1361. PMID: 7684753

49. Carlton JM, Hirt RP, Silva JC, Delcher AL, Schatz M, et al. (2007) Draft genome sequence of the sexually transmitted pathogen Trichomonas vaginalis. Science 315: 207–212. PMID: 17218520

50. Kaur S, Khurana S, Bagga R, Wanchu A, Malla N (2008) Antitrichomonas IgG, IgM, IgA, and IgG subclass responses in human intravaginal trichomoniasis. Parasitol Res 103: 305–312. doi: 10.1007/s00436-008-0971-y PMID: 18437425

51. Corthesy B (2013) Multi-faceted functions of secretory IgA at mucosal surfaces. Front Immunol 4: 185. doi: 10.3389/fimmu.2013.00185 PMID: 23874333

52. Provenzano D, Alderete JF (1995) Analysis of human immunoglobulin-degrading cysteine proteinases of Trichomonas vaginalis. Infect Immun 63: 3388–3395. PMID: 7642267

53. Alderete JF (1988) Alternating phenotypic expression of two classes of Trichomonas vaginalis surface markers. Rev Infect Dis 10 Suppl 2: S408–412. PMID: 3055209

54. Pereira-Neves A, Benchimol M (2007) Phagocytosis by Trichomonas vaginalis: new insights. Biol Cell 99: 87–101. PMID: 17029588

55. Bar AK, Phukan N, Pinheiro J, Simoes-Barbosa A (2015) The Interplay of Host Microbiota and Parasitic Protozoans at Mucosal Interfaces: Implications for the Outcomes of Infections and Diseases. PLoS Negl Trop Dis 9: e0004176. doi: 10.1371/journal.pntd.0004176 PMID: 26658061

56. Martin DH, Zozaya M, Lillis RA, Myers L, Nsuami MJ, et al. (2013) Unique vaginal microbiota that includes an unknown Mycoplasma-like organism is associated with Trichomonas vaginalis infection. J Infect Dis 207: 1922–1931. doi: 10.1093/infdis/jit100 PMID: 23482642

57. El Sayed Zaki M, Raafat D, El Emshaty W, Azab MS, Goda H (2010) Correlation of Trichomonas vaginalis to bacterial vaginosis: a laboratory-based study. J Infect Dev Ctries 4: 156–163. PMID: 20351456

58. Garber GE, Lemchuk-Favel LT (1989) Characterization and purification of extracellular proteases of Trichomonas vaginalis. Can J Microbiol 35: 903–909. PMID: 2819601

59. Garber GE, Lemchuk-Favel LT (1994) Analysis of the extracellular proteases of Trichomonas vaginalis. Parasitol Res 80: 361–365. PMID: 7971921

60. Alvarez-Sanchez ME, Avila-Gonzalez L, Becerril-Garcia C, Fattel-Facenda LV, Ortega-Lopez J, et al. (2000) A novel cysteine proteinase (CP65) of Trichomonas vaginalis involved in cytotoxicity. Microb Pathog 28: 193–202. PMID: 10764610

61. Mendoza-Lopez MR, Becerril-Garcia C, Fattel-Facenda LV, Avila-Gonzalez L, Ruiz-Tachiquin ME, et al. (2000) CP30, a cysteine proteinase involved in Trichomonas vaginalis cytoadherence. Infect Immun 68: 4907–4912. PMID: 10948104

62. Arroyo R, Alderete JF (1989) Trichomonas vaginalis surface proteinase activity is necessary for parasite adherence to epithelial cells. Infect Immun 57: 2991–2997. PMID: 2789190

63. Kummer S, Hayes GR, Gilbert RO, Beach DH, Lucas JJ, et al. (2008) Induction of human host cell apoptosis by Trichomonas vaginalis cysteine proteases is modulated by parasite exposure to iron. Microb Pathog 44: 197–203. PMID: 18024074

64. Vancini RG, Pereira-Neves A, Borojevic R, Benchimol M (2008) Trichomonas vaginalis harboring Mycoplasma hominis increases cytopathogenicity in vitro. Eur J Clin Microbiol Infect Dis 27: 259–267. PMID: 18040730

65. Schmitt N, Ueno H (2015) Regulation of human helper T cell subset differentiation by cytokines. Curr Opin Immunol 34: 130–136. doi: 10.1016/j.coi.2015.03.007 PMID: 25879814

66. Lopez-Romero GC, Quintero J, Astiazaran-Garcia H, Velazquez C (2015) Host Defences Against Giardia Lamblia. Parasite Immunol.

67. Dann SM, Manthey CF, Le C, Miyamoto Y, Gima L, et al. (2015) IL-17A promotes protective IgA responses and expression of other potential effectors against the lumen-dwelling enteric parasite Giardia. Exp Parasitol 156: 68–78. doi: 10.1016/j.exppara.2015.06.003 PMID: 26071205

68. Dreesen L, De Bosscher K, Grit G, Staels B, Lubberts E, et al. (2014) Giardia muris infection in mice is associated with a protective interleukin 17A response and induction of peroxisome proliferator-activated receptor alpha. Infect Immun 82: 3333–3340. doi: 10.1128/IAI.01536-14 PMID: 24866800

69. Makinde HM, Zariffard R, Mirmonsef P, Novak RM, Jarrett O, et al. (2013) IL-22 levels are associated with Trichomonas vaginalis infection in the lower genital tract. Am J Reprod Immunol 70: 38–44. doi: 10.1111/aji.12100 PMID: 23445169

70. Littman DR, Rudensky AY (2010) Th17 and regulatory T cells in mediating and restraining inflammation. Cell 140: 845–858. doi: 10.1016/j.cell.2010.02.021 PMID: 20303875

71. Zenewicz LA, Flavell RA (2011) Recent advances in IL-22 biology. Int Immunol 23: 159–163. doi: 10.1093/intimm/dxr001 PMID: 21393631

72. Phukan N, Parsamand T, Brooks AE, Nguyen TN, Simoes-Barbosa A (2013) The adherence of Trichomonas vaginalis to host ectocervical cells is influenced by lactobacilli. Sex Transm Infect 89: 455–459. doi: 10.1136/sextrans-2013-051039 PMID: 23720602

73. Fettweis JM, Serrano MG, Huang B, Brooks JP, Glascock AL, et al. (2014) An emerging mycoplasma associated with trichomoniasis, vaginal infection and disease. PLoS ONE 9: e110943. doi: 10.1371/journal.pone.0110943 PMID: 25337710

74. Waugh DJ, Wilson C (2008) The interleukin-8 pathway in cancer. Clin Cancer Res 14: 6735–6741. doi: 10.1158/1078-0432.CCR-07-4843 PMID: 18980965

75. Kolaczkowska E, Kubes P (2013) Neutrophil recruitment and function in health and inflammation. Nat Rev Immunol 13: 159–175. doi: 10.1038/nri3399 PMID: 23435331

Chapter 4 : Summary and Discussion

Summary

Trichomonas vaginalis is an important human pathogen, especially because most infections are asymptomatic[1], thus allowing greater spread by asymptomatic carriers. While metronidazole, the mainstay treatment, has been in use since the 1960s[2], in depth molecular understanding of the targets of the drug had remained elusive. The studies in this dissertation, identified more Mz protein targets, thus challenging the prevailing hypothesis of limited, selective targets[3], and also demonstrated some Mz-adducted cysteine residues (Chapter 2). In addition, the results presented in Chapter 3 demonstrate that the presence of *M. hominis* might explain some aspect of observed range and severity of symptoms in clinical presentation.

Insight into metronidazole drug targets

Previous investigation of metronidazole targets in *T. vaginalis* using two-dimensional gel (2DE) identified seven cytosolic proteins, including thioredoxin reductase[3]. Investigations into other protozoa using similar methodology also identified limited number of proteins[4,5].

T. vaginalis has a large protein-coding genome with significant amplification of gene families[6]. Thus, different isolates of the parasite could have different assortments of orthologs to function. In the two strains used in our drug target identification, the only difference was the expression of flavin reductase 1 in the sensitive strain[7]. This likely contributed to the seven proteins shared between the adductomes. This stands in contrast to the eight proteins identified in the G3 strain by their adducted cysteine residues. Our observations across several proteomics studies in the lab have shown that G3 proteomes can vary significantly from other strains.

Following up this study in various other metronidazole-sensitive and -resistant strains would allow the identification of shared targets, especially ones that are conserved in resistant

strains. Mechanistically, drug activation potential is limited in resistant strains. For example, in B7268-EV parasite which lacks flavin reductase 1, and thus a decreased capacity to reduce and eliminate oxygen[7], it is conceivable that capacity of functional thioredoxin reductase to activate metronidazle[3,8] is decreased, as seen with the flavin inhibitor diphenyleneiodonium[9]. Interestingly, the weak driving force for activation of metronidazole preserves resistant strains under lower concentration of drug, while sensitive parasites activate more of the drug, leading to more extensive adduction and subsequent dysfunction. Thus, identification of shared targets that are characterized to be essential for the viability of *T. vaginalis* could be developed as novel drug targets.

Beyond *T. vaginalis*, the use of Mz-alkyne can be implemented even in bacterial species such as *Helicobacter pylori* and *Clostrium difficile*, which were once more susceptible to metronidazole. This approach could unlock potential new targets in those organisms as well.

Insight into immune response to *T. vaginalis*-*M. hominis* co-infection

We observed that monocytes co-cultured with heat-inactivate parasites harboring *M. hominis* elaborated more cytokines than when *M. hominis*-free parasites are used. Previous works suggest that *T. vaginalis* is sensed through TLR4[10] and *M. hominis* is sensed through TLR2[11]. Although both TLR2 and TLR4 share common downstream signaling pathways for inflammatory cytokine expression[12], our observations suggest that TLR2-mediated signaling is more significant.

While we do not observe statistically significant difference in cytotoxic effect secondary to *M. hominis* endosymbiosis, previous study did[13]. It is likely that the contribution of *M. hominis* to cytotoxicity might depend on the background cytotoxic effect of the axenic *T.*

vaginalis. Moreover, the presence of *M. hominis* could lead to greater immune recognition of co-infection, thus leading to symptoms such as leukorrhea, for instance. Epithelial cells are important agents in host defense and the different epithelia express different TLRs[14]. As vaginal epithelium does not express TLR4[14], sensing of the parasite through TLR4 would not be expected to happen unless tissue-resident immune cells were encountered. However, the presence of *M. hominis*, which can be sensed by TLR2[11], a TLR expressed by vaginal epithelium[14], would result in more robust response, likely leading to more symptoms, which might prompt a patient to present to the clinic for treatment.

References:

1. Schwebke, J. R. & Burgess, D. Trichomoniasis. *Clinical Microbiology Reviews* vol. 17 794–803 (2004).

2. Cosar, C. & Julou, L. Activity of (Hydroxy-2'Ethyl)-1 Methyl- 2 Nitro-5 Imidazole (8823, R.P.) in Experimental Trichomonas vaginalis Infections. *Ann. Inst. Pasteur* **96**, 238–41 (1959).

3. Leitsch, D. *et al.* Trichomonas vaginalis: Metronidazole and other nitroimidazole drugs are reduced by the flavin enzyme thioredoxin reductase and disrupt the cellular redox system. Implications for nitroimidazole toxicity and resistance. *Mol. Microbiol.* **72**, 518–536 (2009).

4. Leitsch, D., Kolarich, D., Wilson, I. B. H., Altmann, F. & Duchêne, M. Nitroimidazole action in Entamoeba histolytica: A central role for thioredoxin reductase. *PLoS Biol.* **5**, 1820–1834 (2007).

5. Leitsch, D., Schlosser, S., Burgess, A. & Duchêne, M. Nitroimidazole drugs vary in their mode of action in the human parasite Giardia lamblia. *Int. J. Parasitol. Drugs Drug Resist.* **2**, 166–170 (2012).

6. Carlton, J. M. *et al.* Draft genome sequence of the sexually transmitted pathogen Trichomonas vaginalis. *Science (80-.).* **315**, 207–212 (2007).

7. Leitsch, D., Janssen, B. D., Kolarich, D., Johnson, P. J. & Duchêne, M. Trichomonas vaginalis flavin reductase 1 and its role in metronidazole resistance. *Mol. Microbiol.* **91**, 198–208 (2014).

8. Leitsch, D., Drinić, M., Kolarich, D. & Duchêne, M. Down-regulation of flavin reductase and alcohol dehydrogenase-1 (ADH1) in metronidazole-resistant isolates of Trichomonas vaginalis. *Mol. Biochem. Parasitol.* **183**, 177–183 (2012).

9. Leitsch, D., Kolarich, D. & Duchêne, M. The flavin inhibitor diphenyleneiodonium renders Trichomonas vaginalis resistant to metronidazole, inhibits thioredoxin reductase and flavin reductase, and shuts off hydrogenosomal enzymatic pathways. *Mol. Biochem. Parasitol.* **171**, 17–24 (2010).

10. Zariffard, M. R. *et al.* Trichomonas vaginalis infection activates cells through toll-like receptor 4. *Clin. Immunol.* **111**, 103–107 (2004).

11. Peltier, M. R., Freeman, A. J., Mu, H. H. & Cole, B. C. Characterization and Partial Purification of a Macrophage-Stimulating Factor from Mycoplasma hominis. *Am. J. Reprod. Immunol.* **54**, 342–351 (2005).

12. Lai, Y. & Gallo, R. L. Toll-like receptors in skin infectious and inflammatory diseases. *Infect. Disord. Drug Targets* **8**, 144 (2008).
13. Vancini, R. G., Pereira-Neves, A., Borojevic, R. & Benchimol, M. Trichomonas vaginalis harboring Mycoplasma hominis increases cytopathogenicity in vitro. *Eur. J. Clin. Microbiol. Infect. Dis.* **27**, 259–267 (2008).

14. McClure, R. & Massari, P. TLR-dependent human mucosal epithelial cell responses to microbial pathogens. *Frontiers in Immunology* vol. 5 (2014).